PhD degree in Molecular Medicine

European School of Molecular Medicine (SEMM)

University of Milan and University of Naples "Federico II"

Faculty of Medicine

Settore disciplinare: MED/04

Expression and Initial Characterization of the Cell Fate Transcription Factor PRDM1 in Adult Neural Progenitors and Glioblastoma Multiforme

Chiara Biancotto

IFOM-IEO Campus, Milan

Matricola R07946

Supervisor: **Saverio Minucci MD PhD**
Department of Experimental Oncology
IEO (European Institute of Oncology)

Anno Accademico 2011-2012

TABLE OF CONTENTS

LIST OF ABBREVIATIONS

PRDM	(PRDI-BF1 and RIZ)-Domain Containing Protein
PRDI	Positive Regulatory Domain 1
RIZ	Retinoblastoma Interacting Zinc finger
BCL	B Cell Lymphoma
Blimp-1	B Lymphocyte-Induced Maturation Protein-1
PRDM1α	PR-Domain Containing Protein 1 alpha
PRDM1β	PR-Domain Containing Protein 1 beta
EVI1	Ecotropic Virus Integration site 1 protein homolog
MDS1	MyeloDysplasia Syndrome-associated protein 1
SET	Suppressor of variegation 3-9, Enhancer of zeste and Trithorax
PHD	Prevent Host Death protein
HDAC	Histone DeACetylase
HMT	Histone MethylTransferase
WT	Wild Type
KO	Knock Out
PGC	Primordial Germ Cell
ED	Embryonic Day
EGFP	Enhanced Green Fluorescent Protein
BMP	Bone Morphogenic Protein
ExE	EXtra-embryonic Ectoderm
VE	Visceral Endoderm
HOX	Homeobox protein
GO	Gene Ontology
Ig	Immunoglobulin
TCR	T Cell Receptor
NC	Neural Crest cell
RB	Rohon-Beard sensory neuron
Wnt	WiNgless-Type MMTV integration site family member
FGF	Fibroblast Growth Factor
EGF	Epidermal Growth Fator
PDGFRA	Platelet Derived Growth Factor Receptor Alpha
VEGF	Vascular Endothelial Growth Factor
ENU	EthylNitrosoUrea
Ubo	U-boot zebrafish mutant
Nrd	Narrow minded zebrafish mutant
Prmt	Protein Arginine Methyltransferase
ChIP	Chromatin ImmunoPrecipitation
IRF	Interferon Regulatory Factor
LSD1	Lysine-Specific histone Demethylase 1
GFAP	Glial Fibrillary Acidic Protein
CNS	Central Nervous System
SVZ	SubVentricular Zone
SGZ	SubGranular Zone
BrDU	Bromo-DeoxyUridine
FACS	Fluorescence-Activated Cell Sorting
NCS	Neural Stem Cell
NSPCs	Neural Stem and Progenitor Cells
Notch	Notch homolog 1, translocation-associated
Shh	Sonic hedgehog

bHLH	basic Helix-Loop-Helix
DLBCL	Diffuse Large B Cell Lymphoma
GCB	Germinal Center B cell
ABC	Activated B Cell
NF-kB	Nuclear Factor-KappaB

FIGURES INDEX

TABLE INDEX

ABSTRACT

PRDM1 is a master transcriptional regulator in multiple cell lineages and it is required for the development of many species. However the reason and the mechanisms underlying its pleiotropic functions remain largely unknown as the full array of tissues and target genes that it controls. Our results indicate a completely unexplored field where to study PRDM1 regulatory network that is the brain and its most aggressive cancer, the Glioblastoma multiforme (GBM). We identified that PRDM1 is expressed in adult neural progenitor cells and that it correlates with the maintenance of cellular multipotency, possibly by interfering with pro-differentiation pathways (e.g. HIF1α signaling). We generated the first genome wide profile of PRDM1 binding in mammalian cells, expanding the pool of known direct target genes and providing a new solid ground for mechanistical studies that suggest a role for PRDM1 in stable and heritable gene silencing during differentiation.

Finally we found that PRDM1 expression associates with a specific subtype of human GBM called mesenchymal and that it is highly expressed in GBM cancer derived stem cells. Consequently we have also exploited the functional relevance of PRDM1 in a spontaneous mouse model of GBM related to the human pathology.

Taken together our data add further to the already established role of PRDM1 as a cell fate regulator identifying that PRDM1 is involved in normal and aberrant mammalian neurogenesis. We also provided a consistent dataset to functionally and mechanistically characterize PRDM1 dependent cell fate transitions.

Chapter 1 - INTRODUCTION

1.1 PRDM transcription factor family

In complex multicellular organisms, cells – that share identical genome – encounter diverse lineage choices: a process that determines cell type specific gene expression programs[1]. Current evidence strongly supports a model where cell fate determination is orchestrated by lineage determining regulators and chromatin marks - that may be transmitted across cell generations - originally instructed by pioneer transcription factors[2]. These transcription factors can engage nucleosomes and compacted chromatin or may function as "placeholders": in fact they can modulate the local epigenetic state of chromatin[3] in a way to keep active or silent developmental specific genes. The aberrant expression of such transcription factors often leads to cell transformation linked to an inappropriate program of cellular differentiation[4]. However, relatively few examples of such regulators have been identified and little is known about how tissue-specific programs are established (review in[5]).

In this scenario, increasing evidence suggests, the master regulator PRDM1, and more in general the PRDM family of proteins, to act as a key instructive transcription factor required for the control of cell-fate determination in developing organisms and to maintain tissue homeostasis in many organs.

The PR (PRDI-BF1 and RIZ)-domain containing proteins (PRDMs) derive the name from the firstly identified members: positive regulatory domain I-binding factor 1 (PRD1-BF1)/PRDM1 and retinoblastoma-interacting zinc finger protein 1 (RIZ1)/PRDM2.

PRDMs have been described to play critical roles in different kind of developmental processes [6] [7]. They appear to be highly cell type/tissue specific transcriptional regulators using either enzymatic activity towards histones or recruitment of interaction partners to modify the expression of target genes.

PRDM1 was identified and cloned by two different groups almost at the same time[8]: Keller and Maniatis originally identified PRDM1 as a transcriptional repressor of the interferon beta (IFNβ) promoter following viral infection of U2OS human osteosarcoma cell-line[9], while Turner and co-workers identified the mouse homologue by subtractive cloning of transcripts that were induced during differentiation of B cell lymphoma 1 line (BCL1) and they called the protein Blimp-1 (B lymphocyte-induced maturation protein-1)[10].

The other founding member of the family, the zinc finger gene RIZ1 (or PRDM2) was isolated in a functional screening for Rb interacting proteins[11] and in the same article, the authors recognized the homologous amino-terminal 100 amino acids region shared between RIZ1 and the PRDI-BF1/Blimp1. Subsequently, the RIZ1 PR domain peptide was used as a query for a Genbank homology search showing that the predicted translation product of Mds1-Evi1 locus (also called Mecom or Prdm3, fusing Evi1 gene with what had previously considered an independent upstream locus – Mds1) is homologous to the amino end of RIZ1[12]. This analysis allowed the identification of the Mds1-Evi1 gene as a PRDM gene that normally produces at least two different length products: the PR containing MDS1-EVI1 (PRDM3) protein and the PR lacking EVI1 protein.

The family grew further as additional proteins in vertebrate were identified on the basis of the PR domain conserved in mouse, rat and human with a sequence identity reaching 40%.

This class of genes originated in metazoans and is evolutionary conserved. Gene duplication and loss events[13] [14] have changed PRDMs number among different species. In invertebrates, the orthology assignment yielded two genes for nematodes and three genes for arthropods, while in vertebrates there are 17 putative PRDM orthologs in primates (Fig.1) and 16 putative orthologs in rodents, birds and amphibians, possibly meaning that the functional specialization of PRDMs has increased during the evolution[15]. Moreover since no PR peptides were detected in the yeast genome, it's plausible to hypothesize that the PR domain may have evolved as a result of a special need of multicellular organisms.

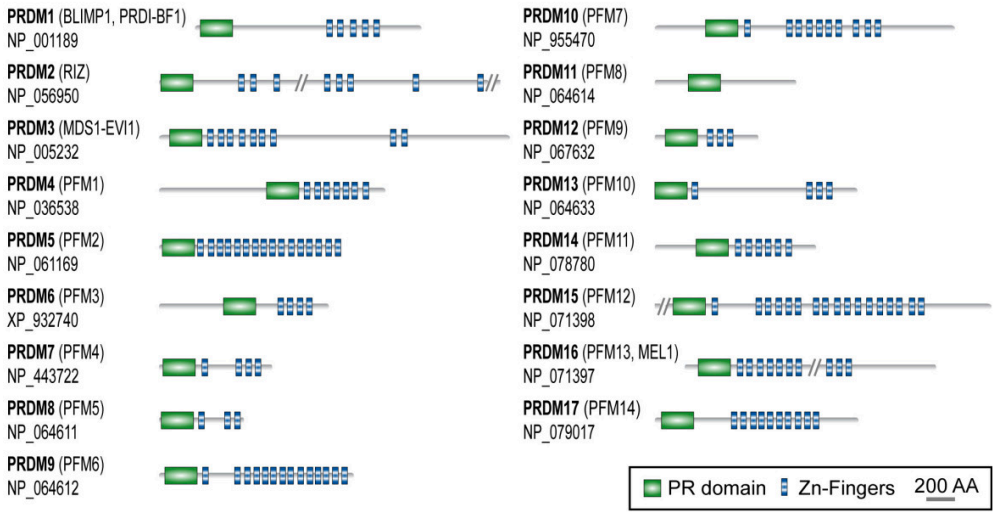

Figure 1. PR-domain containing proteins (PRDMs) family. Figure adapted from Fumasoni et al. BMC Evolutionary Biology 2007 7:187. Domain architecture of the human PRDM paralogs. For each PRDM protein, the corresponding RefSeq Accession Number and additional names are provided.

1.1.1 PR and SET domains: analogies and differences

Using bioinformatics tools, PR domain was shown to share consistent sequence homology with SET domain (named after the *Drosophila* factors Suppressor of variegation 3-9, Enhancer of zeste and Trithorax were originally identified) that is characteristic of protein lysine methyltransferases[16 17 18 19].

Consequently, PR domain has been considered as a sub-type of SET domain even if it diverged from the canonical SET structure.

The aminoacidic sequence similarity between PR and SET domains is typically around 20% nonetheless they are distinct because identities within PR domains or within SET domains are usually higher than 40%.

SET domain containing proteins encompass many members that have been structurally characterized [20 21 22 23 24]. The catalytic domain is composed of a conserved core SET domain, surrounded by a limited set of variable regions (the I-SET and post-SET) that form the binding groove for the substrate peptide and the co-factor binding pocket. The post-SET (immediately at the carboxyl terminal of core-SET) is a dynamic feature, important for the substrate recognition.

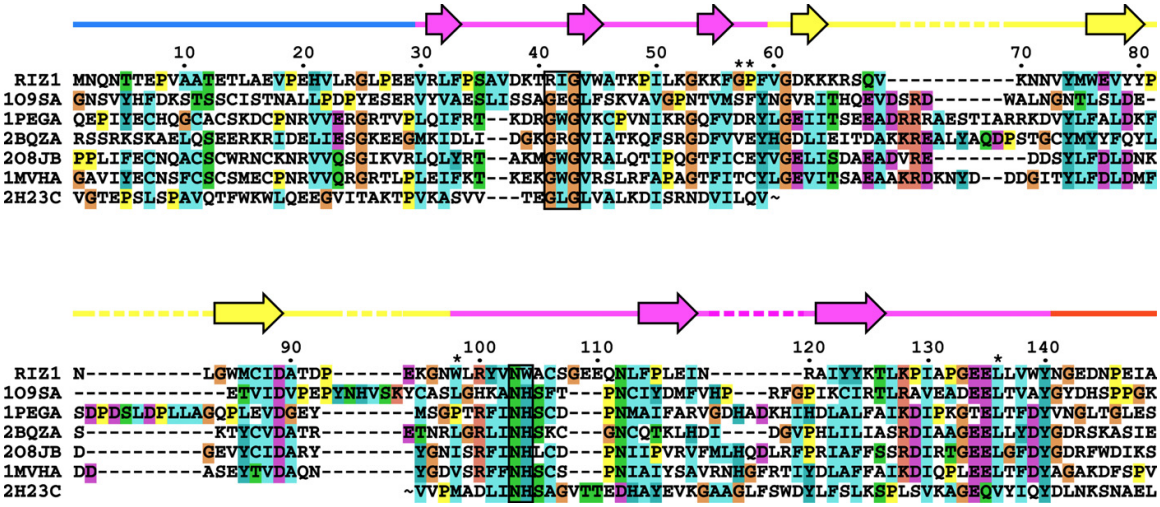

Figure 2. Sequence alignment of the PR domain from RIZ1 and several canonical SET domains. Figure adapted from Briknarova K. et al, Biochemical and Biophysical Research Communications 366 (2008). PR-domain from RIZ1 and SET domains from SET7/9 (1O9SA), DIM-5 (1PEGA), SET8/PR-SET7 (2BQZA), human euchromatic histone methyltransferase 2 (EuHMT2) (2O8JB), Clr4 (1MVHA), and Rubisco large subunit N-methyltransferase (LSMT) (2H23C). Sequence homology is highlighted by the default ClustalX color scheme.. RIZ1 residue numbers are marked above the sequences. β-strands in RIZ1 that are also conserved in most other SET domains are outlined on top. In this diagram, the conserved SET core is purple, N-flanking region is blue, C-flanking region is red and the more variable inserted region is yellow. Two motifs that are highly conserved in canonical SET proteins, GXG and NH, are framed. Positions that are invariant in human PR proteins are marked with asterisks (*).

Unlike SET domain, there is little structural information available for PR domain[25 26] and significant sequence diversity between the two domains impedes the solution of a confident homology model.

Despite sequence similarity, some key residues are not conserved between the two domains: in the SET family, mutations in the conserved H/RxxNHxC motif abolish the catalytic activity[17]. However, all PR domains lack this motif. Conversely, only four residues are constant in human PR domains: Gly57, Pro58, Trp98 and Leu136. Of these, only Leu136 is conserved in canonical SET domains (Fig.2).

Moreover, SET domains are primarily found at the carboxyl termini of proteins that contain various motifs (including the chromo domain, A/T hooks, zinc finger, PHD fingers and GTP binding motifs), which lack obvious DNA binding ability, whereas PR domains (all but PRDM11) are located at the amino-termini of a repeated arrays of Krüpple type zinc fingers (C_2H_2 zinc fingers)[19] (Fig.3).

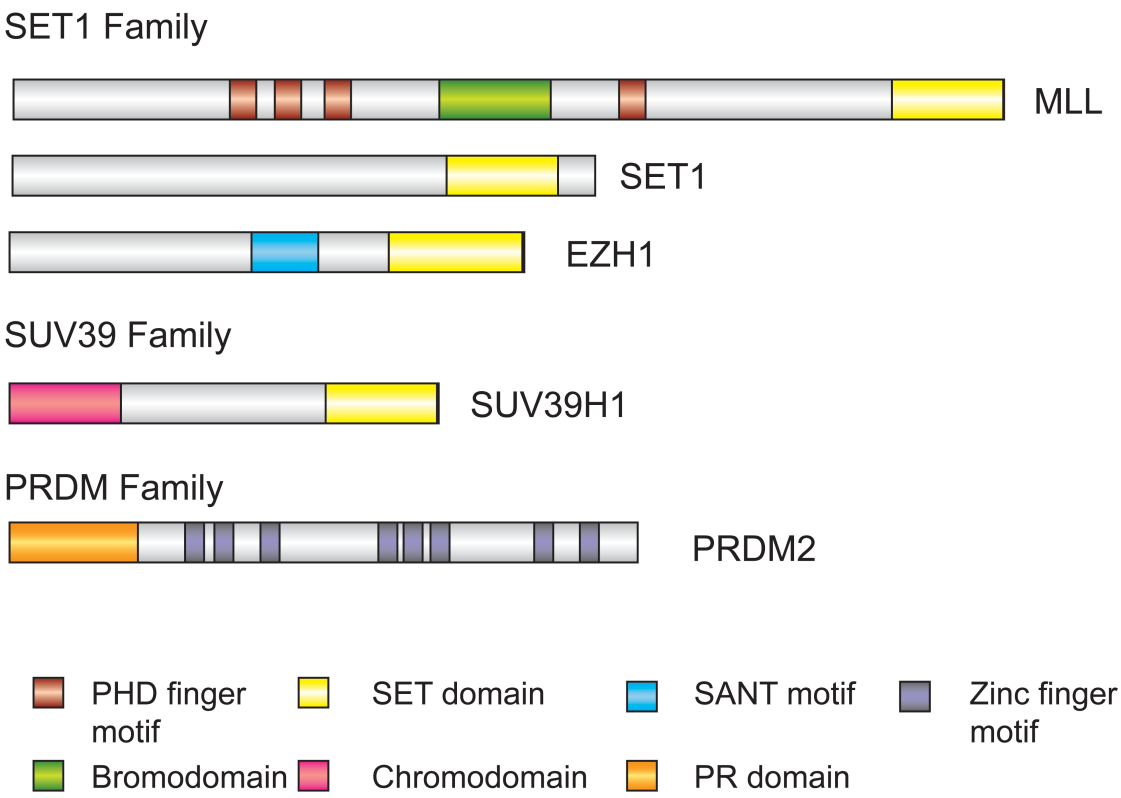

Figure 3. Prototype members of the various families of Histone Methyltransferases (HMTs). Conserved structural features are indicated according to the legend showed at the bottom.

Taking into account all these features, PR domain seems to be a derivative of SET domain as both of them are involved in development, cancer and chromatin regulation but with diverse molecular mechanisms.

SET proteins methylate directly histone lysine residues, this being a post-translational epigenetic modification that controls the expression of genes by serving as markers for the recruitment of particular complexes that direct the organization of chromatin. For PRDMs, the enzymatic activity – postulated for the homology with SET – has been found only in few PRDMs: by in vitro methylation assays recombinant RIZ1 and PRDM8 were both shown to act as repressive histone methyltransferases by catalyzing the dimethylation of lysine 9 of histone H3 (H3K9me2), while PRDM9 was found to catalyze the activating trimethylated lysine 4 of histone H3 (H3K4me3)[26] [27] [28]. More recently it has been demonstrated that PRDM3/PRDM16 double null cells have reduced levels of H3K9me1, which is responsible for a decrease of Suv39h-dependent H3K9me3 levels in cell

chromatin. This effect compromises the structure of pericentric heterochromatin and the nuclear lamina of the cells that then undergo senescence. The authors show that PRDM3 and PRDM16 are cytoplasmic enzymes but they did not provide direct mechanisms for their involvement in the maintenance of heterochromatin and nuclear lamina structure[29].

Comparing SET and PR tridimentional structures, only a cysteine residue (C106) is shared between RIZ1 PR domain and SET proteins catalytic domain and the mutation of such aminoacid in RIZ1 and in SUV39H1 decreases or abolishes their enzymatic activity [26]. Nevertheless, it is not conserved among the others PRDM members possibly explaining the weak biochemical activity for PRDMs. Crystallization studies have shown that the flexible carboxyl terminal sequence in RIZ1 PR domain is necessary for functional activity - a property that SET proteins use for substrate recognition - but the exact molecular details of the complex between RIZ1 and histone H3 await further structural investigation.

Although mainly "not catalytic", all PRDMs are present in chromatin remodeling complexes. In fact, as mentioned before, from the structural point of view, PRDM proteins have two core domains – the PR domain and a series of C_2H_2 zinc fingers – and other smaller domains that serve as scaffolds for the recruitment of co-factors and enzymes to the target promoters in a cell-type and context specific manner. For example, PRDM6 maintains the proliferative potential of smooth muscle cells through the formation of a complex with p300 histone acetyltransferase[30] while it co-localizes with H4K20 methylation in endothelial progenitors[31]. On the other hand, PRDM5 was found to bind in-vitro G9a and class I histone deacetylases (HDACs) and to recruit them to the target promoters yielding H3K9 methylation and H3 and H4 deacetylation, respectively [32]. Some PRDM members contain also proline rich domain (PRDM1[8], PRDM3[33] and PRDM16) through which they bind histone modifiers.

Growing evidence suggests an important role for Krüpple type C_2H_2 zinc fingers, originally identified as DNA-binding domains, in protein binding[34]: for example the first

two zinc fingers of PRDM3 serve for SUV39H1 binding[35] while PRDM16 uses them for CEBP-β[36] and PPR-γ recruitment [37].

Functionally, PRDMs are transcriptional regulators that bind target promoters via their C_2H_2 zinc fingers in many developmental contexts[38] [35] and they are important master regulators of different cell-fate transitions. For example, PRDM14 was recently demonstrated to be important in the maintenance of human embryonic stem cells[39] and together with PRDM1 regulate the formation of mouse primordial germ cells[40] while PRDM3 and PRDM16 are both critical for the early hematopoiesis[41] [42,43].

1.2. PRDM1 is a master cell fate regulator

PRDM1 is a prototype of PRDM family because it represents well all of the features mentioned above and available evidence suggests an involvement in different tumors.

PRDM1 is expressed in a variety of embryonic tissues[42] and it is highly conserved developmental regulator in many organisms. In mammals, as well as in other model organisms, PRDM1 has been implicated in a large number of regulatory networks suggesting that its function is finely tuned. However the full array of tissues and molecular mechanisms regulated by PRDM1 are in need of further investigation and constitute the scope of this work.

PRDM1 knock-out (KO) in mouse is embryonically lethal at day 10.5 of gestation and the major abnormalities observed indicate its fundamental role in the specification of primordial germ cells (PGCs) other than secondary defects including the formation of the placenta, the branchial arches and the loss of integrity of the blood vessels [44].

Whole-mount in situ hybridization (comparing wild type and KO mice) has been used to investigate the role of PRDM1 in the first stages of mammalian development. Surprisingly, even though PRDM1 localizes in the region (axial mesendoderm) from which antero-posterior axis and head structures originate in early vertebrates, the formation of the anterior patterning and of the neural crest were unaffected by PRDM1 loss[44]. This

observation was unexpected and in disagreement with what has been observed in other vertebrates: in fact, in *Xenopus* and *zebrafish* (see below), PRDM1 transcript localizes in the same structures (anterior mesendoderm and the prechordal plate) where it is functionally active for forebrain and early axis formation[45,46].

Despite largely expressed in many compartments, PRDM1 deficient mice die for placental abnormalities and mutant embryos display quite restricted tissue impairments.

The generation of transgenic mice and derived transgenic primary cells - in which a reporter gene (i.e. EGFP, membrane-target Venus)[47] was cloned under the control of PRDM1 regulatory elements - allowed to recapitulate the dynamic expression of embryonic PRDM1 and to overcome the limits of KO mice. This model was widely used for the understanding of PGCs specification (below) but also it was adopted for the study of other tissues especially for skin epithelial cell lineages.

In fact, it has been assessed that PRDM1 is expressed in a particular population of unipotent progenitors in the skin able to give rise to proliferative cells, which in turn differentiate (by repressing c-Myc) into sebum-secreting cells. PRDM1 expressing cells are also able to induce and mobilize multipotent progenitors when homeostasis of the gland is perturbed [48].

These findings, coupled with immunohistochemical staining of PRDM1 in epithelial tissues, gave the rational to perform conditional deletion of PRDM1 in epidermis[49]. PRDM1 is normally expressed in the granular layer keratinocytes where it regulates keratinocyte transition from granular to cornified layer, the components of the barrier that protect the organism from the external enviroment. In the absence of PRDM1, the granula layer of newborns is expanded and contains abnormally undifferentiated enlarged cells. The mice develop big scarring other than spenomegaly and enlarged lymphonodes and die around 14 weeks. The observed delay in the differentiation process culminates in an abnormal cornified layer and in the hyperkeratinization of the hair follicle infundibulum.

In an attempt to understand the mechanisms regulated by PRDM1 in epidermal keratinocites, the epidermis of 1-day-old mice (wild type and KO) has been used for gene expression profiling. The differentially expressed genes encompass different categories involved in metabolism, signalling, structural genes of the cornified layer and carriers for membrane trafficking. The search for PRDM1 consensus binding site (as it was identified in lymphocytes[50]) in the KO up regulated genes returned six genes (dusp16, elf5, fos, nfat, prdm1 and sprr1a) that were confirmed also in-vivo by Chromatine Immunoprecipitation (ChIP). Of particular interest is the regulation of Nfat, which serves for the activation of transporters that regulate cellular osmosis and promotes water uptake. The unsuccessful down regulation of Nfat in PRDM1 KO mice determines the increased cell size of granular layer cells and of corneocytes resulting in the abnormal cornified layer.

Finally, in order to bypass placental defects PRDM1 was conditionally deleted only in the embryo proper, lengthening the lifespan until ED 18.5[51] and assessing that early lethality of PRDM1 null embryos was a consequence of extra-embryonic lineages defects and not of endothelial cell defects.

The rescue of early lethality consented to show that PRDM1 plays essential roles in the formation of posterior forelimb, secondary heart field and sensory vibrissae and that in general PRDM1 is a transcriptional regulator of signalling pathways important for fate decision of multipotent progenitors.

1.2.1 PRDM1 in primordial germ cells

The importance of PRDM1 in primordial germ cells (PGCs) formation was delineated from single cell gene expression profiling studies [52] [53,54] aimed to identify the cell of origin of germ cells and the fundamental players of the differentiation process.

In mouse, and probably in all mammals, the formation of germ cell lineage (haploid gametes) is not predetermined at fertilization, but it is initiated in incipient somatic cells (diploid epiblast cells) that, under specific signals, partially revert to a pluripotent state and escape from the somatic program of differentiation – a process called “epigenesis” [53].

There are three principal events that characterize the "epigenesis" program: a) escaping the somatic program; b) up regulation of pluripotency associated genes and c) ensuing genome wide epigenetic reprogramming (Fig.2) [52].

PGCs originate from a founder population of proximal epiblast cells encircled by the extra-embryonic ectoderm (ExE) and the visceral endoderm (VE) in the post-implantation embryo. At embryonic day (ED) 6.25, this group of cells is stimulated by morphogens (BMP4, BMP8 and BMP2) that are secreted from the ExE and induces the expression of the interferon-inducible transmembrane protein (fragilis/mil-1/ifitm3) [55] [56]. Immediately after, some of these epiblast cells start to express PRDM1, which from that point onward will characterize the lineage-restricted precursors[57]. As mentioned above these pluripotent epiblasts give rise to both germ cells and somatic cells as it has been demonstrated, by lineage tracing experiments, that early PRDM1 expressing cells are positive also for mesodermal genes (Hox genes, brachyury-T, Fgf8, Snai1, Mesp1, Sp5) [58].

During early gastrulation PRDM1 positive cells repress the somatic genes (Hoxa1 and Hoxb1) and at ED 7.5 the established precursors of germ cells are a cluster of 40 alkaline phosphatase and stella (or small nuclear cytoplasmic shuttling protein/Dppa3/Pgc7) positive cells located in the extraembryonic mesoderm[55]. Finally, these cells proliferate further and, at ED 10.5, colonize the embryonic gonads where they will differentiate into mature germ cells. PRDM1 positive cells contribute to stella positive cells confirming that PRDM1 is the earliest marker for lineage-restricted PGCs (Fig.4).

PRDM1 mutant embryos are able to form no more than half of the PGCs as compared to wild type (WT) mice and moreover these immature cells are not able to efficiently proliferate and migrate along the developing hindgut endoderm.

A detailed analysis done by the laboratory of Mitinori Saitou described the transcriptional changes occurring in PGCs at different stages of the maturation process (the initial 48 hours occurring from ED 6.25 to ED 8.25 with 12 hours of interval) and compared them to their somatic or PRDM1 null counterparts[54].

The first observation made by the authors was that while somatic cells during differentiation exhibited a homogenous enrichment of Hoxb1 positive cells and a homogenous decrease of Sox2 positive cells, the specifying PGCs (PRDM1 positive) transited in a "somatic like" expression pattern (Hoxb1 high and Sox2 low) to then specifically revert to the Hoxb negative, Sox2 positive state. Pairwise comparison of PRDM1 positive PGCs at different developmental stages demonstrated that the major expression level changes were between the passage form Hoxb1 positive PGCs to Hoxb-1 negative PGCs (E6.75-E7.0) during which the cells up regulate 493 genes (also called "specification genes") and down regulate 330 genes (also called "somatic genes"). The "specification genes", based on Gene Ontology (GO) functional annotation were enriched for terms associated with: germ cell development (mainly transcription factors-Prdm1, Prdm14, Sox3, Dppa3, Ifitm3, Dnd1, Elf3, Elk1, Isl2, Mycn, Klf2, Smad3, Kit and AP2γ), morphogenesis and organism development (Sox2, Nanog, and Epc1). On the other hand the "somatic genes" were enriched in cell-cycle regulators (CyclinE1, CyclineD1, Cdc25a, Cdc6, Pold2, E2F3, Myc and Cdk2), de novo DNA methyltransferases (Dnmt3a and 3b), Uhrf1 that recruits Dnmt1 to the replication foci, histone methyltransferase Glp (Ehmt1) and Hox cluster genes other than proteins involved in mesoderm induction and organ development.

In PRDM1 deficient cells many of the "somatic genes" were not correctly repressed and many of these showed similar expression levels to the somatic neighbour cells. Conversely, PRDM1 deficient PGCs acquire to some extent germ cells proprieties but then fail to revert to the pluripotent state meaning that PRDM1 independent mechanisms might regulate some of the initial "specification genes". Thus, the main function of PRDM1 in the formation of PGC is the repression of the "somatic program" by the down regulation of somatic-mesodermal genes, which include cell-cycle regulators and epigenetic modifiers. However, also the activation of the "specification genes" is partly impaired in PRDM1-null PGCs, confirming that PRDM1 is the master regulator of the entire process.

Germ cells from ED 7.75 onwards are subjected to a global epigenetic reprogramming that includes the erasure of the parental imprints, reactivation of inactive X chromosome and genome-wide CpG demethylation[59] [60]. The major epigenetic changes involve a global reduction of H3K9me2 (the levels of G9a are invariant, but embryonic GLP methyltransferase is repressed) and of DNA methylation. The dimethylated H3K9, mainly associated with repressed regions on euchromatin, is removed at around ED 8.0 and then maintained at constant low level until ED 12.5. At ED 9.5 all the migrating germ cells have low DNA mathylation signals, a consequence of DNA methyltransferases loss from the nuclei of the PGCs. At ED 8.0 the "maintenance methyltransferase" Dnmt1 is absent from germ cells nuclei for the duration of a cell cycle (16 hours) and immediately after also Dnmt3b and Dnmt3a, the "de novo methyltransferases", are absent or expressed at very low levels, respectively. Conversely, the levels of H3K27me3 (a more labile marker of gene repression in embryonic stem cells) and of H3K4me and H3K9 acetylation (markers of gene expression and active chromatin) increase in germ cells. In somatic cells H3K27me3 is mainly restricted to the X chromosome undergoing inactivation, while in migrating germ cells at around ED 8.5-9.0 large spots of H3K27me3 characterize euchromatic regions that subsequently will be covered by hyperactive marks[59].

Interestingly, another PRDM family member (PRDM14) is part of the "specification genes" and has recently been demonstrated to be the key regulator of epigenetic reprogramming and reacquisition of potential pluripotency in germ cells PMID[61]. PRDM14-null mice born and develop normally, but they are sterile because of complete lack of germ cells. Mutant PGCs failed to activate Sox2 and Dppa3 at the wild type levels and they showed also an impaired reduction of H3K9me because GLP methyltransferase is not properly repressed. These evidences strongly demonstrate that PRDM14 is responsible for the epigenetic reprogramming in germ cells and that two PRDMs are the major transcriptional regulators of germ cells formation in mice (Fig 4). [62] [63]

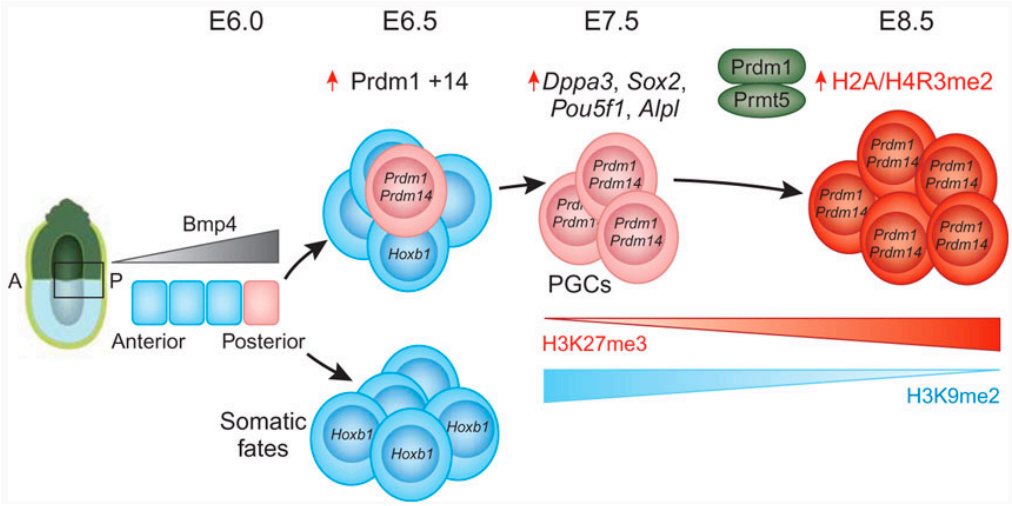

Figure 4. PRDM1 is a master regulator of primordial germ cells (PGCs) formation in mouse and PRDM14 is required for epiblasts reprogramming. Figure adapted from Nature Genetics 40, 934 - 935 (2008). PRDM1 and PRDM14 are fundamental players of germ cells formation in mouse. PRDM1 and PRDM14 are induced in proximal epiblats by BMP signals from extra embryonic ectoderm. PRDM1 and PRDM14 serve for repressing the somatic program and epigenetically reprogram epiblast cells that will generate the PGCs. These cell will up regulated germ cell (stella or Dppa3) and pluripotency markers (Sox2, Pou5f1 and alkaline phosphatase – Alpl). Afterwards (at embryonic day 8.5) H3K9me2 histone marks are erased from these cells, the levels of H3K27me3 increase and PRDM1-Prmt5 complex mediate H2A and H4R3 methylation.

1.2.2 PRDM1 in lymphocytes

Since PRDM1 was originally isolated in a screening for factors that were induced in B cell lymphomas differentiating towards Ig secreting cells, its relevance in lymphoid compartment has been investigated by generating conditional mouse models.

The laboratory of Kathryn Calame has studied extensively the abrogation of PRDM1 in B cell compartment crossing PRDM1 floxed mice with transgenic mice that express Cre recombinase under the control of CD19 promoter[64]. These studies confirmed and extended previous observations[65] [66], demonstrating that PRDM1 is the master regulator of plasmacell differentiation and it is absolutely necessary for Ig secretion from long-lived plasma-cells [67,68]. Briefly, in adaptive immunity, the process of maturation of an antigen-specific B-cell comprises two main processes: the formation, in the germinal centre, of fast proliferating cells that undergo class switch recombination and antigen affinity maturation and the formation of non-proliferating antibody secreting cells. Interestingly, the choice of the activated B-cell fate is determined by the antagonism of two master regulators that reciprocally counteract: BCL6 for the formation of the cellular component that will

constitute the immunological memory and PRDM1 for the maturation of the humoral compartment that will constitute the long-lived plasmacell in the bone marrow survival niches [69,70].

In particular, PRDM1 is continuously required for the maintenance of plasmacytic phenotype likely establishing a transcriptional program that characterize terminally differentiated B cells[6] by the induction of Syndecan, J chain rearrangement and immonuglobulin secretion.

Moreover, PRDM1 ectopic expression alone is able to force the differentiation of BCL-1 lymphoma cell line and of mouse primary splenocytes in antibody-secreting cells by repressing PAX5, a marker of activated B cells, and allowing expression of XBP-1[71 72].

Apparently PRDM1 expression was restricted to B cells compartment since, in thymocytes, PRDM1 mRNA was detected at a very steady state level. Nonetheless PRDM1 expression is much higher in antigen-experienced cells and the genetic ablation of PRDM1 in T cell compartment revealed that it also regulates developmental steps in diverse lymphocytic lineages[73,74]. In fact, these mice develop severe colitis due to an altered T cell homeostasis: in PRDM1 conditional KO mice the absolute number of naïve $CD4^+$T cells in thymus was decreased while, in response to TCR stimulus, the effector $CD4^+$T cells showed a hyperproliferation and hyperactivation (Fig. 5). Furthermore, the autoimmune inflammation was, in this work, correlated to an impairment of KO regulatory T cells (T_{reg}) in protecting against colitis in vivo.

PRDM1 is also highly expressed in effectors T helper type 2 (Th2) lymphocytes where it is mainly involved in contrasting Th1 response during Th2 lineage differentiation in order to favour humoral Th2 responses[75].

Finally, PRDM1 is additionally required for the terminal differentiation of effector $CD8^+$ T cells[76,77]. After virus-specific infection naïve $CD8^+$ T cells differentiate into two kinds of effectors, the cytotoxic short-lived effector cells and the cytokine producing effector cells that give rise to the memory compartment[78]. The cells defective for PRDM1 preferentially

commit though the memory precursor fate while they were insufficient in clearing acute infection.

As it was highlighted for plasmacell formation, also during T lymphocytes differentiation PRDM1 and BCL6 are mutually exclusive cell fate determinants. In fact, in some effectors the determination of cell lineage is dependent on the expression of such transcription factors: for example in $CD4^+$ T cells, BCL6 stimulate a kind of effectors (called follicular helper T cells [79]) that help the generation of germinal centre[80] while they do not express PRDM1, which instead characterizes, at different levels, other effectors (Th1, Th2, Th17 and T_{reg})[81]. Again, in $CD8^+$T, PRDM1 controls the cytotoxic effectors[73,74,76] and when deleted, the cells express more BCL6 in comparison to the WT cells.

The dichotomy between PRDM1 and BCL6 in the context of B and T cells is a maintained mechanism and PRDM1 seems to be important for cell cycle exit of the cells and for the terminal differentiation of specialized effectors.

Only in innate immunity this rule of thumb seems subverted: in fact, although always required for maturation and homeostasis of effector functions, in natural killer lymphocytes PRDM1 function is independent by BCL6 repression[82].

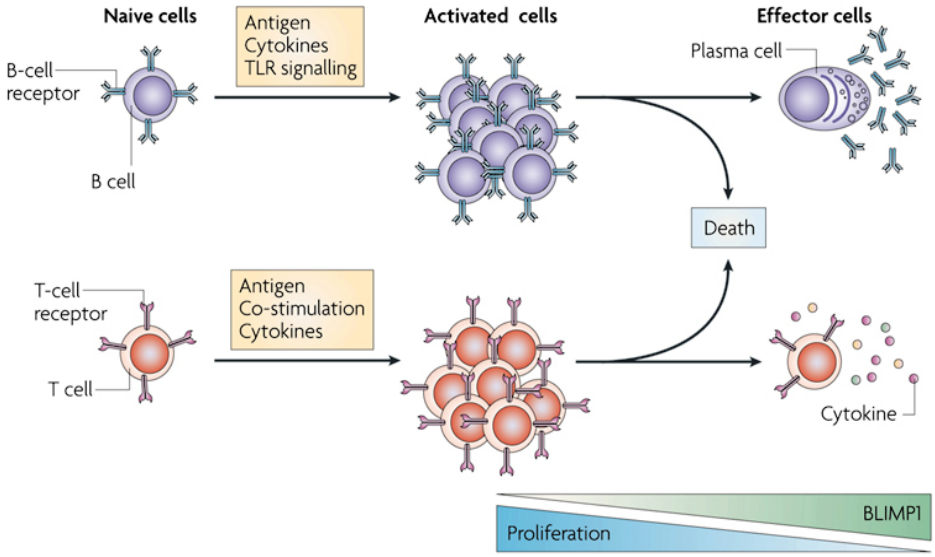

Figure 5. PRDM1 is a transcriptional repressor important for B an T lymphocytes terminal differentiation. Figure adapted from Nature Reviews Immunology 7, 923-927 (December 2007). PRDM1 controls the terminal differentiation antibody secreting cells and it maintains the homeostasis of effector T cells. In both cases the effector cells require PRDM1 to complete their developmental program. Most effector cells in either lineage are short-lived and die through apoptosis. The appropriate transition of activated lymphocytes to short and long-lived effector cells requires BLIMP1 function.

1.2.3 PRDM1 target genes and mechanism of target regulation in PGC and lymphocytes

PRDM1 has been extensively studied in germ cells and in lymphocytes but the identification of direct target genes was limited by the accessibility of such specific cell types that are restricted in number. Moreover the ectopic expression of PRDM1 leads to high citotoxicity. Consequently PRDM1 target genes were often evaluated indirectly as well as the molecular mechanisms associated with their regulation.

In PGCs PRDM1 appeared to be essential for the repression of all the "somatic genes" since PRDM1 deficient PGC-like cells fail completely to down regulate them.

The exact molecular mechanism that PRDM1 uses in PGCs for target genes regulation is currently under investigation but a pioneer work[58] demonstrated that in germ cells PRDM1 complexes with Prmt5 – an arginine methyltransferase – and that they direct the symmetrical dimethylation of H2A and H4 histones (H2A/H4R3me2s).

In vitro methylation assay of PRDM1 revealed a strong activity towards H2AR3 and H4R3, a modification that was never associated before with the PR/SET domain. Interestingly Prmt5, which is a class II arginine methylatransferase responsible for the symmetrical NG,N'G-dimethylation of arginine, was highly expressed in PGCs with a pattern similar to PRDM1. PRDM1 and Prmt5 co-expressed in the nuclei of germ cells between ED 8.5 and ED 10.5 and this time point coincides with the maximal accumulation of H2A/H4R3me2s in the nucleus (Fig. 4 and 6).

Additionally, it has been demonstrated that only when PRDM1 and Prmt5 are coexpressed in the nucleus are able to exert their repressive function towards a direct target gene – the RNA helicase Dhx38. After ED 11.5, the complex dissociates and Prmt5 shuttle to the cytoplasm while Dhx38 is up regulated both in female and male PGCs.

The authors were able to recognize four PRDM1 consensus binding site in Dhx38 whole gene body, and using ChIP experiments they showed that the consensus encompassing

exon 11 was directly bound by PRDM1-Prmt5 complex in ED 10.5 PGCs and it coincides with H2A/H4R3me2s and gene repression (Fig 4).

This mechanism seems to be conserved from Drosophila to humans. In fact in D. *melanogaster* Capsuleen protein, which is the homologous to mouse Prmt5, interact with Tudor in germ plasm. Proteins that contain Tudor domain are able to read the covalent modifications imposed by arginine methyltransferases and are expressed also in mammalian germ cells.

Also in seminoma tumors, which are thought to derive from PGCs, the complex between PRDM1, Prmt5 and H2A/H4R3me2s is maintained.

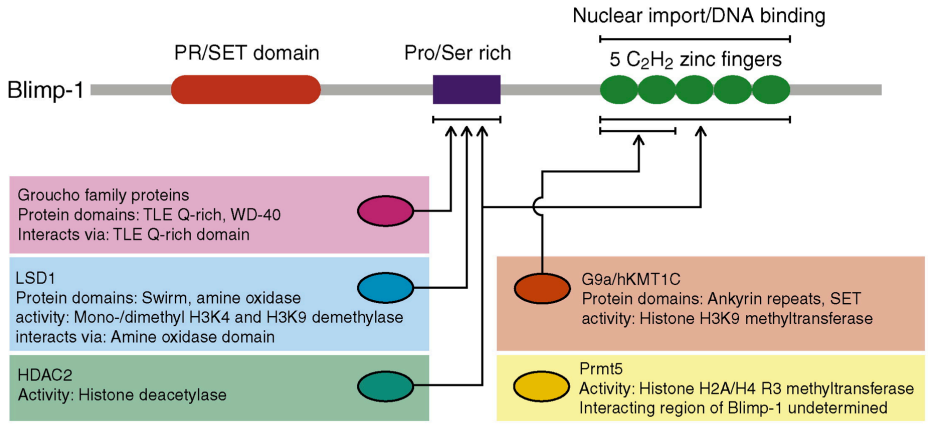

Figure 6. PRDM1 functional domains. Figure adapted from Current Opinion in Genetics & Development 2009, 19:379–385. Domain architecture of PRDM1. PRDM1 serves as a scaffold for the recruitment of co-repressor proteins and enzymes that catalyze histone tail modifications. PRDM1 contains an N-terminal PR/SET domain, a proline/serine rich region and five C-terminal C2H2 zinc fingers. Groucho family co-repressor proteins and LSD1 interact with the proline/serine rich region during plasma cell differentiation. The five C2H2 zinc fingers of PRDM1 mediate nuclear localization, DNA binding but also serve as a binding interface for interacting proteins (G9a and HDAC2 to some extent). The SET domain histone methyltransferase G9a interacts with the first 2 zinc fingers of PRDM1 while HDAC2 displays interacts with both the zinc fingers and proline/serine rich region. PRDM1 interacts also with the arginine methyltransferase Prmt5 for the formation of primordial germ cells (PGC) in mouse.

The specificity of PRDM1 function in B and T lymphocytes corresponds to a divergence in the transcriptional networks that govern the different immunological responses. Hence PRDM1 direct target genes and coregulators are often distinct for each specialized target cell.

Despite different pathways that characterized B and T cells, some functional categories of regulated genes are conserved in the processes of PRDM1 in driving the terminal differentiation of effector cells: in both cases cell metabolism concentrate the efforts for protein production rather than proliferation.

The first category regulated by PRDM1 is the inhibition of both cellular proliferation and survival. In fact, PRDM1 stimulates B cells to differentiate into post-mitotic Ig secreting cells and in T cells it regulates the terminal differentiation of effector cells. This function comprises in B cells the inhibition of c-Myc gene[83], which is a PRDM1 direct target gene[84], and of E2F1[72] other than the inhibition of anti-apoptotic factors. We have already explained the redundancy of PRDM1 and BCL6 reciprocal inhibition in almost all the lymphocytes, but also bcl2a1[85] – an anti-apoptotic member of the Bcl2 family – is down regulated in both the lineages. Even if direct evidences of PRDM1 binding are not provided, it has been demonstrated that bcl2a1 is induced in PRDM1 deficient Th1 cells. This effect may account for the accumulation of $CD4^+$T cells in the periphery since these cells are more resistant to in-vitro cell death after cytokine withdrawal[74]. Finally, the pro-proliferating gene Id3[86] is expressed in the subsets of effectors in which PRDM1 is absent: in germinal center B cells[72], in follicular helper T cells[80] and in PRDM1-deficient $CD8^+$T cells[76]. The repression of Id3 in short-lived effector $CD8^+$T cells has been recently demonstrated to be important for the cells to switch between programmed cell-death and memory phenotype.

The second class of target genes that is functionally important is the induction of the secretory machinery: the Ig for B cells[67] and the cytokines for T cells[87]. In B-cells the genes responsible for protein synthesis and secretion are regulated by Xbp1 gene, which is positively associated with PRDM1 transcription in gene expression profiles of splenic B-cells[88]. Nevertheless the molecular mechanism of such regulation is currently uncertain (maybe dependent on Pax5[89]). In T cells the same mechanism appears much more clear and it involves the repression of IL2 [90-92]. PRDM1 (itself induced by IL2 but with a slow

kinetic[74]) represses IL2 both directly and indirectly by repressing Fos (a part of AP1 activator complex) possibly contributing to regulatory T cell function in vivo.

The last important category that is controlled by PRDM1 in lymphocytes is the repression of the activated effector phenotype: the germinal center B cells and the Th1 cells. Direct targets for silencing the "B-cell program" are: Pax5[93], class II transactivator (CIITA)[94,95] - required for MHC class II expression in antigen presentation - and Spib gene[72]. PRDM1 is also promoting the polarization of Th2 lineage (that has humoral characteristics) opposing the expression of three genes important for Th1 differentiation[75]: INF-γ gene that is directly bound by PRDM1 in a region up-stream to the promoter characterized by H3K4me3 in Th1 and H3K27me3 in Th2 and T-bet gene that is the principal regulator of Th1 sub-population as it rapidly induces IFN γ and BCL6.

Transcriptional regulation of target genes is achieved when PRDM1 binds the DNA via two of its five zinc-fingers [96]. Attached to a specific sequence of DNA – similar to that of interferon regulatory factor (IRF) 1 and IRF2 - it acts as bait, recruiting co-repressors complexes[97] (Fig.6).

PRDM1 represses mouse c-Myc promoter by directly recruiting HDAC1/2[97] through two association domains: one located within residues 557 to 715 and the other located within the proline-rich domain. Histone deacetylation increases the net positive charge of the histones, presumably rendering them more effecting in associating with negatively charged DNA to form a more compacted chromatin structure that results in gene repression[98]. PRDM1 causes a deacetylation of histone H3 in the region of c-Myc promoter and the treatment with HDAC inhibitor tricostatin A abrogate c-Myc repression in co-transfection assay[97].

Subsequently it was demonstrated that PRDM1 is able to bind a heterologous test promoter and to recruit – by a repression domain mapped between 331 and 398 aminoacids – the co-repressor proteins of the Groucho family (in particular hGrg, TLE1 and TLE2). Interestingly the same repression domain was discovered to be necessary for PRDM1

induced apoptosis in immature B-cells[99] and it contains two proline rich sequences highly conserved between human and mouse homolog proteins (hence the same region that mediate HDACs recruitment for c-Myc repression). Moreover, HDAC2 interacts with PRDM1 both indirectly by associating with Groucho proteins and directly through the association with PRDM1 zinc-fingers[97], so PRDM1-HDACs-Groucho might cluster together in repressor complexes (Fig. 6).

The repressive function of PRDM1 was firstly discovered for its capacity to inhibit human IFNβ transcription after viral infection[9]. The mechanism of IFNβ repression requires the binding of PRDM1, which directly recruits the lysine methyltransferase G9a able to silence the target promoter causing H3K9me2 [38]. In this case the methylation of IFNβ promoter is strictly dependent on the functional activity of G9a that is recruited by PRDM1 by using its zinc finger region[38] (even if another work reports the binding also through the proline rich domain[100]).

More recently the histone demethylase LSD1 has been linked to PRDM1-mediated target repression in plasmacell. In fact, it has been demonstrated that they interact through the proline rich domain and that they colocalize in the nucleus and in the binding region of the target promoter (CIITA). LSD1 depletion leads to a decrease of IgM secretion and to an increase of H3 acetylation, H3K4me2 and H3K4me3 levels in CIITA promoter determining gene derepression[100]. Nonetheless LSD1 knockdown did not affect H3K9me2 level suggesting that more factors can act in concert to establish dynamic repressive machinery orchestrated by PRDM1 in the B-cell epigenetic program (Fig. 6).

1.2.4 PRDM1 in neural development

PRDM1 homolog has been extensively studied in zebrafish[45,101] where it localizes in the areas of the developing forebrain - the leading anterior mesendoderm and prechordal plate – other than in a variety of other tissue precursors: slow muscle precursor cells; otic vesicle; the branchial arches and unidentified cells of the central nervous system.

In particular, PRDM1 during zebrafish development gradually distributes in the signalling centres of neural commitment and at midgastrulation its expression marks the boundary between neural and non-neural ectoderm[101,102]. Here it plays an important role for the specification of different cell types such as neural crest (NC) cells, Rohon-Beard (RB) sensory neurons and the neural crest derived craniofacial skeletal elements.

In vertebrates, NC cells are a transient embryonic population that arises from the dorso-lateral edge of the neural plate and migrates to differentiate into different specialized nervous cells (neurons, glia of the peripheral nervous system, melanocytes, cartilage and bones of the face). Critical transcription factors induced signalling (belonging to BMP, Wnt and FGF families) between the neural and non neural ectoderm are needed for cell fate acquisition[103]. From the same region also RB non-migrating sensory neurons originate and in the dorsal spinal cord they mediate the mechanosensory touch response and remain in the central nervous system[104].

In zebrafish, the specification of different cell types seems to be governed by BMP gradient along the embryo that induces PRDM1 expression in different cell compartments at the neural plate border[105-108]. Different studies have defined that PRDM1 is involved in the development of both NC cells and RB neurons[109,110]. In particular PRDM1 is transiently expressed in the cells at the neural plate border from where NC cells and RB neurons arise but not in the developing cells. Genetic screenings of ethylnitrosourea (ENU) mutagenized zebrafish identified two similar phenotypes associated with PRDM1 impairments: the u boot^{trp39} (ubo) and the nrd^{m805} narrowminded (nrd). The major abnormalities observed in ubo affect the differentiation of myoblasts into slow muscle fibres[111,112], the formation of pectoral fins[113] – the equivalent of vertebrate forelimbs – and the specification of neuronal precursors[109]. The origin of these defects was determined by two point mutations in PRDM1 ortholog, which impair the DNA binding ability of the protein. The Ubo mutants display a reduction in the levels of *sna2* – a marker of pre-migratory NC cells – and later on, they show developmental impairment in the

specification of NC derivatives: the cells of the cranial trigeminal ganglia (NC origin) were smaller and unable to specify in the correct ganglia neurons, the dorsal root ganglia - composed by sensory neurons (NC origin) normally organized in ordered segments along the spinal cord - was also defective; and finally the mutants have a reduced number of melanocytes (NC origin). Also RB sensory neurons fail to specify.

Interestingly the ectopic expression of PRDM1 mRNA into the fertilized eggs of mutant embryos did not rescue completely the phenotype, which resulted in a supernumerary RB cells, without any significant change in the NC numbers. This observation helps in defining the pathway of neural specification in zebrafish, where PRDM1 ortholog, after BMP signalling, is required for the commitment of neural progenitor cells (of both NC cells and RB neurons) that by default differentiate into RB sensory neurons and that only in the presence of a correct notch-delta signalling are able to specify also in NC cells.

At the same time another group identified the narrowminded (nrd) mutant zebrafish in which neurogenesis and neural crest formation were affected[110]. Also in this case a point mutation hits PRDM1 ortholog, causing a null product completely lacking the zinc fingers domain. The mutant nrd failed to form RB sensory neurons while NC cells were present early during embryogenesis but then compromised in the ability to differentiate in NC derivatives. Contrary to what observed in the previous work, this time the authors were able to phenocopying nrd defects by using morpholino depletion and to rescue the phenotype by using misexpression of PRDM1. This discrepancy is attributed to the different effects of the mutations occurred. In fact, nrd appears to be a null allele, while ubo is more likely a hypomorfic allele with a less severe phenotype. These experiments suggest also that different PRDM1 levels - from BMP signalling - are needed for specifying RB sensory neurons (low levels) and NC cells (high levels).

A more detailed view of PRDM1 in the nascent lateral border of the embryo would be needed to understand if NC cells and RB sensory neurons are really arising from the same

PRDM1-positive precursors or if NC cells are initially responding to PRDM1-independent signals.

PRDM1 expression has been found also in the neural plate of Xenopus embryos[114] showing many analogies with zebrafish neural development.

1.3. Mammalian neurogenesis

Since our data drove the development of experimental efforts for dissecting the role of PRDM1 during adult brain homeostasis, we will briefly introduce some background notions about neurogenesis during development and in adult organisms.

During embryogenesis a portion of the ectoderm specifies to become neural ectoderm. This region of the embryo is called neural plate and will form the neural tube from which brain and spinal cord (the components of the central nervous system) originate.

In the developing cerebral cortex, the original neural tube is lined by a ventricular zone, composed of a single layer of rapidly dividing neural stem cells called neuroepithelium (also known as germinal epithelium). The pseudostratified appearance of the neuroepithelium is due to the so-called "nuclear migration" of the neural precursors - rapidly dividing stem cells – that extend from the apical to the basal surface of the cortex, but have nuclei at different height accordingly with the cell-cycle phase in which they are.

Around ED 9-10 neuroephitelial cells start to acquire features of glial cells (they are called radial glial cells): they are lengthening the radial processes along with the thickening of the cortex and they begin to express astroglial markers such as astrocyte-specific glutamate transporter (GLAST), brain lipid-binding protein (BLBP), Tenascin C (TN-C), intermediate filament proteins (nestin, vimentin) and glial fibrillary acidic protein (GFAP). Moreover these neuroephitelial cells begin to make astrocyte-like specialized contact with endothelial cells of the developing growing vasculature.

It is now widely accepted that these glial cells are effectively the neural stem cells that undergo distinct mode of cell division in order to generate all the cell types that constitute the central nervous system (CNS). From this point onward the cells proliferate

asymmetrically to maintain the undifferentiated population – that remain in the ventricular zone - and to produce a more committed daughter cell that could be a post mitotic neuron, which migrates radially, or an intermediate progenitor with more restricted developmental potential that populate the embryonic sub-ventricular zone. Consequently during embryogenesis radial glia can either work as scaffold of fibers for migrating neurons or can itself divide and translocate to the cortical plate and differentiate in more specialized cell-types.

After birth the majority of radial glial cells convert into astrocytes, while a small population maintain the contact with the ventricular surface and continue to function as neural stem cell in the neonate.

In the last decades, it has been demonstrated that neurogenesis persists also in postnatal and adult brains in two different districts: the subventricular zone (SVZ) in the walls of the lateral ventricles and in the subgranular zone (SGZ) of the dentate gyrus of the hippocampus[115-117]. More recently a large number of proliferating cells have been found also in the region between the hippocampus and the corpus callosum[118]. The major contribution to the field has been done by the usage of bromodeoxyuridine (BrdU), a nucleotide analog, as a lineage tracer through which continuous neurogenesis has been visualized in mammals, including humans[117,119].

The SVZ contains quiescent neural stem cells - also known as B cells - that resemble radial glial properties (retain apical-basal polarity and are part of the ventricular epithelium) and that can give rise to actively-dividing progenitor cells (called C cells), which in turn differentiate in neuroblasts (A cells). These neuroblasts migrate along the rostral migratory stream (RMS) to the olfactory bulb (OB) through chain migration and differentiate into local interneurons with specialized functions in olfaction.

The SGZ instead produce neurons with specialized function for learning and memory. It contains quiescent neural stem cells that divide asymmetrically to generate more

committed progenitor cells (type 2 cell), [120]which in turn differentiate into glutamatergic dentate granule cells[121].

Neural stem cells (NSCs) can be separated from the other neural components and cultured in-vitro by using the neurosphere assay[122,123], which consists in the continuous exposure of neural cells to mitogens in a serum-free medium. These conditions – adopted also for non-neural tissues such as the mammary epithelium and the cardiac muscle[123] - ensure that only neural stem cells and undifferentiated progenitors will be able to proliferate in-vitro whereas all the other cell populations will extinguish in culture. The proliferating cells detach from the plate and form a sphere, which contain only a small fraction (10-50%) of neural stem cells while the rest undergoes spontaneous differentiation. Repeated cycles of spheres dissociation and replating ensure a progressive enrichment and expansion of the neural stem cells in culture, decreasing the presence of nonstem progenitors that have limited replication ability.

The direct isolation of neural stem cells from fresh tissues through the identification of specific cell surface markers and fluorescence-activated cell sorting (FACS) has also been intensively investigated. The surface antigen CD133 – a five-transmembrane protein also known as prominin-1 – is a marker for neuroepithelial cells other than other adult stem cells (hematopoietic, liver)[124,125]. Mouse and human fetal brain NSCs isolated with antibodies against CD133 are able to self-renew and to differentiate into neural cell types[126,127]. Other antigens used to separate NSC and radial glia from more differentiated cells were: the carbohydrate moiety CD15 (also known as stage-specific embryonic antigen – SSEA1 – or LeX) alone[128,129] or in combination with CD184 (a G protein-coupled receptor)[108], and CD24, a cell adhesion molecule[130]. In addition, NSCs and neural progenitors have been isolated from dissociated human brain cells by using genetic promoter-reporters of NSC specific markers[131,132] Anyway selective markers to discriminate neural stem from neural progenitor cells are still missing.

In normal conditions adult neurogenesis is restricted to neurogenic areas in response to physiological and pharmacological stimuli. Alternatively different kind of injuries may activate adult neurogenesis like psychiatric diseases, stroke, neurodegenerative disorders and cancer. Therefore understanding the mechanisms of NSCs self renewal and differentiation is extremely important since they can be used in clinics to treat impaired tissues.

Autocrine and paracrine impulses activate intricate signalling pathways, characterized by the expression of specific transcription factors, under which NSCs are able to proliferate or to become a specialized cell of the CNS. Four networks are mainly involved in self-renewal and differentiation of NSCs: a) the Notch signalling; b) the Wnt/β-catenin pathway; c) Sonic hedgehog-Gli signalling and d) growth factors (FGF and EGF) signalling.

Moreover embryonic and adult NSCs are characterized by the expression of SOXB1 factors (Sox1, Sox2, Sox3). In fact, it has been demonstrated that SOXB1 mutants have defects in brain development[133-135] and, both in-vivo and in-vitro, Sox2 and Sox3 expression correlate with proliferating cells [136,137]. Also, BMI-1, a polycomb family transcriptional repressor is fundamental for the maintenance of NSCs and progenitors by silencing the cyclin-dependent kinase inhibitors - p16Ink4 and p19Arf - and p21-Rb pathway[138,139]. The pathway that is mainly involved in NSC maintenance and proliferation is the Shh-Gli signalling pathway and its direct effectors Gli-1, Gli-2 and Gli-3 [140].

Conversely Notch and Wnt signalling pathways are involved both in neurogenesis and in differentiation signals. The activation of Notch cascade determines the induction of diverse effectors (Hes1, Hes5, C-promoter binding factor1 (CBF1/RBP-J) and Musashi-1) that are involved in self renewal activity in both embryonic and adult stem cells. Following the interaction between Notch and its ligands (Delta and Jagged), the intracellular domain of Notch translocate to the nucleus where it complexes with CBF1/RBP-J and activates Hes1 and Hes5 that inhibit neural differentiation of NSCs during development[141,142].

Moreover Musashi-1 reinforces the effect of Notch signalling by inhibiting its target mNumb[143]. Nonetheless Notch can also trigger the progression of neurogenesis. In fact, if expressed at low levels, Notch is able to up regulate the basic Helix-Loop-Helix (bHLH) factors such as Neurogenin2 (NGN2) and Mammalian achaetescute homolog1 (MASH1) that promote neuronal differentiation[144].

The Wnt signalling pathway has been demonstrated to be relevant both in hippocampal and olfactory bulb neurogenesis and to promote the proliferation of adult NSCs[145]. However the Wnt signalling is able also to activate NeuroD1, a pro-neurogenic basic helix-loop-helix (bHLH) transcription factor, required for the formation of neurons[146].

The early differentiation of NSCs is triggered by lineage-determinant transcription factors that make the cells to commit through a more differentiated progenitor and to loose multipotency.

The forced expression of mammalian achetescute homologue (MASH1) in neural crest stem cells induces morphological differentiation and expression of neuronal markers[147,148] such as anti-proliferative transcription factors (PHOX2a and cycline-dependent kynase inhibitor p27) and pro-neuronal proteins (Neurogenin-1 and NeuroD)[148,149].

Again, PAX6 activates a cascade of factors that are negative regulators of the cell cycle and promoters of the neural cell-fate such as NGN2, which in turn represses SOXB1 group while it up-regulates HES6.2 a repressor of the Notch signalling[150,151]. NGN1, another important pro-neuronal factor, makes the progenitor cells to escape from the differentiation in other lineages by sequestering a CREB binding complex, called mothers against decapentaplegic homolog 1 (CBP-SMAD1), from the promoters of astrocytes promoting genes and by inhibiting signal transducer and activator of transcription-3 (STAT3) necessary for gliogenesis[152]. STAT3 and SMAD1 instead are the up stream signalling factors[153,154] that activate the transcriptional expression of glial proteins such as (GFAP), OLIG-1 and OLIG-2[154].

Beside the well characterized pathways, many others remain to be elucidated. Quite recently it has been assessed that different members of the PRDM family are expressed in diverse areas of the developing mammalian brain and are regulated by the Notch signalling[155]. In particular PRDM8 was shown to be associated with Notch-Hes signalling down regulation in post-mitotic neurons while PRDM16 rapidly increased together with Notch-Hes stimulus in neuronal progenitor cells. Since in zebrafish PRDM1 homolog enable Notch-bHLH signalling to specify primary sensory neurons and that its expression has not been evaluated in adult mouse brain, we cannot rule out the possibility that PRDM1 might control neurogenesis also in complex organism and this study argues in favour of this hypothesis.

1.4. PRDM1 in tumors

PRDMs also play a role in human cancer, where they have been mainly characterized as tumor suppressor genes[156].

In tumors different mechanisms, other than gene inactivation and protein stability can interfere with PRDM protein function. Remarkably, both transcriptional repression ability and tumor suppressor role of various PRDM proteins, rely on an intact PR/SET domain[12,157,158] and, in human tumors, naturally occurring truncated isoforms of some of the PRDM gene family proteins have been identified so far, in which the PR domain is disrupted[159,160].

However, although the expression of these alternative isoforms has been linked to oncogenesis of multiple tumor types, the function of the PR domain has not been clearly defined[161,162].

Evidence exists for PRDM1 to act as a putative tumor suppressor: a) PRDM1 directly represses c-Myc, which is frequently de-regulated in B cell tumors[83]; b) the ectopic expression of PRDM1 is toxic in multiple cell types leading to apoptosis in lymphoma cell lines[99]; c) the genomic region where PRDM1 gene resides – on chromosome 6q21-22.1 – is frequently deleted in several tumors including in B cell lymphomas [65] and d) PRDM1 is

mainly known as a transcriptional repressor interacting with different co-repressor proteins such as G9a, HDAC2, PRMT5 and LSD1[163].

Indeed, experimental indications agreed with the idea that PRDM1 is a candidate tumor suppressor at least in diffuse large B cell lymphoma (DLBCL).

DLBCL, the most common subtype of non-Hodgkin's lymphoma, is a genetically and clinically heterogeneous disease that - based on gene expression profiling - has been classified into three different subsets which resemble the different stages of B cells differentiation: the germinal center B cell-like (GCB) DLBCL; the activated B cell-like (ABC) DLBCL and primary mediastinal large B cell-like lymphomas[164].

The attempt to identify new genetic lesions that characterize the different sub-types of diffuse large B cell lymphoma (DLBCL) brought to the identification of diverse inactivating mutations (in both the alleles) in PRDM1 gene. In particular, PRDM1 mutations were confined to the ABC subtype in 24% of the cases[165,166] and in the 77% of ABC-DLBCLs PRDM1 protein was not expressed at all, suggesting an alternative mechanism – other than mutations – of protein inactivation.[65]. The spectrum of the identified mutations in PRDM1 was very variegated ranging from point mutations (nonsense, missense, splicing aberrations) to large intra-chromosomal rearrangements while no mutations were found in GCB DLBCL subtype.

Furthermore, ABC-DLBCL displays a constitutive active NF-kB pathway necessary for survival and resistance to chemotherapy treatment[167-169] and it is the most aggressive type of DLBCL with poor clinical prognosis.

Recently two studies[170,171] definitely demonstrate that PRDM1 is a tumor suppressor in the development of ABC-like DLBCL and highlighted the interplay between PRDM1 and NF-kB pathways during the pathogenesis.

The authors analyzed diverse DLBCLs in which they identified a group of missense mutations affecting the stability and the function of PRDM1 other than cases of epigenetic silencing when BCL6 was co-expressed.

Furthermore, in two mouse models of PRDM1 conditional KO (in B cells or restricted to GC cells) there was an increased incidence of lymphoproliferative disease and of DLBCL with constitutively active NF-kB pathway, resembling the human ABC-DLBCL phenotype[170].

In another work, using a more sophisticated mouse model that combines NF-kB activation with PRDM1 inactivation, Calado and co-workers showed that the two altered pathways cooperate in the development of lymphoma[171]. This last observation is even more interesting from a therapeutic point of view: in fact the standard treatment CHOP (cyclophosphamide, doxorubicin, vincristine and prednisone) is ineffective for half of the patients that develop DLBCL (and in particular ABC-DLBCL). It has been demonstrated that some chemotherapy resistant B cell lymphoma cell lines express a shorter isoform of PRDM1, also known as PRDM1β. The treatment of resistant cell lines with rituximab and doxorubicin decreases both PRDM1β level and the phosphorylated form of NF-kB. In addition the treatment with NF-kB signal inhibitors down regulate PRDM1β and affect cell growth. These observations suggested that NF-kB in this tumors regulates PRDM1β levels and open new perspectives in the diagnosis and the treatment of these tumors[172].

As mentioned above, some of the PRDM genes generate more than one isoform: the full-length product and an alternative product that lacks the PR domain but is otherwise identical for the rest of the protein. Interestingly, the different products behave in a so-called "yin-yang" fashion where the full-length proteins participate in tumor suppression and cell cycle arrest, while a high relative expression of the isoform missing the PR domain is linked to oncogenesis[173].

The shorter product of PRDM1 (referred as PRDM1β, while the full length is PRDM1α) was identified as a transcript highly expressed in human myeloma cell lines, starting from a single novel exon upstream of the exon 4 of PRDM1 gene and in frame with the rest of the protein. Consequently the relative protein retains the DNA binding ability but completely lacks the amino terminal 101 aminoacids containing the PR domain (Fig.7) [160].

In a luciferase reporter assay PRDM1β showed weak repressive ability towards the heterologous promoter even if it was functionally able to recruit HDACs. Recently it has been demonstrated that the loss of PRDM1β promoter methylation is frequent in B lymphoma cell lines and in primary DLBCL[174] and might account for the unbalanced PRDM1α/PRDM1β ratio in tumors compared with normal plasmacell.

Immunocytochemical staining for PRDM1 and tissue microarray analysis reported PRDM1 expression also in other B cells neoplsms – like lymphoplasmacytic lymphoma, plasmablastic lymphoma and oral mucosa lymphoma – as well as in T-cell lymphomas. Moreover this study showed a subset non-ABC DLBCL co-expressing PRDM1 and BCL6 (independently from IRF4 expression) and correlated with worst prognosis[175]. Despite in this last article the authors presented a consistent collection of healthy and pathological samples they did not consider a differential expression between PRDM1α and PRDM1β and in general PRDM1 protein functionality[176].

In T-cell malignancies, like for DLBCL, it has been found a relationship between PRDM1β expression and chemotherapy resistance. The treatment of PRDM1β expressing resistant cells with the proteosome inhibitor bortezomid blocks NF-kB transcription and contemporary decreases PRDM1β, IRF4 and c-myc expression that regulate T-cell transformations. Also in this case PRDM1β expression could be related to NF-kB pathway and it might suggest new ways of treatment[175].

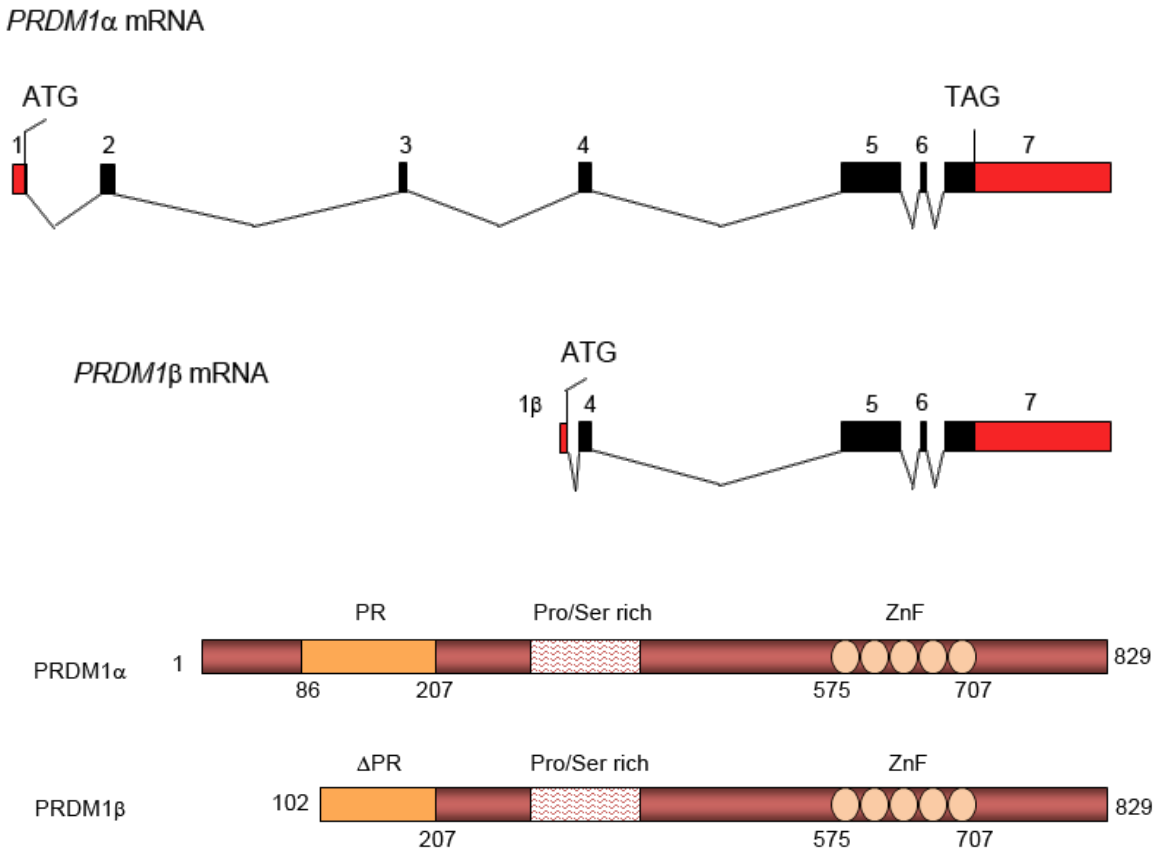

Figure 7. PRDM1 human gene. (Top) The gene encompasses 23,6 kb DNA in humans, from 106534195 to 106557814 (hg19-Feb, 2009) in the long arm of chromosome 6. It encodes 7 exons. The open reading frame spans all 7 exons. The mRNAs encoded by PRDM1 have two transcript isoforms, PRDM1alpha and PRDM1beta, which are 5164 and 4675 bp long, respectively. The shorter isoform is generated by usage of the alternative promoter located in intron 3 and contains a different 5' untranslated region. It lacks the 5' in frame portion of the coding region present in PRDM1alpha.
(Bottom) PRDM1α is the larger isoform and contains 825 amino acids. It has a PR domain at the N-terminal portion (86-207 aa) of the protein, which is related to the SET domain found in many histone methyltransferases. In contrast to bona fide SET-domain proteins, the PR domain in PRDM1 does not possess intrinsic histone methyltransferase activity. Five C2H2-type zinc fingers which represent the DNA binding domain, are present at the C-terminal portion of the protein (575-707 aa). The middle part of PRDM1 (about 300-400 aa) is rich in proline and serine. PRDM1β lacks the N-terminal 101 amino acids of the PRDM1alpha, and has a truncated PR domain. PRDM1β has been shown to be functionally impaired in its transcriptional repression activity (Gyory et al., 2003). The proximal 3 zinc fingers in PRDM1/Blimp-1 delta exon 6 variant are disrupted (Schmidt et al., 2008).

5. Glioblatoma multiforme

Our initial data indicated that PRDM1 is expressed not only in early neural progenitors of adult brain but also in the most common adult brain tumor, the glioblastoma multiforme (GBM). The observed evidence turned our attention on a previously unidentified role of PRDM1 in normal brain homeostasis and in its aberrant counterpart. Consequently we consider worthwhile to mention some important aspects of high-grade gliomas.

The high-grade glial tumor GBM is the most common and aggressive – with a median survival of 14 months after diagnosis - brain tumor in adulthood. Morphologically it represents a heterogeneous collection of distinct diseases comprising astrocytic, oligodendroglial and mixed neoplasms[177] whereas histologically GBM is designated as a grade IV high grade glioma (with necrosis and microvascular proliferation) according to the world health organization (WHO) classification[178]. The majority of GBMs are primary lesions, while a minority of them can arise from a previous lower-grade tumor and they are called secondary GBMs[179,180].

Glioblastoma multiforme (GBM) comprises also a fraction of cells with similar characteristics of neural stem cells. Increasing evidence supports the hypothesis that GBMs arise from the transformation of neural stem cells residing in the SVZ.

Infact, high-grade gliomas can be generated when the appropriate genetic lesion are directed in either neural progenitor or glial cell types[181-183]. There is a large consensus, however, on neural stem and progenitor cells representing a likely candidate for the origin of human gliomas[184], in spite of difficulties in retrospectively determining if human gliomas originated from a differentiated cell (astrocytes or oligodendrocytes) that acquired trans-differentiation abilities (necessary to generate and maintain glioma cell-type heterogeneity) or if common glial progenitors had overcome anti-proliferative restrictions. However the cell of origin of human gliomas is under debate and the generation of mouse models recapitulating human pathogenesis will help in clarifying this issue.

In the last few years the improvement of high-throughput sequencing technologies contributed to the identification of the critical pathways involved in the pathogenesis of GBMs (Fig. 6). The major effort has been done by The Cancer Genome Atlas (TCGA) which create a collection of data that helped in classifying different tumors - histopathologically indistinguishable – on the basis of their molecular profile[185-188] (http://tcga-data.nci.nih.gov/). Moreover new bioinformatic tools have been developed in

order to integrate genomic, expression and epigenetic data and identify different classes of GBMs on the basis of overlapping features[188,189].

The pathogenesis of GBM involves the inactivation of tumor suppressive pathways (p53 and Rb) and the oncogenic activation of receptor kinase pathways, which result in uncontrolled cell proliferation, invasion and angiogenesis (Fig. 8). The activation of signalling pathways might be achieved at different levels: a) through the overexpression of cell growing stimuli (PDGF, bFGF, FGF2, EGF, TGFα and IGF1) and of their receptors (EGFR, ERBB2, PDGFRA, MET), b) trough the deletion of negative regulators of the signalling pathways (PTEN, NF1) and c) by mutations that results in constitutively active receptors (such as EGFRvIII).

According with the TCGA classification, four GBM classes have been recognized to possess distinct molecular subtypes: proneural, classical, mesenchymal and neural [183,190].

Proneural GBMs are characterized by a transcriptional profile similar to that of neural development and they are frequently occurring in younger patients. The genes more frequently activated in proneural subtype comprise factors important for oligodendrocytic (PDGFRA, OLIG2, TCF3, NKX2-2) and neural (SOX, DCX, DLL3, ASCL1 and TCF4) differentiation. Recently also the mutation of isocitrate dehydrogenase 1 (IDH1) and to a lesser extent of IDH2 has been identified in some proneural tumors as well as in other lower grade gliomas and secondary GBMs. The gene is mutated, only in one single copy, in the active site for substrate recognition, determining an aminoacid sobstitution (R132H) that is responsible for a gain of function event. In fact, the mutated copy acquired a higher affinity for α-ketoglutarate which is converted, with a NADPH dependent reduction, into R(-)-2-hydroxyglutarate (2-HG). This metabolite alters many functions of the cell such as hypoxic sensing, demethylation and fatty acid metabolism, which determine a characteristic cell expression profiling. The identification of IDH1 related mutation had important implications for diagnosis since it was seen to correlate with better prognosis.

Therefore it represents a good example of how clinics and molecular medicine have to be integrated in order to stratify patients that will receive more focused treatments[191].

Highly proliferative cells and major chromosomal losses or amplifications are the principal characteristics of classical GBMs. In particular gain of chromosome 7, and losses of chromosomes 10 and 9p21.3 determine EGFR amplification and the deletion of PTEN and CDKN2A respectively. Transcriptionally these tumors resemble neural precursors and stem cells expression such as activated Notch and Sonic hedgehog signalling pathways. Classical GBMs derived the name for the property they have to respond to classical radiotherapy since p53 pathway is not perturbed.

Mesenchymal subtype shows frequently mutated NF1, p53 and CDKN2A. Furthermore two recent studies went more into the details of the mesenchymal transcriptional program[188,189]. In the first study[188] combining computational analysis and targeted functional assay the authors identified two transcription factors (C/EBPβ and STAT3) as the master regulators of the genetic regulatory networks that initiate and maintain the malignant and aggressive state of the mesenchymal subtype. Togheter with these two major players other four transcription factors – RUNX1, FOSL, bHLH-B2 and ZNF-238 – control the entire signature. In the second study[189] the HIPPO pathway transducer TAZ was seen to co-segregate with mesenchymal GBMs while to be epigenetically silenced in other lower-grade gliomas. In addition TAZ was seen to augmente the grade and the penetrance of a mouse model of high-grade glioma.

Finally neural subtype strictly separates form the others but none alteration is particularly enriched and it is characterized by the expression of neuronal markers (NEFL, GABRA1, SYT1 and SLC12A5).

This complex characterization might also contribute to the improvement of current therapies since standard treatment protocols have remained relatively unchanged and involve aggressive radio- and chemo-therapeutic treatment following surgery[192]. Also prognosis might take advantage of this database by identifying single molecules that

follow the histology. At the moment the prognostic markers are confined to IDH mutation that we mentioned before[181], the methylation status of the DNA repair enzyme O6-methylguanine-DNA methyltransferase (MGMT) that is predictive of sensitivity to alkylating chemotherapy[193,194] and of progression incidence[195], and finally the 1p/19q co-deletion in oligodendroglioma[196].

Additional studies will clarify glioblastoma biology integrating genomic studies, animal models of disease and careful study of the human tissue.

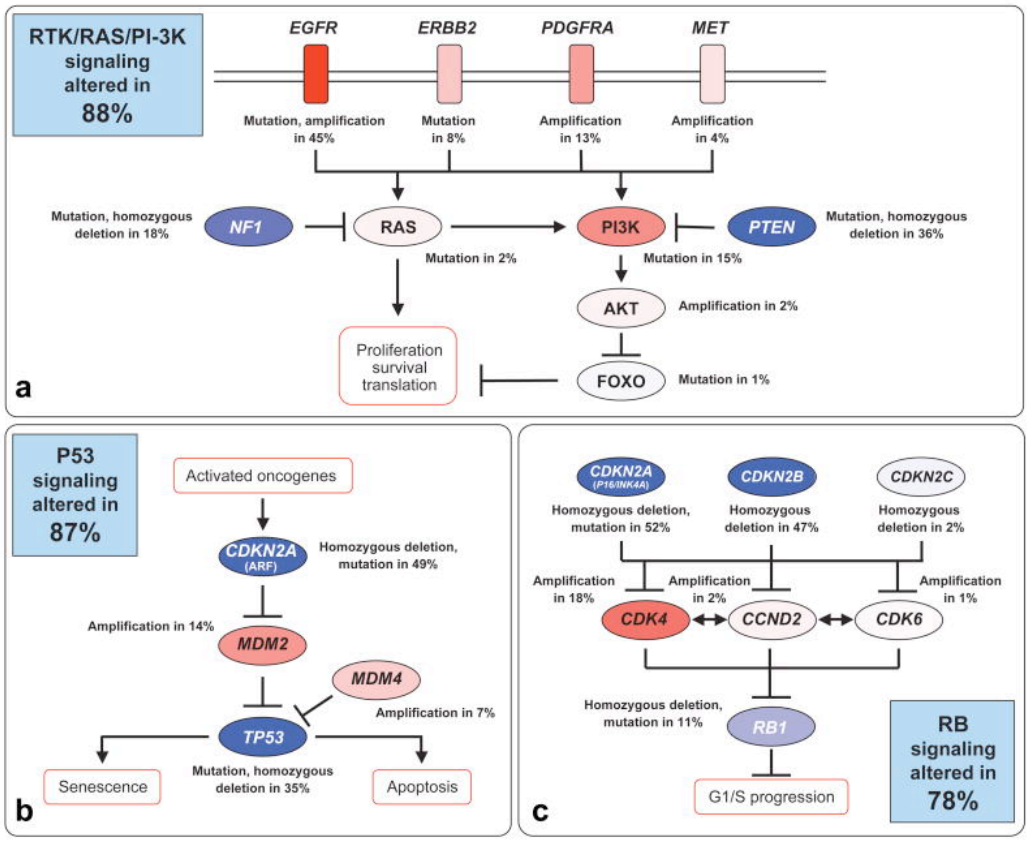

Figure 8. **Aberrantly signaling pathways in GBM.** Figure adapted from Nature 2008 Oct 23;455(7216):1061-8. The Cancer Genome Atlas (TCGA) Network has recently released an integrated analysis of genomic and transcriptomic data in order to delineate the molecular profile of human Glioblastoma multiforme (GBM). These studies revealed a number of recurrent mutations that involve different signaling networks. Herein the primary sequence alterations and amplifications of a) RTK/Ras/PI(3)K, b) p53 and c) signaling pathways are shown. Red indicates activating genetic alterations, with frequently altered genes showing deeper shades of red. Conversely, blue indicates inactivating alterations, with darker shades corresponding to a higher percentage of alteration. For each altered component of a particular pathway, the nature of the alteration and the percentage of tumours affected are indicated. Boxes contain the final percentages of glioblastomas with alterations in at least one known component gene of the designated pathway.

Chapter 2 - MATERIALS AND METHODS

2.1 Isolation and culture of mouse sub-ventricular stem cells

The brain form mouse was removed and placed in PBS with penicillin and streptomycin (0.1 mg/ml). The tissue corresponding to the periventricular region (SVZ) was dissected and incubated in Earl's balanced salt solution (EBSS) containing papain (1 mg/ml), EDTA (0.2 mg/ml) and cystein (0.2 mg/ml) at 37°C for 1 hour. The disgregated tissue was collected by centrifugation at 200 g for 10 minutes and resuspended in 1 ml of NEC medium and plated in uncoated flask at a concentration of 8x103 cells/cm2. NEC medium contains: Neurocult NS-A Basal medium (Stem Cell Technology), 10% proliferation supplement (Stem Cell Technology), 2 μg/ml heparin, (Sigma) 10 ng/ml hFGF (PrepoTech), 20 ng/ml hEGF (Prepotech). When neurospheres reached approximately 300-500 microns in diameter were passaged harvesting them by centrifugation (200 g per 10 minutes) and triturating in 200 μl of medium with automatic pipette.

2.2 Cell culture

Ntera2-D1 were grown in Dulbecco's Modified Eagle Medium (DMEM) supplemented with 10% FBS, 2mM glutamine and 1% penicillin/streptomycin, passed every 2-3 days with 0.005% trypsin-EDTA for the efficient expansion of the cell line. To induce differentiation cultures were treated with 10 μM of all-trans-retinoic acid (ATRA R2625, Sigma-Aldrich company), supplemented every 48 hours.

Murine E14Tg2a embryonic stem cells (ESCs) were grown without feeders in standars ES medium supplemented with b-mercaptoethanol 14.3 mM (GIBCO), LIF 1000 U/mL (Chemicon) and 2i [1uM MEK – PD0325901 (Cayman chemicals) and 3uM GSK3 – CHIR99021 (Axon biochemicals)]. The cells were incubated at 37°C in a humidified 5% CO2 incubator.

Pelicci G. group kindly provided cancer stem cells lysates derived from human glioblastoma tumors. The samples were collected accordingly with the Ethical Committee

for human experimentation of IEO (European Institute of Oncology) and all patients signed and approved consent document prior to surgery.

2.3 Quantitative real time (RT) PCR

Total RNA was prepared from 1x106 cells using RNAeasy Kit (Qiagen) following manufacturer's instructions. Total RNA was used for first strand cDNA synthesis using random primers and M-MuLV reverse transcripase (Finnzymes) according with manufacturers' instructions.

Each SYBR green reaction was performed in 20 µl containing 10 µl of 2x SYBR green master mix (Applied Biosystem), 1 µl of 0.5 µM primer mix and 8 ng of cDNA. Oligos were designed at the boundary of exon-intron to avoid amplification of genomic DNA.

The PCR reaction was run on HT9700 PCR machine with the following cycling parameters: 1 cycle at 50°C for 2 min, 1 cycle at 95°C for 10 min followed by 40 cycles where the temperature ramp from 95°C to 60°C in 1min. Each sample was run in duplicate. The mean value of the replicates for each sample was calculated and expressed as cycle treshold (CT: cycle number at which each PCR reaction reaches a threshold, set within the linear range of all reactions). For each sample, the CT value of the endogenous control (GAPDH) was subtracted to the CT value of the target gene (ΔCt) to obtain comparable values. Then, the relative amount of gene expression is calculated as the difference (ΔΔCt) between the ΔCt of the test sample and of the control sample. Finally, the relative expression is expressed as $2^{-\Delta\Delta Ct}$.

2.4 RNA-sequencing

After quality control, mRNA was processed following the standard Solexa protocol recommended for mRNA sequencing. Paired-end 50bp-reads were aligned to the mm9 reference genome and to the Mus Musculus transcriptome (Ensembl build 63, Flicek et al. 2012) using TopHat 1.3.1 (Trapnell et al. 2009). We allowed up to two mismatches and specified a mean distance between pairs (-r) of 120 bp.

Transcripts abundances were quantified using Cufflinks 1.2.1 (Trapnell et al. 2010). Differentially expressed genes were called using Cuffdiff 1.2.1 (Trapnell et al. 2010). For the next steps of the analyses we considered the quantifications at the level of single genes. Genes showing an FPKM (fragments per kilobase of exon per million fragments mapped) equal or higher than one in at least one sample were retained. Differentially expressed genes were defined using an FDR <= 0.05 and no threshold on the fold change. For transcript quantification we used options –N (upper-quartile normalization) and -u.

Tracks for the UCSC genome browser (Fujita et al. 2011) were generated considering only the uniquely alignable fraction of the total reads. Tracks were linearly re-scaled to the same sequencing depth.

2.5 Chromatin Immunoprecipitation (ChIP) – sequencing and ChIP-qPCR

For ChIP cells were fixed on the bulk with 1% formaldehyde in PBS. Cross-linking was allowed to continue for 10 minutes at 37°C and stopped by addition of glycine (0.125 M as final concentration) followed by an additional incubation of 5 minutes. Fixed cells were washed twice with PBS and then lysed in SDS Buffer (50 mM Tris pH 8.1, 0.5% SDS, 100 mM NaCl, 5mM EDTA and protease inhibitors). Cells were pelleted by centrifugation and resuspended in 5 ml of IP Buffer (100 mM Tris pH 8.6, 0.3% SDS, 1.7% Triton X-100, 5 mM EDTA). Cells were disrupted by 12-15 pulses (30 seconds each) of sonication with a tapered J-microtip (6.5 mm) in a Branson digital sonifier 250D, at a power setting of 50%, yelding genomic DNA fragments with a bulk size of 200-500 bp. For each immunoprecipitation, 1 ml of diluted lysate (15x106 cells/ml) was precleared by addition of 50 µl of blocked protein A beads (50% slurry protein A- Sepharose from Amersham; 0.5 mg/ml fatty acid free BSA, Sigma). Samples were immunoprecipitated at 4°C with magnetic dynabeads protein G and A (Invitrogen) mix 1:4 previously saturated with two different antibodies specific for PRDM1 (anti-PRDM1 polyclonal rabbit serum got from Surani lab and BLIMP-1/PRDI-BF1 (C14A4) rabbit mAb #9115) or with normal rabbit IgG (Santa Cruz Biotechnology sc-2027). Beads were washed and crosslink was reversed

with Elution Buffer (1% of SDS, NaHCO3 0.1M and proteinase K) overnight at 65°C and the DNA was directly used for quantitative PCR or quantified with picogreen for sequencing. We tried to improve ChIP experiment performing a repeated cycle of immunoprecipitations. Basically following the over-night immunoprecipitation with the first antibody we collected the unbound fraction and we used it for a second-round IP with the other antibody (two different sequential IP were done exchanging antibodies order). In this way we increased the probability to sequester PRDM1-chromatin complexes reaching different protein epitopes that may be masked by fixing the cells and finally obtaining a reasonable DNA amount for sequencing purposes.

Raw 36bp-reads were aligned to the hg18 genome using Bowtie 0.12.7 (Langmead et al 2009). All the reads with a unique match to the genome with two or fewer mismatches (-m 1 –v 2) were retained. Peak calling was performed against input DNA using MACS v1.4 (Zhang et al 2008) with default parameters. Peak lists were annotated over RefSeq genes lists using GIN (Cesaroni et al 2008, priority set to "gene" and promoter definition to "-20000").

For ChIP of the histone marks, we used standard procedure using anti- H3K4me3 (Ative Motif 31210), H3K27me3 (Millipore 07-449), H3K9me3 (ChIP grade ab8898) and H3K9me2 (ChIP grade mAbcam 1220) antibodies. Real-time PCR was performed with 6 μL of DNA per reaction and 200 nM primers, diluted in a final volume of 20 μL in SYBR Green Reaction Mix (Perkin Elmer, Boston, MA). Accumulation of fluorescent products was monitored by real-time PCR using a GeneAmp 9700 Sequence Detector (ABI). Each PCR reaction generated only the expected specific amplicon, as shown by the melting-temperature profiles of final products (dissociation curve, automatically measured by the Taqman 9700).

2.6 Immunoblot

To prepare total cell extracts tissue-cultured cells were harvested by centrifugation, washed in PBS and directly lysed in Laemly 5x buffer followed by sonication for 30 seconds in a

Tekman CV26 sonicator set at 25% amplitude. The lysates were clarified and loaded in 8% SDS-polyacrylamide gel. The immunoblot was performed with Immobilon-P (Millipore) transfer membrane previously equilibrated in methanol. Rabbit monoclonal antibody anti-PRDM1 (Cell Signaling) was diluted 1:500 in 5% milk PBS-tween 0.1% and used for protein detection.

2.7 Immunofluorescence

Cells were fixed in 4% paraformaldehyde, washed in PBS and incubated in blocking buffer (PBS, 2% BSA, 0.1% Triton). Primary antibody was incubated at 4°C overnight. Primary rabbit polyclonal anti-PRDM1 antibody (Abcam ab59369) and secondary anti-rabbit FITC-conjugated antibody were diluted 1:25 and 1:50 respectively in blocking solution.

Images were acquired with an Olympus fluorescence microscope with the ScanR automated image acquisition software. Image analysis was performed with the ImageJ software.

2.8 BrdU proliferation assay

For proliferation assay cells (3x106) at different time points were pulsed for 10 minutes in medium containing 33 μM BrdU. Harvested cells were pelleted and resuspended in 750 μl of PBS and fixed by adding 2250 μl of pure ethanol for 30 minutes in ice. Fixed cells were resuspended in 1 ml of 2N HCl and incubated at room temperature for 25 minutes and after 3ml of 0.1 M Sodium Borate addition (Na2B4O7) incubated for other 2 minutes at RT. The cells were stained with anti-BrdU antibody diluted 1:5 in PBS, 1% BSA and with secondary anti-mouse Cy5 conjugated antibody.

2.9 Animal experiments

PRDM1-mVenus mice were imported from Saitou M. Lboratory. PRDM1-NestinCre and PRDM1-ErCre were generated by crossing PRDM1flox/flox mice with Nestin-Cre mice or Cre-ERT2 (The Jackson Laboratory). P53HE-ErCre and PRDM1-P53HE-ErCre mice were generated by crossing TP53 heterozygous mice (The Jackson Laboratory) with Cre-ERT2 or PRDM1-ErCre. The latter two mice were subjected to intracranial orthotopic

inoculation of concentrated lentivirus resuspended in PBS (106 copies/ml) expressing mutated Ras (HRasV12). In anesthetized mice (by intraperitoneal injections of Avertin 0.1mg/10g body weight) 2 µl of virus were stereotaxically injected into the nucleus caudatus (coordinates: 0.7 mm posterior, 3 mm left lateral, 3.5 mm in depth from the dura) of 8-weeks-old mice. A cohort of mice were administered by oral gavage with 5mg of tamoxifen dissolved in 80 µl of corn oil for two treatments of 5 days each separated by one week of no treatment. The mice were maintained until development of neurologic signs and then killed for the analysis of tumor histology and immunohistochemestry.

The mice were housed in plastic cages and were kept in a regulated enviroment (22°C; 55% humidity) with a 12 hours light/dark cycle (lights on at 7:00 AM). Food and water ad libitum.

2.10 Tissue histology

For histology, mouse brains were formalin fixed and paraffin-embedded. 5 µm sections were cut and placed onto polysine slides (Thermo Scientific). For Hematoxylin and Eosin staining sections were deparaffinized in xylene, rehydrated in a graded alchol series and stained in Mayer hematoxylin. After counterstain in eosin-phloxine B solution the sectiones were dehydrated in alchol and cleared in xylene.

Chapter 3 - RESULTS

3.1 PRDM1 expression correlates with multipotency in neural stem and progenitor cells (NSPCs)

In order to functionally and mechanistically characterize PRDM1 as a developmental regulator, we first needed to identify an appropriate experimental framework where to perform genome wide studies. Following initial screenings in different model systems we decided to assay for previously unanticipated role of PRDM1 in the mammalian central nervous system (CNS).

Available in situ hybridization data suggest that PRDM1 is highly expressed in neural territories during mouse development: in particular it is expressed in the key precursor structures (the leading anterior mesendoderm and the prechordal plate) from which the forebrain originates[42,51] (Fig. 9A, source http://genome.ucsc.edu/cgi-bin/hgVisiGene?hgp_listSpec=prdm1&hgp_doSearch=search). However in neuronal derived tissues PRDM1 expression is confined to the primitive retinal neurons (Fig. 7B) in the outer neuroblastic layer from about embryonic day (ED) 11 until birth and PRDM1 null embryos are not affected in the development of the head structures[42].

In the adult brain PRDM1 expression is undetectable (Fig. 9C) and it is slightly higher in the olfactory bulbs (Fig. 9D-F http://brainstars.org/probeset/1420425). Nonetheless, since PRDM1 protein is often restricted to a small cell population in a particular developmental stage, in situ hybridization (ISH) and gene expression profiles might not be sensitive enough to appreciate PRDM1 expression differences.

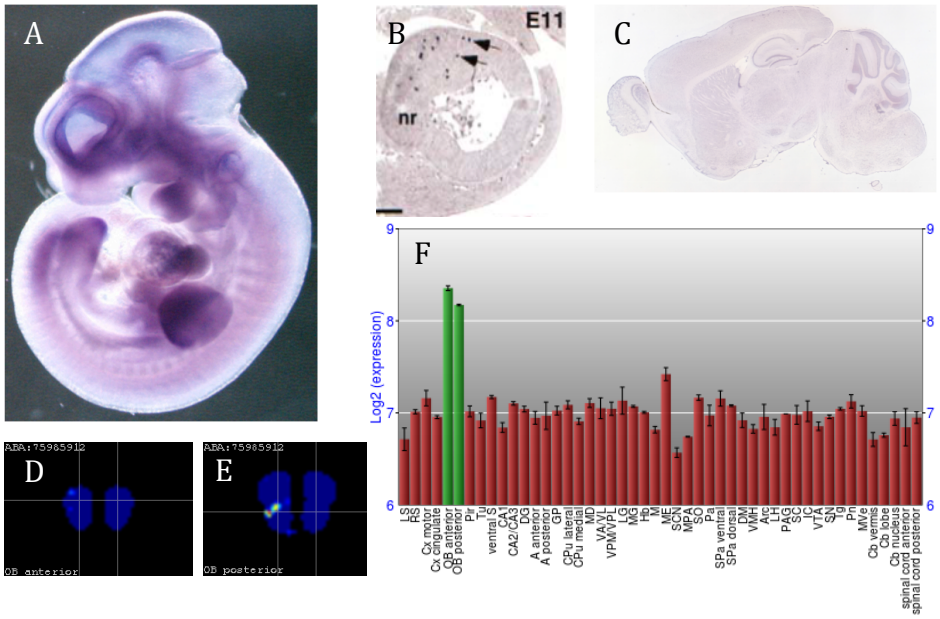

Figure 9. PRDM1 expression in mouse neural tissues. A) In situ hybridization (ISH) of PRDM1 in mouse embryo. PRDM1 is induced early in the anterior definitive endoderm, mesoderm of head process and prechordal plate. Source: Mahoney Lab: MGI Reference: Mouse Brain Organization Revealed Through Direct Genome-Scale TF Expression Analysis. B) Immunohistochemistry (IHC) of PRDM1 in ectoderm-derived tissues. Sagittal section through the eyes of ED11 embryo. PRDM1 is expressed in the outer neuroblastic layer of neural retina. Source: MGI Reference: The dynamic expression pattern of B lymphocyte induced maturation protein-1 (Blimp-1) during mouse embryonic development. C) PRDM1 is not detectable in mouse brain after birth using IHC. Source: Allen Brain Atlas (ABA). D) and E) expression energy cross section images of PRDM1 in the olfactory bulb anterior and posterior respectively. Source: Allen Mouse Brain Atlas, Allen Instiute for Brain Science. F) Mouse PRDM1 relative gene expression in adult brain compartments. Source: BrainStars classification of 48 brain regions by multi-state gene analysis.

As previously described, in zebrafish PRDM1 is expressed in neural progenitors and in mammals it is critical for homeostasis of many tissues. These observations prompted us to better investigate if PRDM1 might be involved also in adult mouse neurogenesis.

To test this, we took advantage of PRDM1mVenus mice[47], a transgenic reporter strain that expresses membrane-targeted Venus (mVenus) under the control of PRDM1 regulatory elements (Fig. 10). Following mVenus tracer is possible to recapitulate directly in vivo the dynamic expression pattern of PRDM1. From the brain of C57BL/6 wild type (WT) and PRDM1mVenus adult mice we isolated the cells residing in the subventricular zone (SVZ) of the cerebral cortex (the adult neural stem cell niche), a compartment enriched for neural stem and progenitor cells (NSPCs). In a few days, from the cell suspension neurospheres started to form and we expanded them in culture in order to enrich for NSPCs (schematic representation in Fig. 11).

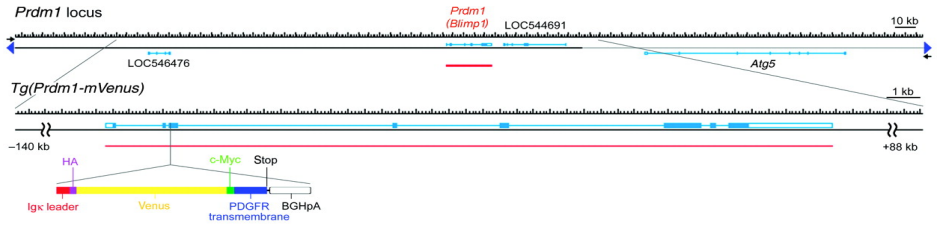

Figure 10. Scheme of the Prdm1mVenus transgene. The genomic loci and exon–intron structures of the Prdm1. The position at which sequences of the fluorescent reporters are recombined are also shown. Source: Ohinata Y et al. Reproduction 2008;136:503-514

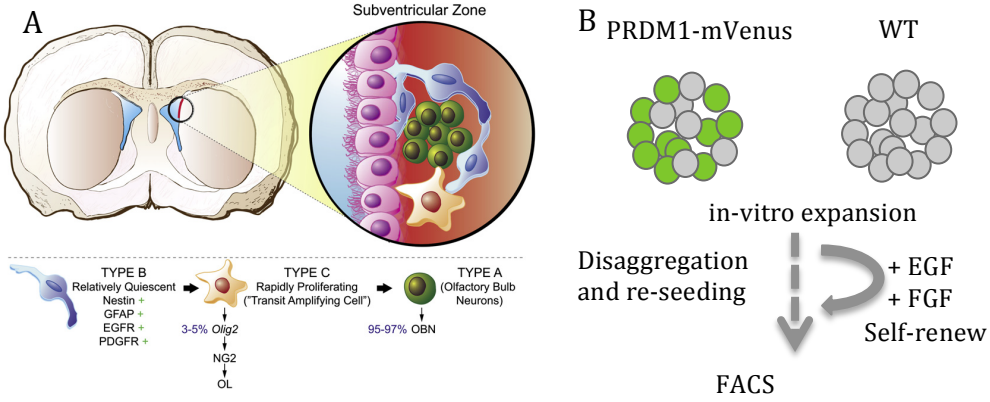

Figure 11. Derivation and expansion of mouse neural stem and progenitor cells (NSPCs) from adult brain. A) Picture adapted from Charles D. Stiles and David H. Rowitch, Neuron 58, June 26, 2008. Scheme of frontal section of the adult mouse brain showing the subventricular zone (SVZ) (red and enlarged on the right) adjacent to the lateral ventricle. SVZ progenitors include type B (blue), C (amber), A (green) cells and ciliated ependymal cells (pink) that line the lateral ventricle. Type B cells divide very slowly and express the markers indicated. They give rise to transient amplifying type C cells that in turn generate type A neuroblasts that contribute to the rostral migratory stream in most cases. B) Stem and progenitor cells derived from the sub-ventricular zone (SVZ) of adult WT and PRDM1mVenus reporter mice were propagated in culture as neurospheres. At each passage the spheres were disaggregated and seeded as single cells to expand the pool of NSPCs to be analyzed by FACS.

After some passages (around 10) the dissociated neurospheres were subjected to flow cytometry. We realized that the population of NSPCs was morphologically heterogeneous both in WT as well as in PRDM1mVenus derived cells and it could be separated in two subpopulations, called P1 and P2 (Fig. 12A and B). Both of them were gated and analysed for fluorescence emission. Interestingly a significant enrichment of Venus positive events was detected in both the subpopulations but more significantly in the one with higher side scatter (SSC), the P1 (equal to the 22.9% Fig 12E and F), while considering the total

NSPCs (P1 and P2 together) the percentage of Venus positive cells was 4% if compared with the total WT NSPCs (Fig. 14D and 14B respectively). Neurospheres are composed of different population of cells, which are believed to have various levels of differentiation potential. The most primitive NSC, among other markers, can be discriminated using FACS analyses by means of physical properties such as size and granular complexity, forward (FSC) and side scatter (SSC), respectively (Fig. 12-14). The total Venus-positive (Fig. 13B) and Venus-negative cells (Fig. 13A) of PRDM1mVenus sample were independently plotted in order to see differences in the morphology of the cells and we noticed that putative PRDM1 expressing cells were augmented in SSC^{high} while PRDM1 negative clustered in FSC/SSC^{low}. Furthermore, a stringent gate was set on WT neurosphere cells in order to identify the lowest fraction of cells with the NSC properties characterized by high FSC/SSC (Fig. 14A and 14C). This population resulted to be highly similar between WT and transgenic animals neurospheres. Interestingly, when Venus-positive neurosphere cells were separately analyzed we found fourfold-enrichment in the FSC/SSC^{high} population (Fig. 14E), indicating that Venus expressing population is enriched for NSC. We also observed an eight-fold enrichment of SSC^{high} cells that is a morphological feature of adult NSCs.

Although promising, these first evidence were indirect proves of PRDM1 expression in neurogenic areas that we directly corroborated by testing PRDM1 presence in different brain compartments. Firstly, we confirmed that PRDM1 protein was indeed expressed in NSPCs while it was not detectable in primary cortical astrocytes (Fig. 15), moreover PRDM1 expression level counter-correlated with GFAP level (astrocytic marker) in a NSPCs in vitro differentiation assay (Fig. 16). Afterwards, we examined the PRDM1 transcript in brain lysates. While in the majority of the tissues analyzed PRDM1 was not revealed (or it was expressed at very low level), in line with the ATLAS database, I found relatively higher PRDM1 expression in the olfactory bulb (OB) and in rostra migratory

stream (RMS) (Fig. 17), two neurogenic areas that contain migrating neural progenitors which differentiate to become functionally effective.

Collectively the data indicated that by means of lineage tracing protein and gene expression experiments we demonstrated that PRDM1 is expressed in the brain of the adult mice and that it correlates more with properties of uncommitted neural progenitors.

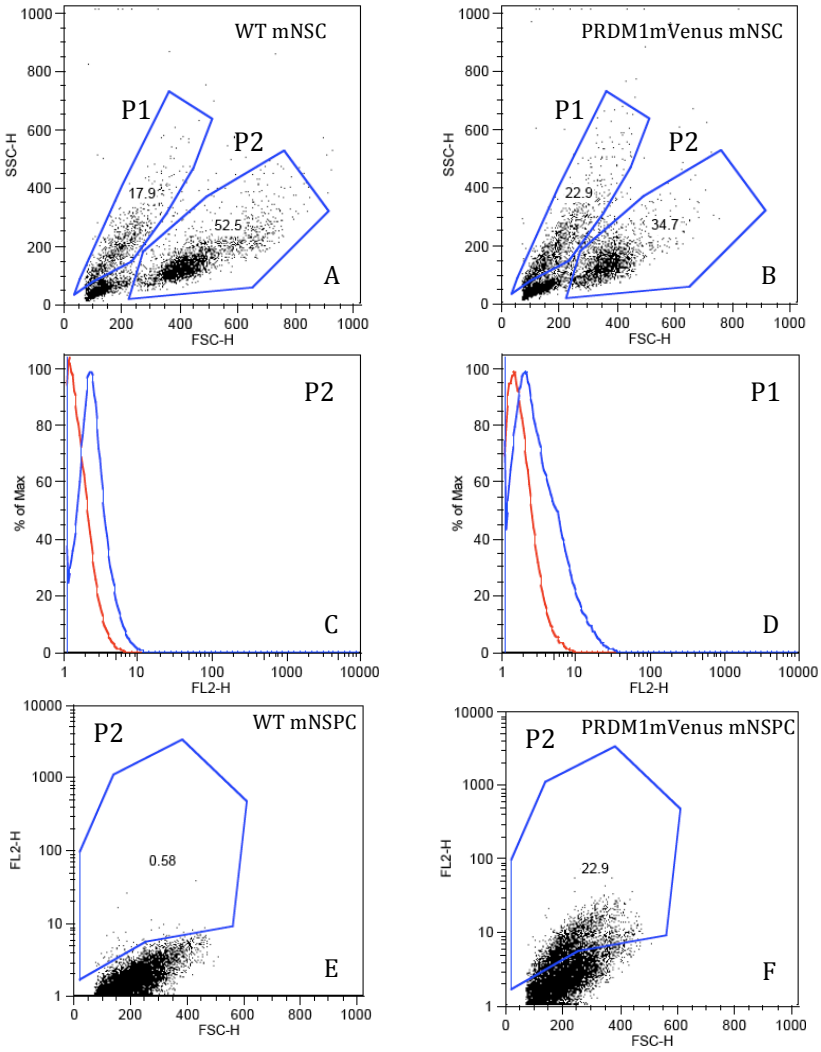

Figure 12. Initial characterization of PRDM1 expression in adult mouse brain.
A and B) FACS analysis of freshly dissociated NSPCs. Stem and progenitor cells derived from the subventricular zone (SVZ) of adult WT (A) and PRDM1mVenus (B) reporter mice were propagated in culture as neurospheres and then FACS analysed as single cells (see scheme in Fig. 9). C and D). The cells separate in two morphologically different sub-populations (P1 and P2 in the top panels) and both of them are enriched for Venus positive cells (blue curve) if compared with the non-fluorescent WT cells (red curve). E and F) The Venus positive cells correspond to the 22.9% of the P2 population in PRDM1mVenus (F) compared to the negative WT control (E). Laser exitation at 488 nm and emission detected in FL2-H channel (at 542 nm).

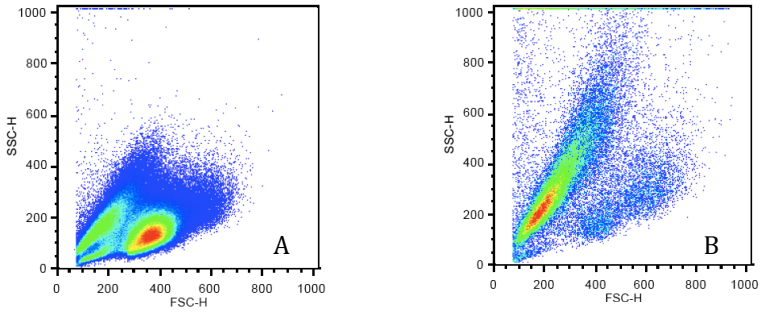

Figure 13. Venus-negative and Venus-positive NSPCs are morphologically different. (A) Cells from PRDM1Venus mice. Distribution of the TOTAL Venus negative population. (B) Distribution of the TOTAL Venus positive population.

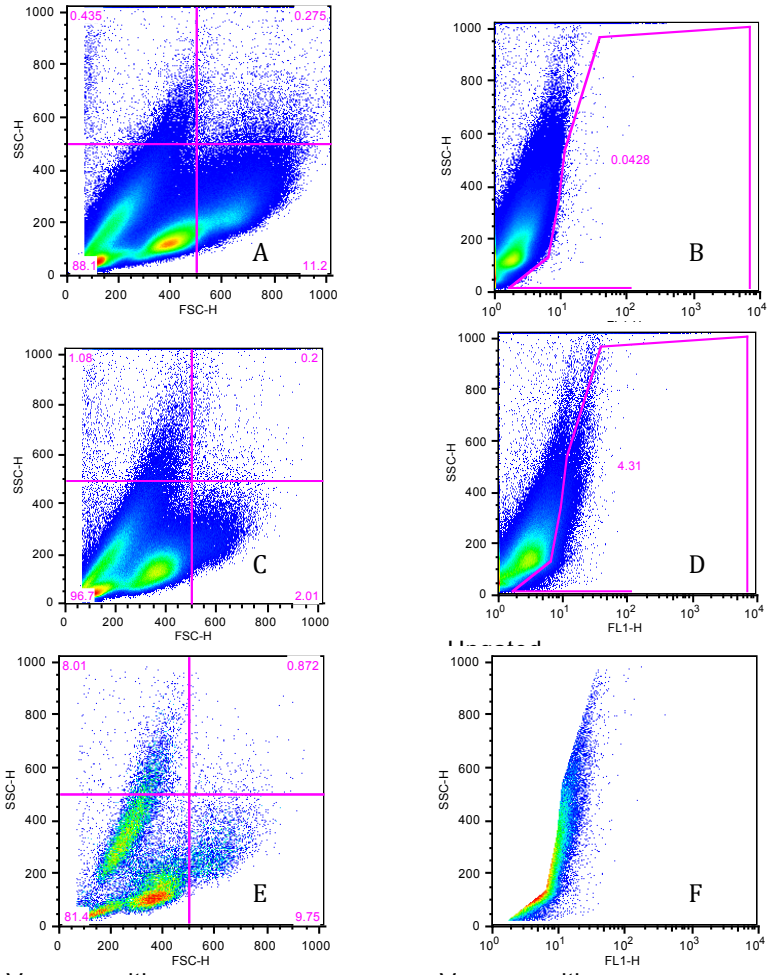

Figure 14. NSPCs morphological analysis. A stringent gate was set on NSPC cells (A and C) in order to identify the lowest fraction of cells with the NSC properties of high FSC/SSH. This population resulted to be highly similar between WT (0.275 in A) and transgenic animals neurospheres (0.2 in C). Interestingly, when Venus positive neurosphere cells (F) – resulting from the subtraction of PRDM1mVenus positive events (D) from the negative control (B) - were separately analyzed we found a four fold enrichment in the FSC/SSC high population (0.872 in E) and eight fold enrichments in SSC high population (1.08 in C and 8.01 in E) indicating that Venus positive cells may be enriched for NSC.

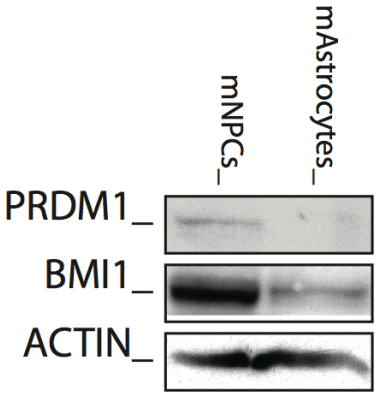

Figure 15. PRDM1 protein is expressed in NSPCs and not in differentiated astrocytes. Primary NSPCs and astrocyte cultures were derived from 7 days old mice using established methods (McCarthy and de Vellis, 1980). BMI1 is normally expressed in stem and progenitor cells and is used as positive control. Actin is used as loading control.

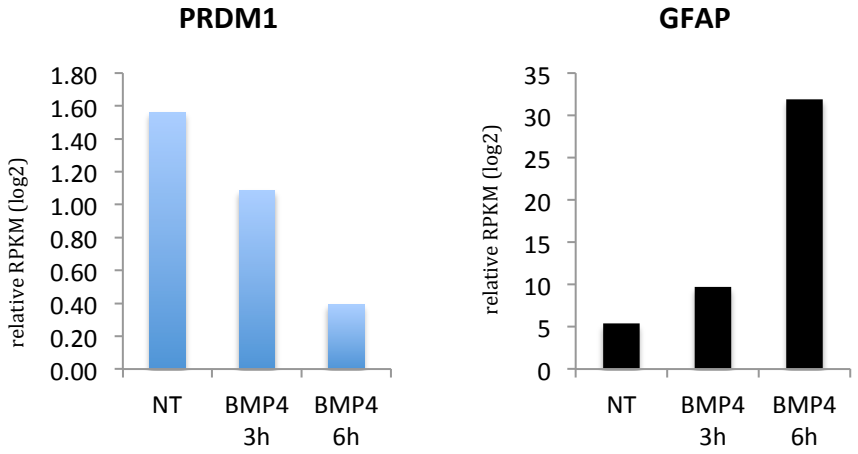

Figure 16. PRDM1 expression is down regulated during in vitro differentiating primary NSPCs. Untreated NSPCs (NT) or treated with 10 ng/mL of BMP4 for 3 and 6 hours. GFAP is used as positive control of cellular differentiation. TBP is used as reference gene for normalization. PRDM1 difference in gene expression between the treatments has been assessed by one-way ANOVA and it is statistically significant (p=0.0163).

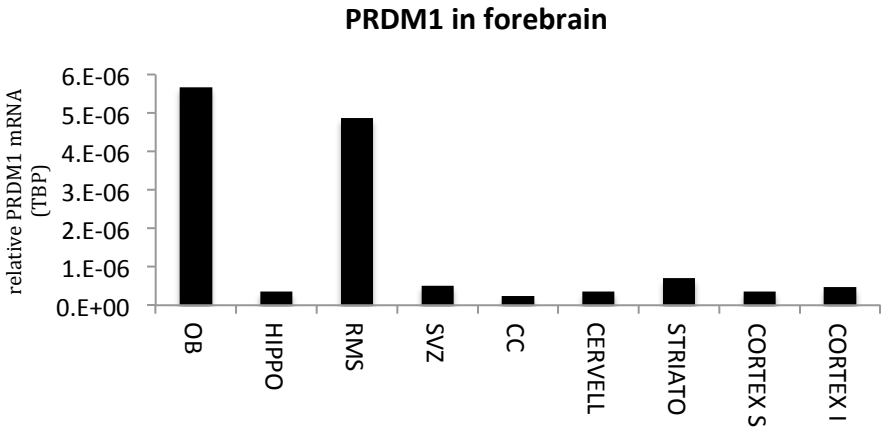

Figure 17. Relative PRDM1 expression in different mouse brain tissues. OB, olfactory bulb; HIPPO, hippocampus; RMS, rostra migratory stream; SVZ sub-ventricular zone; CC, corpus callosum; CERVELL, cerebellum; STRIATO; CORTEX S, temporal cortex; CORTEX I, frontal cortex. TBP is used as reference gene for normalization.

3.2 PRDM1 loss has consequences on NSPCs global gene expression

These data prompted us to better investigate PRDM1 biological function in a previously unexplored context that is the central nervous system (CNS). In order to do this we generated conditional knock out (CKO) mice where PRDM1 expression was abrogated in NSPCs in vivo. This mouse model was obtained by crossing mice that possess loxP sites in introns flanking exons 6 to 8 of the Prdm1 gene (http://jaxmice.jax.org/strain/008100.html) with mice that express Cre recombinase under the control of the rat nestin promoter and enhancer (http://jaxmice.jax.org/strain/003771.html). The efficiency of PRDM1 deletion was assessed both at genomic level in WT, conditional heterozygous (CHE) and CKO NSPCs (Fig. 18) and at expression level in WT and CKO NSPCs and whole brain (Fig. 19). Mice that were homozygous for PRDM1 deletion in the brain were viable, normal in size and did not display any gross physical or behavioural abnormalities.

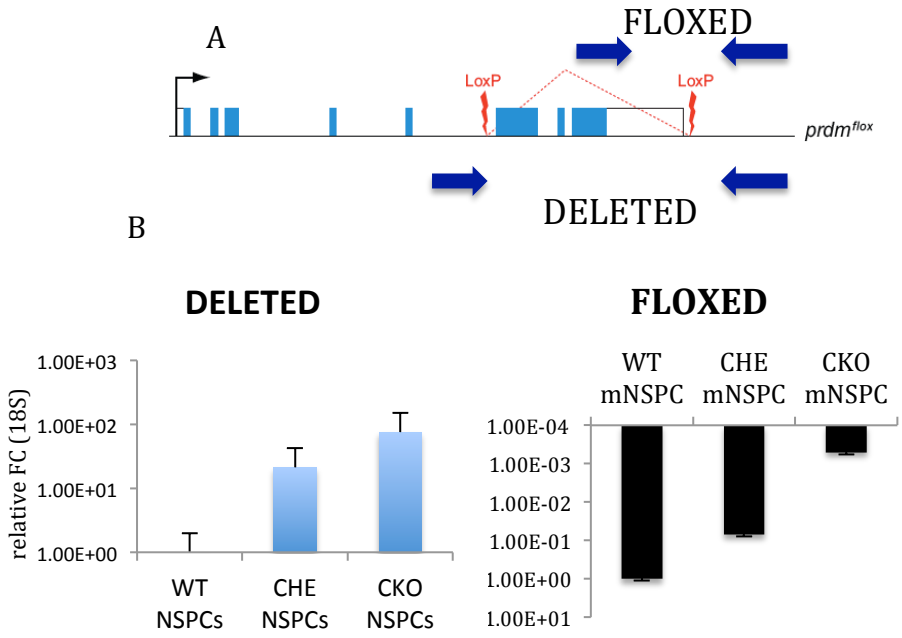

Figure 18. PRDM1 conditional knock out (CKO) mouse model. A) Schematic representation of PRDM1FLOX locus. This mouse model possesses loxP sites in introns flanking exons 6 to 8 of the PRDM1 gene. When these mutant mice are bred to mice that express Cre recombinase, resulting offspring will have exons 6 to 8 deleted in the cre-expressing tissue. Two couples of primers were designed to assess the deletion of PRDM1 gene. The primers called "FLOXED" amplify only WT allele, while "DELETED" primers are able to amplify only in case of recombination (deletion) event. B) Genomic DNA derived from NSPCs of PRDM1flox crossed with Nestin Cre mice and amplified with the two different PCR designed assays. The values are normalized with 18S gene.

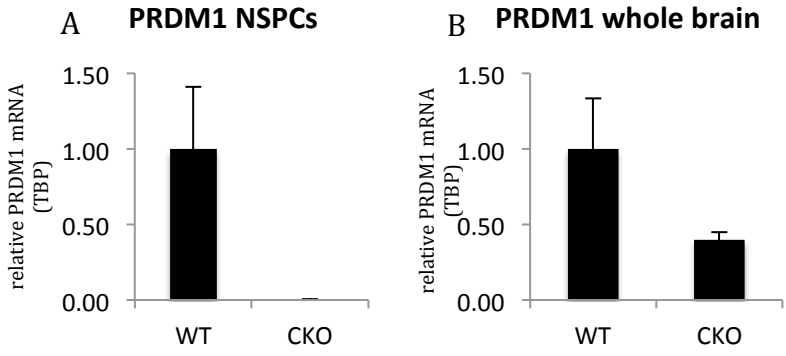

Figure 19. PRDM1 is efficiently deleted in the Nestin expressing cells and in their neural derivatives. PRDM1 qRT-PCR performed with NSPCs (A) or whole brain lysate (B). TBP is used as reference gene for normalization.

In order to obtain a more global view on the effect of PRDM1 loss of function in adult neurogenesis we carried out RNA sequencing in WT and PRDM1 CKO NSPCs. NSPCs were isolated from the subventricular zone of adult mice brain by enzymatic digestion. Dissected regions were mechanically dissociated to obtain single cell suspension that was plated in the selective culture medium (for details see Material and Methods 2.1). By using this methodology, NSPCs formed spherical clusters called neuropsheres, which were mechanically dissociated to a single-cell suspension and replated to expand the pool. After few passages (around 5) we extracted total RNA from WT and PRDM1 CKO neurospheres (Fig. 20). Starting with total RNA, the messenger RNA was first purified using polyA selection (Illumina), then chemically fragmented and converted into single cell cDNA using random hexamer priming. Next, the second strand was generated to create double-stranded cDNA that was ready for library construction for paired-end sequencing.

Transcripts abundance and differentially expressed genes were called and analysed using the parameters described in Material and Methods 2.4 demonstrating that the loss of PRDM1 function influenced NSPCs genome wide gene expression profile. The

overlapping list of co-regulated genes obtained from two independent experiments in the absence of PRDM1 (76 genes were downregulated and 117 upregulated) was significantly enriched for metabolic pathways (glycolysis/gluconeogenesis, fructose and mannose metabolism), amino-acids metabolism (pentose phosphate pathway), nervous system development and function (Wnt/β-catenin signalling), membrane trafficking (clathrin mediated endocytosis) and HIF1α signalling pathway (not indicated in the table but it was the sixth pathway more represented) (Fig. 21). Combining our dataset with a published transcriptome database for astrocytes, neurons and oligodendrocytes[197] we observed that deregulated genes in PRDM1 null NSPCs are variably expressed in all the differentiated brain cell types (Fig. 22).

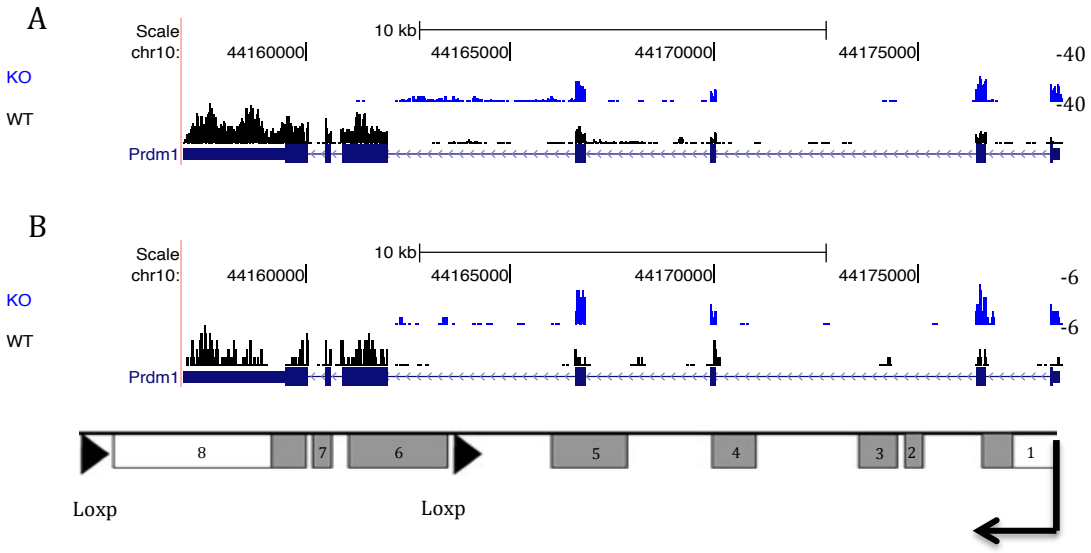

Figure 20. RNA sequencing of WT and PRDM1 CKO NSPCs. The transcriptome of WT (black track) and PRDM1 KO (blue track) neurospheres was obtained from two independent experiments (two WT mice and two CKO mice). A) Genome browser snapshot of replicate 1. B) Genome browser snapshot of replicate 2. In both the replicates is clear the deletion of the region comprising exons 6 to 8 of PRDM1 locus in KO tracks.

Top Canonical Pathways	
Name	p-value
Glycolysis/Gluconeogenesis	4.91E-08
Pentose Phosphate Pathway	2.48E-05
Wnt/β-catenin Signaling	3.19E-05
Fructose and Mannose Metabolism	4.11E-05
Clathrin-mediated Endocytosis Signaling	6.58E-05

Figure 21. Summary of Ingenuity Systems Pathway Analysis (IPA) of PRDM1 KO regulated genes. The analysis showed that the regulated genes in PRDM1 KO NSPCs compared to WT belong more significantly to the listed pathways. Threshold was set up at 5 but HIF1α signaling was the sixth more enriched pathway.

Furthermore, in the same database the authors identified cell-type enriched signalling pathways and interestingly Wnt/β-catenin signalling and glycolysis/gluoconeogenesis were more significantly associated with astrocytes and as mentioned above also over-represented in our list of KO deregulated genes.

In the validation step we observed a fair correlation between RNA-sequencing profile and independent qRT-PCR experiments with approximately 50% of randomly selected genes being defined as deregulated by both platforms (Fig. 23). We believed that these results are on line with the expected degree of variation due to heterogeneity in neurosphere cultures. Notably, however we fully recapitulated by gene expression profiles the more differentiated phenotype of PRDM1 depleted NSPCs as being the glial fibrillary acidic protein (GFAP) - a well-known marker of astrocytes and glial cells – up regulated in KO cultured cells (Fig 24A and 24B). Accordingly with a pro-differentiation effect of PRDM1 deletion, we noticed that KO NSPCs proliferated less than WT (Fig. 25). In fact in neurosphere-assay KO cells were slower in self-renewing ability and formed smaller spheres (Fig. 25A and 25B). Indeed, at high density cell suspension (150 cells per microliter) 2.9% of WT neurospheres were bigger than 100 μm (in diameter), on the other hand only 0.4% of the KO neurospheres reached the same size (see Table 2 for details).

To verify this phenotypic observation we plated low-density (1 cell per microliter) single cell suspension of NSPCs in a 96 well and we waited for new sphere formation. Indeed we saw that KO NSPCs were drastically impaired in the ability to re-form new colonies (Fig. 25C) and in some cases the newly form neurospheres had a differentiated morphology (Fig. 25D and 25E).

Together the data presented here suggested that the loss of PRDM1 impaired NSPCs in-vitro self-renew and it influenced the transcriptional profile of genes that are important in all mouse brain terminally differentiated cells.

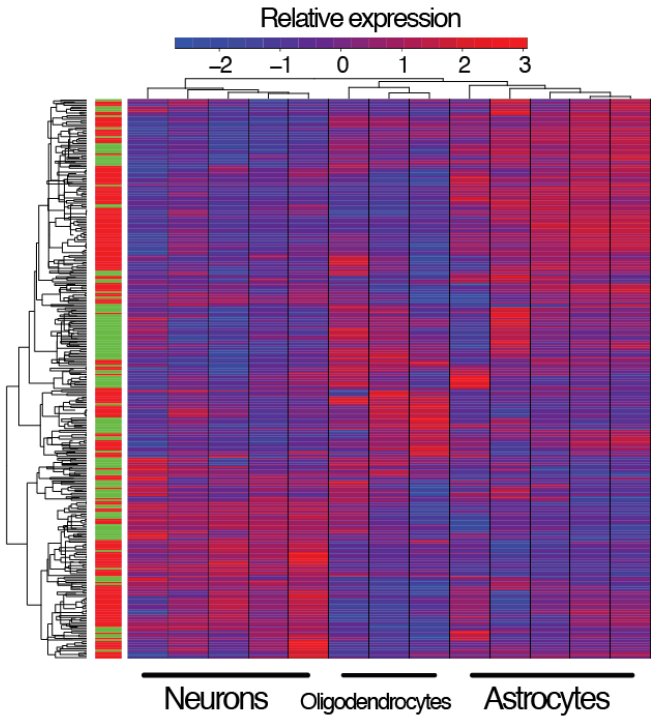

Figure 22. PRDM1 dependent genes are expressed in all mouse brain terminally differentiated cells. Regulated genes after PRDM1 ablation in NSPCs are indicated on the left of the heatmap (down regulated in green and up regulated in red). The heatmap represents the expression level of each individual gene in the three major classes of brain terminally differentiated cells. Source: The Journal of Neuroscience, 2 January 2008, 28(1): 264-278; doi: 10.1523/ JNEUROSCI.4178-07.2008. The expression level was normalized and plotted on a logaritmic color scale, with blue representing low expression and red representing high expression.

DIAMETER (μm)	WT spheres (%)	KO spheres (%)
10 - 20	19.3%	17.3%
20.1 - 50	44%	47.3%
50.1 - 100	34%	35%
> 100	2.9%	0.4%

Table2. Neurospheres counting in WT and KO NSPCs culture.

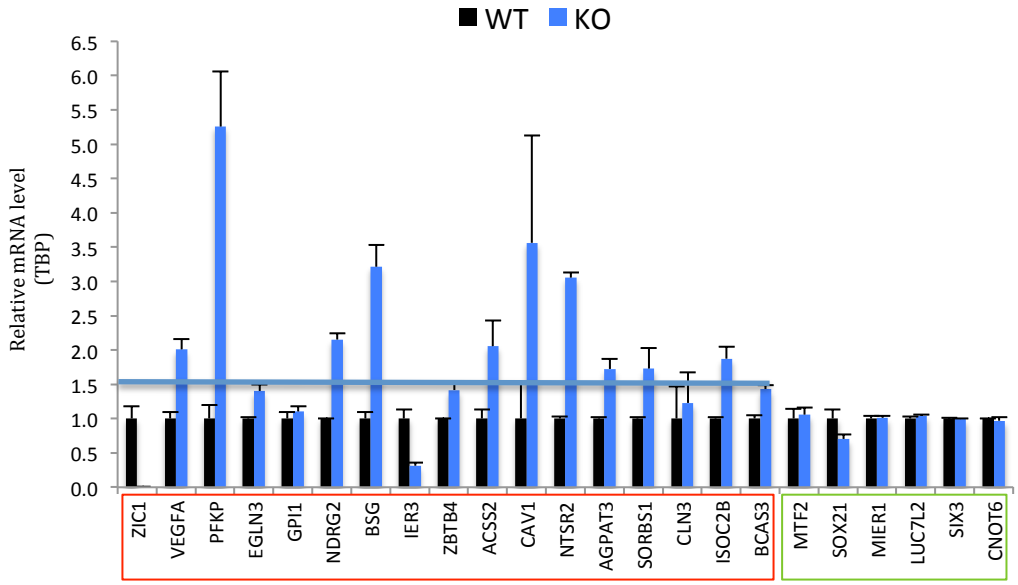

Figure 23. Validation by qRT-PCR of RNA-seq. Expression level of selected genes up regulated (in red) or down regulated (in green) in KO NSPCs was checked in an independent experiment for RNA-seq validation. The graph shows that part of the up regulated genes were confirmed (above the blue line settled at 1.5 fold increase) while down regulated did not recapitulate RNA- seq profile.

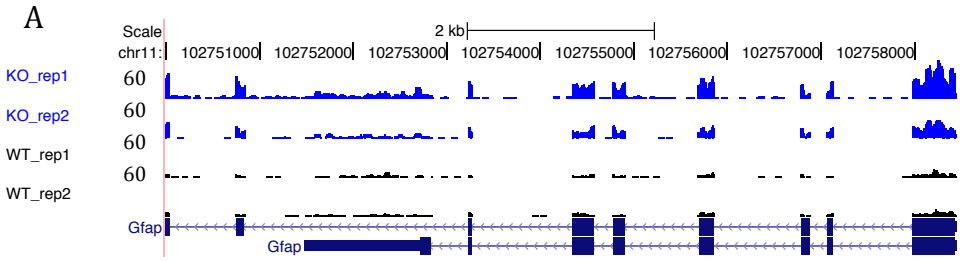

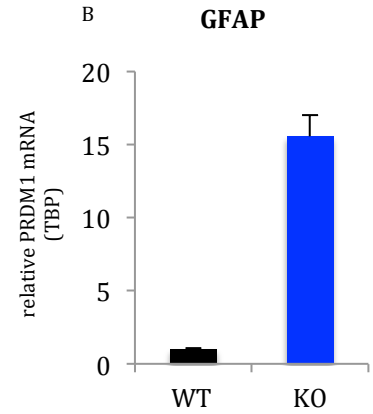

Figure 24. GFAP gene is significantly up regulated in PRDM1 KO NSPCs. A) RNA-seq profile shows GFAP expression pattern in WT NSPCs (black) – almost undetectable - and in KO NSPCs (blue) where it is well expressed. B) qRT-PCR validation of GFAP expression in an independent experiment. TBP is used as reference gene for normalization.

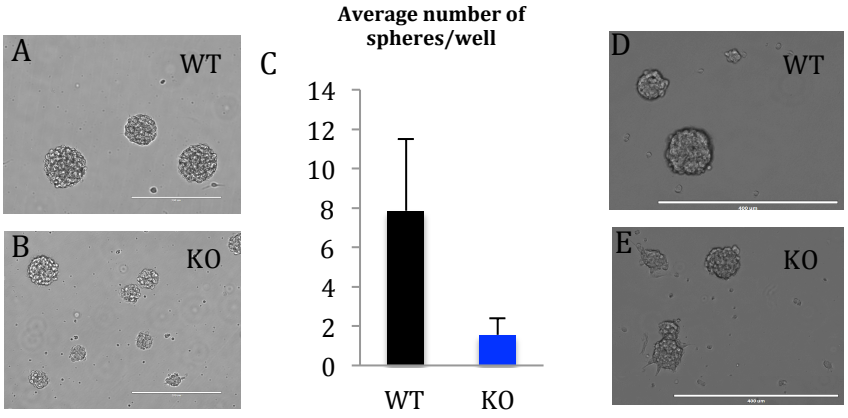

Figure 25. Loss of PRDM1 impairs NSPCs in vitro self renewal. A and B) Phase contrast images of neurospheres WT (A) and PRDM1 KO (B) NSPCs. PRDM1 KO spheres appears generally smaller in size and fewer in number. C) The neurospheres of each sample were disaggregated and plated as single cell in a 96 well plate. The graph represents the average number of new spheres in each well of a 96 well plate. Bars show mean values of spheres/well and corresponding standard error of two independent experiments. KO cells are impaired in the formation of new spheres when plated at low density single cell suspension. D and E) Phase contrast images. The newly formed neurospheres are also morphologically different. KO NSPCs (E) in these conditions show a differentiated morphology compared with WT (D).

3.3 Identification of PRDM1 regulatory network

To gain insight into the molecular mechanism by which PRDM1 regulates developmentally important processes, we overcame the paucity of neurospheres, by moving to an established model system of neural differentiation where we could set-up and perform ChIP-sequencing: the Ntera2-D1 (NT2-D1) embryonic carcinoma cell line. NT2-D1 is widely adopted differentiation model system that shares many properties with human embryonic stem cells (expression of pluripotency markers such as Oct4, Nanog, and Sox2; in vivo differentiation towards different lineages –e.g. teratoma formation; in vitro commitment towards defined developmental routes –e.g. neural commitment) and that can differentiate in vitro into neurons upon exposure to all trans retinoic acid (ATRA). We successfully differentiated NT2-D1 in vitro as revealed by gene-expression, morphology and proliferation changes during ATRA exposure (Fig. 26 and 28).

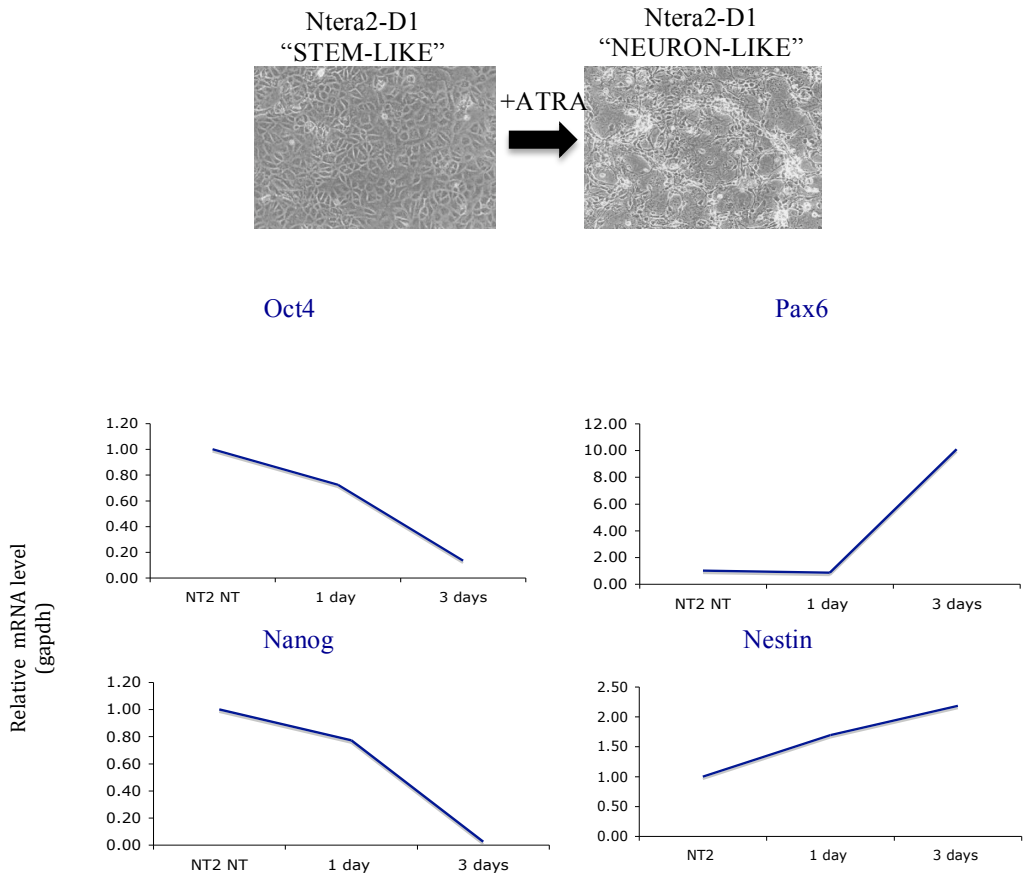

Figure 26. Ntera2-D1 (NT2-D1) cells in-vitro differentiation. (Top) Light microscopy images of NT2 cells not treated and after retinoic acid (ATRA) treatment. (Bottom) ATRA induced NT2-D1 differentiation determine the loss of pluripotency markers as Oct4 and Nanog (graphs on the left) and the acquirement of neural-specific markers as Pax6 and Nestin (graphs on the right). Gene expression changes were detected by real-time quantitative PCR (qRT-PCR) and they are represented as relative intensity by using gapdh housekeeping gene for mRNA level normalization.

Next, we tested for the expression of PRDM1 during NT2 differentiation by using TaqMan tool (Fig. 27) and qRT-PCR (Fig. 28 C): we collected the cells at different time points (not treated, 1, 3, 5, 7 and 14 days exposed to ATRA) to measure expression along with cellular proliferation changes trough 5-bromo-2-deoxyuridine (BrdU) incorporation until day 7. Interestingly, we noticed that the peak of PRDM1 expression coincided with the time point at which the cells start to exit the cell cycle and to commit to a more differentiated state, acquiring morphological changes. In particular, PRDM1 expression pattern correlated with the early stages of cellular differentiation as it was up regulated around the third day of ATRA induction and down regulated immediately after (as detected by transcript and protein level) (Fig. 28C and 28A-B respectively). Consistent with this, BrdU cell incorporation progressively decreased after the third day of ATRA treatment and the cells

started to accumulate in G1 phase from this time point onwards, until they practically exit the cell cycle after one week of treatment (Figure 28 C bottom).

The human PRDM1 gene contains an alternative promoter capable of generating a PR domain deleted protein (called PRDM1-β), which lacks 101 amino acids comprising most of the PR domain. We designed a quantitative real-time PCR (qRT-PCR) assay to discriminate the expression pattern of each of the two isoforms that differentiate for length and for the presence of a unique exon in PRDM1β. In early time points of ATRA induction, PRDM1β was hardly detectable and it started to be expressed at day 7 when the full-length isoform (PRDM1α) was not more detectable (Figure 29).

We further investigate the role of PRDM1 in NT2-D1 differentiation, an interesting model system amenable to mechanistic analyses. We performed Chromatin-immunoprecipitation sequencing (ChIP-seq) experiment for PRDM1 at the third day of ATRA treatment (at the time point in which only PRDM1α is expressed) by two sequential rounds of IP (scheme of the experiment in Fig. 30 B) using two different anti-PRDM1 antibodies. One of these antibodies was kindly provided by Surani A. laboratory and it was already validated for ChIP experiments. We checked the specificity of the other antibody (commercially available) by performing ChIP-western blot (ChIP-WB) (Fig. 30A).

From ChIP-sequencing we obtained 10 millions uniquely aligned reads forming 4700 peaks (IP versus input) calculated with a threshold p-value of 1e-5 on a non-redundant list of genes. The genomic distribution of the peaks shows a clear enrichment for promoters (27%). However, since PRDM1 is also present in substantial amounts at intergenic binding sites (Fig. 30C), it could be additionally involved in long distance mechanisms of gene regulation. The sequences surrounding the peaks (Fig. 30D) were then analysed by MEME to search for enriched de novo DNA-binding motif(s) (Fig. 30E). MEME outcome confirmed at a genomic scale the main PRDM1 consensus motif (IRF-like), and reinforced the confidence in the validity of our approach and of the target genes identified.

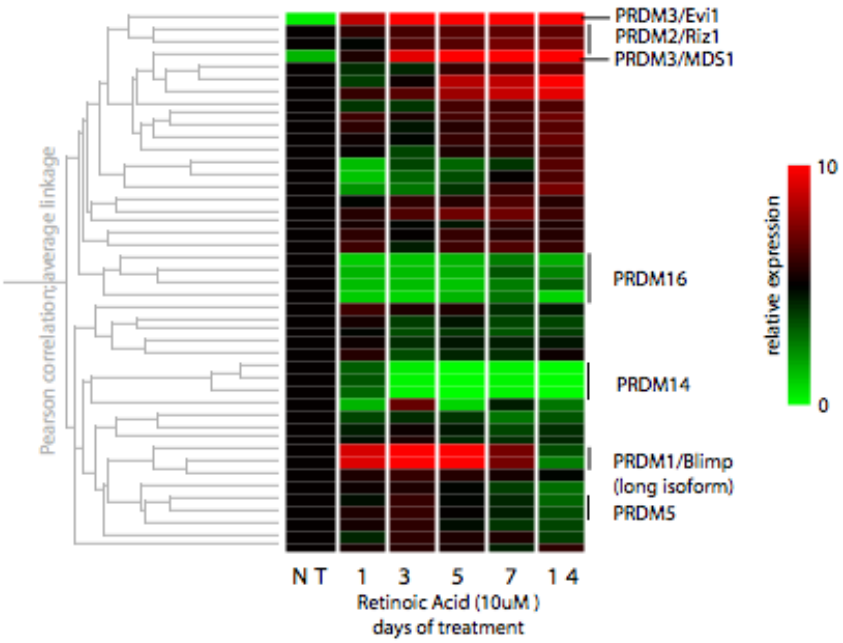

Figure 27. PRDMs expression during ATRA induced NT2-D1 differentiation. In the y, relative mRNA expression level; in the x, days of RA treatment. Data are represented as a heatmap according to the color-code scale shown on the right. Each line corresponds to a TaqMan probe for each PRDM members.

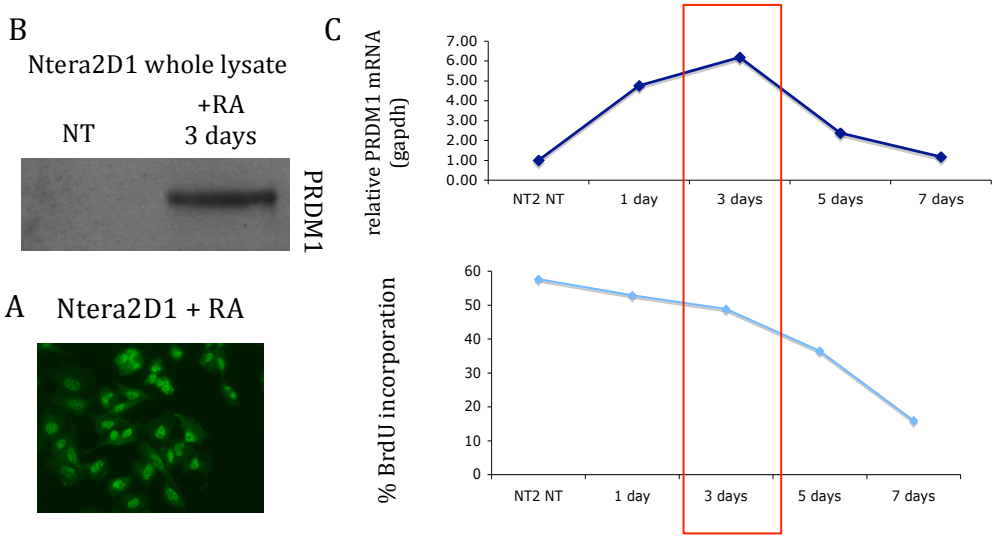

Figure 28. PRDM1 expression pattern during NT2-D1 differentiation. PRDM1 is a nuclear DNA binding protein whose expression is induced upon ATRA treatment. PRDM1 expression peaks at the third day of ATRA treatment as the same time point when the cells start to exit the cell cycle. (A) Immunofluorescence of PRDM1 in NT2-D1 cells exposed to ATRA (detected by anti-PRDM1 polyclonal antibody from Abcam). (B) Immunoblot of endogenous PRDM1 (detected by anti-PRDM1 polyclonal antibody from Cell signaling) in NT2-D1 whole lysate, before and after 3 days of ATRA treatment. (C) (Top) PRDM1 expression level during NT2-D1 differentiation detected by qRT-PCR normalized to gapdh values. In the y, relative mRNA expression level; in the x, days of RA treatment. (Bottom) Percentage of proliferating cells during ATRA differentiation. In the y, percentage of BrdU positive cells; in the x, days of ATRA treatment.

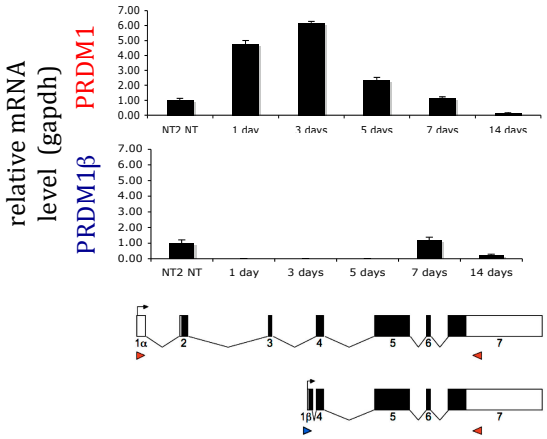

Figure 29. PRDM1α and PRDM1β are counter-regulated during NT2 differentiation. PRDM1α (top) and PRDM1β (bottom) relative expression. The values are normalized to gapdh. In the y relative mRNA level, in the x days of ATRA differentiation. Schematic representation of PRDM1α and PRDM1β genes.

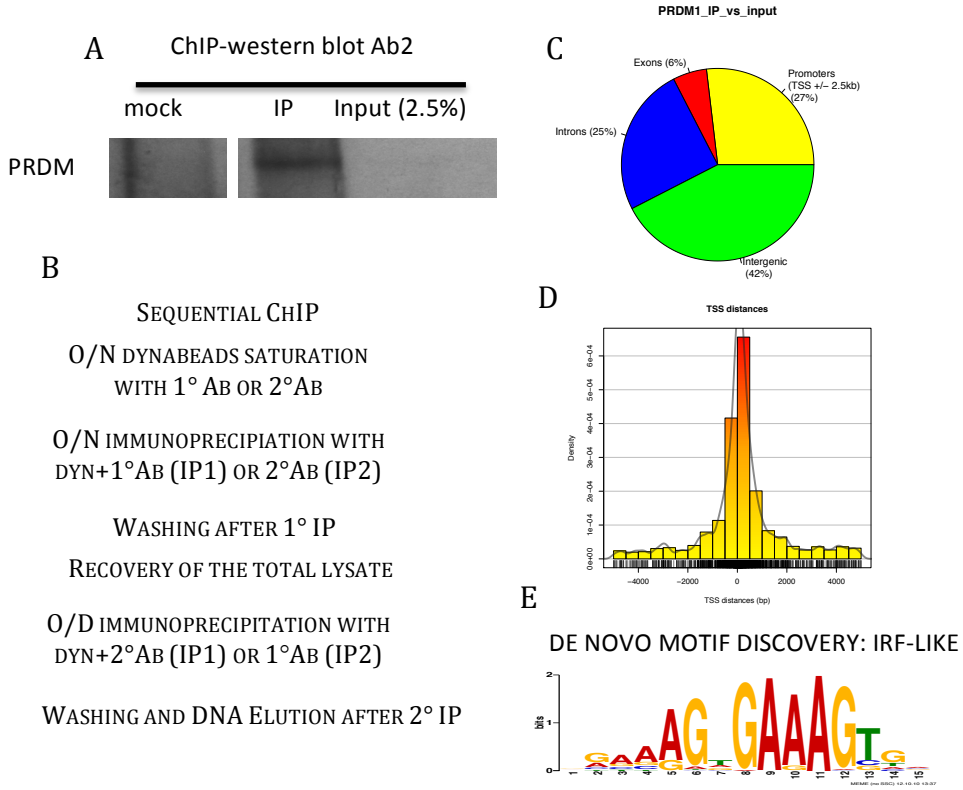

Figure 30. PRDM1 Chromatin immunoprecipitation sequencing (ChIP-seq) in NT2-D1. (A) ChIP of endogenous PRDM1 in NT2-D1 cells at the third day of ATRA treatment using two different antibodies. One got from Surani group, already used for ChIP purposes and the other commercial (Ab2) and validated in chip-conditions (by ChIP western blot) before the usage for ChIP-qPCR. Using both antibodies we obtained enough DNA to sequence. (B) Flowchart of the ChIP experiment. The IP were performed in duplicate (IP1 and IP2) by precipitating chromatin in two IP rounds. C) Genomic distribution of PRDM1 peaks. D) Distribution of the peaks around RefSeq transcription start site (TSS). E) Logo derived from MEME of the de-novo binding motif.

We randomly selected 30 putative target regions from the ChIP-seq (with different binding affinity according to the p-value assigned) for single binding region ChIP quantitative PCR (ChIP-qPCR) validation (Fig 31). The specificity of PRDM1 direct target binding sites was compared with the chromatin immunoprecipitated with rabbit IgG (mock) as negative control (Fig. 31A). Furthermore the ChIP was performed also in the cells untreated (in which PRDM1 is expressed as a basal level) showing, as expected, low PRDM1-binding affinity (Fig. 31B). We were able to confirm the binding for 27 regions measured as the enrichment on the total chromatin before the IP (input) and comparing with mock experiment (some of the validated regions are graphed in Figure 31A-B). We confirmed that the quality of the assigned peaks is high (90% validation), and therefore we proceeded to an in-depth bioinformatic analyses. To find any relation among PRDM1 target genes we searched the Database for Annotation, Visualization, and Integrated Discovery (DAVID) for enriched gene ontology (GO) terms (Fig. 32). We found the top ranking gene clusters in nucleus and in negative regulation of transcription - as expected being a known transcription regulator – but most importantly new classes of genes emerged to be part of PRDM1 regulatory network such as the regulation of RNA metabolic processes (splicing) and factors important for neural differentiation and embryonic morphogenesis (Figure 32). The latter observation is quite remarkable as no role was so far ascribed for PRDM1 in neural development. Moreover the Table 1 shows the lists of PRDM1 direct targets that were also up regulated or down regulated in NSPCs after PRDM1 KO and they represent interesting candidates to understand PRDM1 pathway in neurogenesis.

We concluded that NT2-D1 cell line is a useful tool where to study, at molecular level, some features of neural lineage commitment. As further proof, PRDMs – recently reported to be important for mammalian neurogenesis – were dynamically regulated during NT2-D1 differentiation evaluated at different time points (represented in the heatmap Fig 27).

These data strongly supported the already established role of PRDM1 as a master regulator important for developmental processes and extended it to neural differentiation.

Collectively our results represented the first profile of PRDM1 binding on a genomic scale and pave the way for the discovery of novel biological functions since to date no other comprehensive studies in human or mouse identified the PRDM1 global regulatory network using unbiased methods.

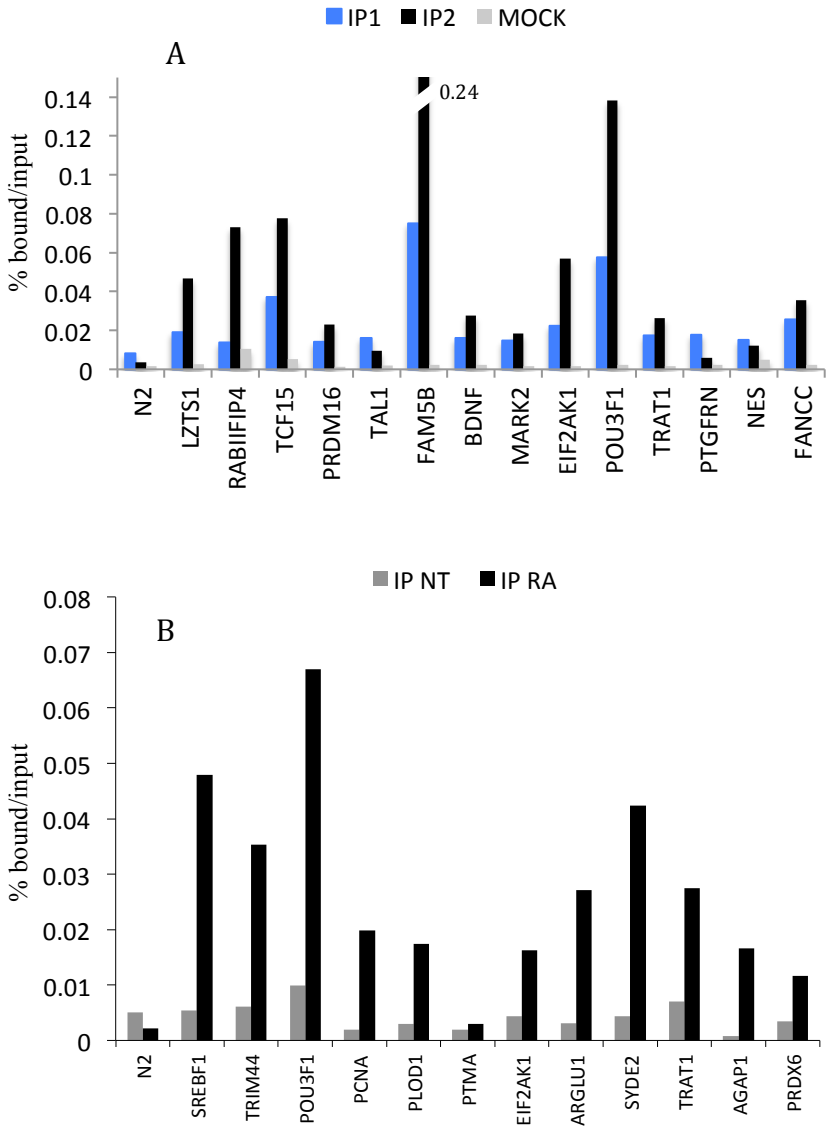

Figure 31. ChIP-qPCR validation of PRDM1 ChIP-seq. (A) Target regions of newly identified PRDM1 binding sites were validated by ChIP-qPCR in two indipendent experiments (IP1 and IP2). (B) Comparison between the ChIP performed in the cells treated with ATRA or non-treated (NT). N2 is a negative region used as control and mock experiment is ChIP performed using rabbit control IgG. In the y, the enrichments are calculated as the percentage on the input chromatin; in the x, the regions selected for primers design.

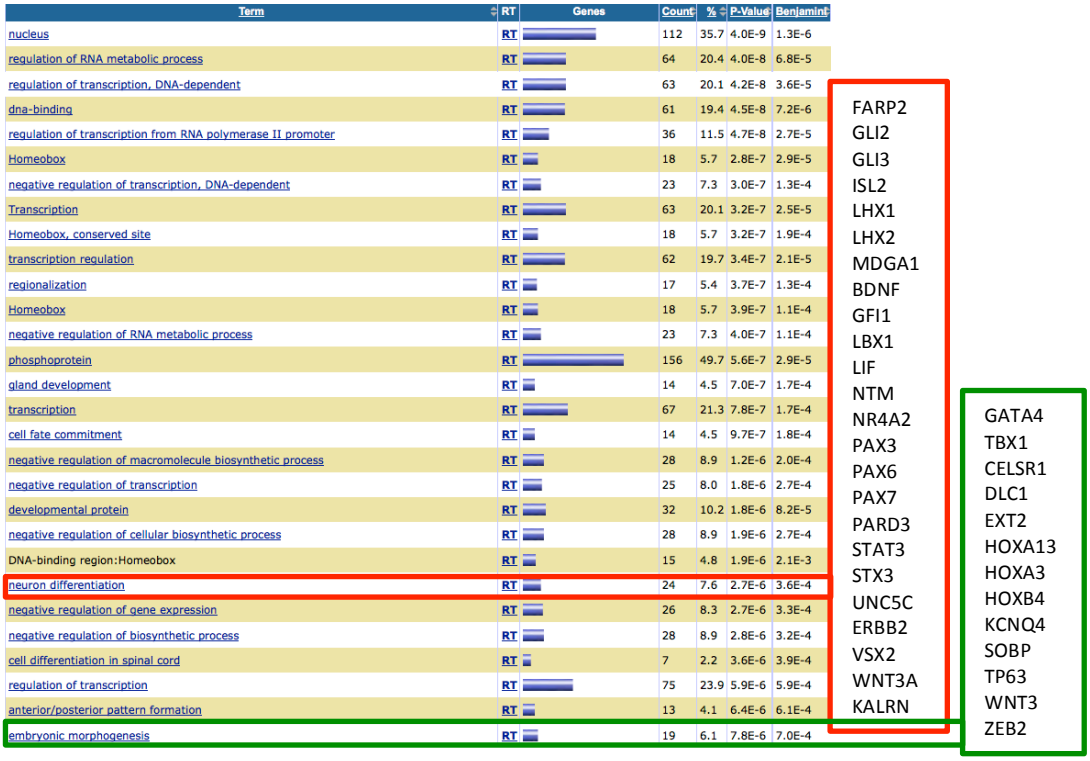

Term	RT	Genes	Count	%	P-Value	Benjamini
nucleus	RT		112	35.7	4.0E-9	1.3E-6
regulation of RNA metabolic process	RT		64	20.4	4.0E-8	6.8E-5
regulation of transcription, DNA-dependent	RT		63	20.1	4.2E-8	3.6E-5
dna-binding	RT		61	19.4	4.5E-8	7.2E-6
regulation of transcription from RNA polymerase II promoter	RT		36	11.5	4.7E-8	2.7E-5
Homeobox	RT		18	5.7	2.8E-7	2.9E-5
negative regulation of transcription, DNA-dependent	RT		23	7.3	3.0E-7	1.3E-4
Transcription	RT		63	20.1	3.2E-7	2.5E-5
Homeobox, conserved site	RT		18	5.7	3.2E-7	1.9E-4
transcription regulation	RT		62	19.7	3.4E-7	2.1E-5
regionalization	RT		17	5.4	3.7E-7	1.3E-4
Homeobox	RT		18	5.7	3.9E-7	1.1E-4
negative regulation of RNA metabolic process	RT		23	7.3	4.0E-7	1.1E-4
phosphoprotein	RT		156	49.7	5.6E-7	2.9E-5
gland development	RT		14	4.5	7.0E-7	1.7E-4
transcription	RT		67	21.3	7.8E-7	1.7E-4
cell fate commitment	RT		14	4.5	9.7E-7	1.8E-4
negative regulation of macromolecule biosynthetic process	RT		28	8.9	1.2E-6	2.0E-4
negative regulation of transcription	RT		25	8.0	1.8E-6	2.7E-4
developmental protein	RT		32	10.2	1.8E-6	8.2E-5
negative regulation of cellular biosynthetic process	RT		28	8.9	1.9E-6	2.7E-4
DNA-binding region:Homeobox	RT		15	4.8	1.9E-6	2.1E-3
neuron differentiation	RT		24	7.6	2.7E-6	3.6E-4
negative regulation of gene expression	RT		26	8.3	2.7E-6	3.3E-4
negative regulation of biosynthetic process	RT		28	8.9	2.8E-6	3.2E-4
cell differentiation in spinal cord	RT		7	2.2	3.6E-6	3.9E-4
regulation of transcription	RT		75	23.9	5.9E-6	5.9E-4
anterior/posterior pattern formation	RT		13	4.1	6.4E-6	6.1E-4
embryonic morphogenesis	RT		19	6.1	7.8E-6	7.0E-4

Figure 32. Enriched gene ontology (GO) in PRDM1 target genes obtained from Database for Annotation, Visualization, and Integrated Discovery (DAVID). The top ranking gene clusters in transcriptional regulator activity. Transcription factors involved in neurogenesis (in red) and embryonic development (in green) were also present in this list and the genes of these classes are indicated.

Common UP vs all	Common DOWN vs all
Ndrg2	Mier1
Agpat3	Slc38a2
Bcas3	Cnot6
Isoc2b	Six3
Zbtb4	Sox21
Pfkp	H3f3a
Ntsr2	Luc7l2
Zic1	Ccnl1
Bsg	Paip2
Acss2	Matr3
Dmrta2	Mtf2
Egln3	Zfp238
Gpi1	Tle4

Table 1. PRDM1 direct target genes are deregulated in NSPCs after PRDM1 KO. List of the genes that are directly bound by PRDM1 (ChIP-seq profile) and regulated after PRDM1 KO in NSPCs (RNA-seq profile).

3.4 Analysis of PRDM1 molecular mechanism

Our data suggested that PRDM1 preferentially represses genes that are essential for determining cell fate decisions during embryonic development as previously shown for Polycomb (PcG) proteins[198,199] via mechanisms that are not yet fully elucidated. Interestingly we observed a significant overlap between PRDM1 target promoters identified in human embryonic carcinoma cell line (NT2-D1) and the regulatory network controlled by PcG in human embryonic stem cells (hESC)[200]. We strengthened this observation by measuring also a substantial overlap between PRDM1 target promoters and H3K27me3 (a reversible repressive modification mediated by PcG) targets in hESC (69 out of 322)[201] (Figure 33A). Consequently we though that the common PRDM1/PcG promoters were more likely to be stably repressed during cellular differentiation. This hypothesis was supported by available datasets in IMR90 cells (a fibroblast cell line in which PRDM1 is expressed) whereby PRDM1 and PcG common genomic targets were enriched for H3K9 methylation (a more heritable repressive marker than H3K27me3)[201] meaning that these genes were stably silenced in the differentiated cells. From our dataset we selected three candidates for the validation of the hypothesis that were also PcG targets and positive for H3K27me3 in undifferentiated NT2 dataset[202]. We designed a "primer walking" (Fig 33 B) centred in the target promoters and we used it to amplify the DNA coming from ChIP performed at different time points during NT2-D1 commitment (untreated NT, 3, 7 and 21 days of ATRA treatment). As you can appreciate from Fig. 34 we observed that in the selected regions H3K9me3 increased during NT2-D1 differentiation. However we did not establish a direct role for PRDM1 in driving PcG complexes to the target promoters neither we correlated this evidence with a diminished expression of the selected genes since in NT2-D1 they were barely expressed and since in this undifferentiated cell line the global levels of both of H3K9 repressive marks were considerably higher than in hESC.

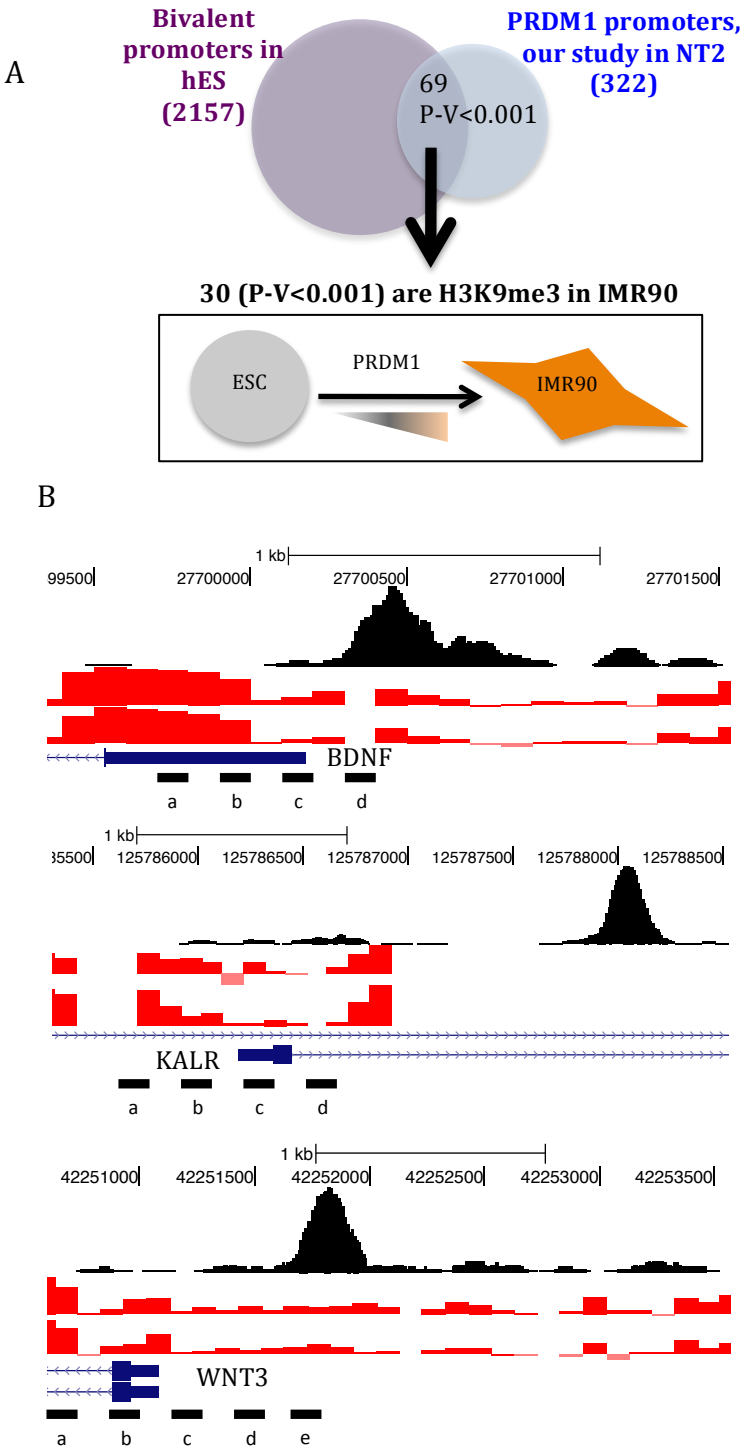

Figure 33. PRDM1 target genes are developmentally important and overlap with H3K27me3 in hESC. A) PRDM1 binding sites at the promoters overlap with bivalent domains in human embryonic stem cells (Venn diagram), source: Cell. 2010 October 15; 143(2): 313–324 B) PRDM1 ChIP-seq peaks in NT2-D1 after ATRA (black track) and H3K27me3 in NT2-D1 untreated cells (red tracks), source: O'Geen H, Squazzo SL, Iyengar S, Blahnik K, Rinn JL, et al. (2007) Genome-Wide Analysis of KAP1 Binding Suggests Autoregulation of KRAB-ZNFs. PLoS Genet 3(6): e89. doi:10.1371/journal.pgen.0030089. Three promoters (BDNF, KALRN and WNT3) were selected to check epigenetic changes during NT2 differentiation. Dashed line and letters (a, b, c, d) indicate the genomic regions where we designed the primers to amplify the DNA obtained from histone marks ChIP (see next picture).

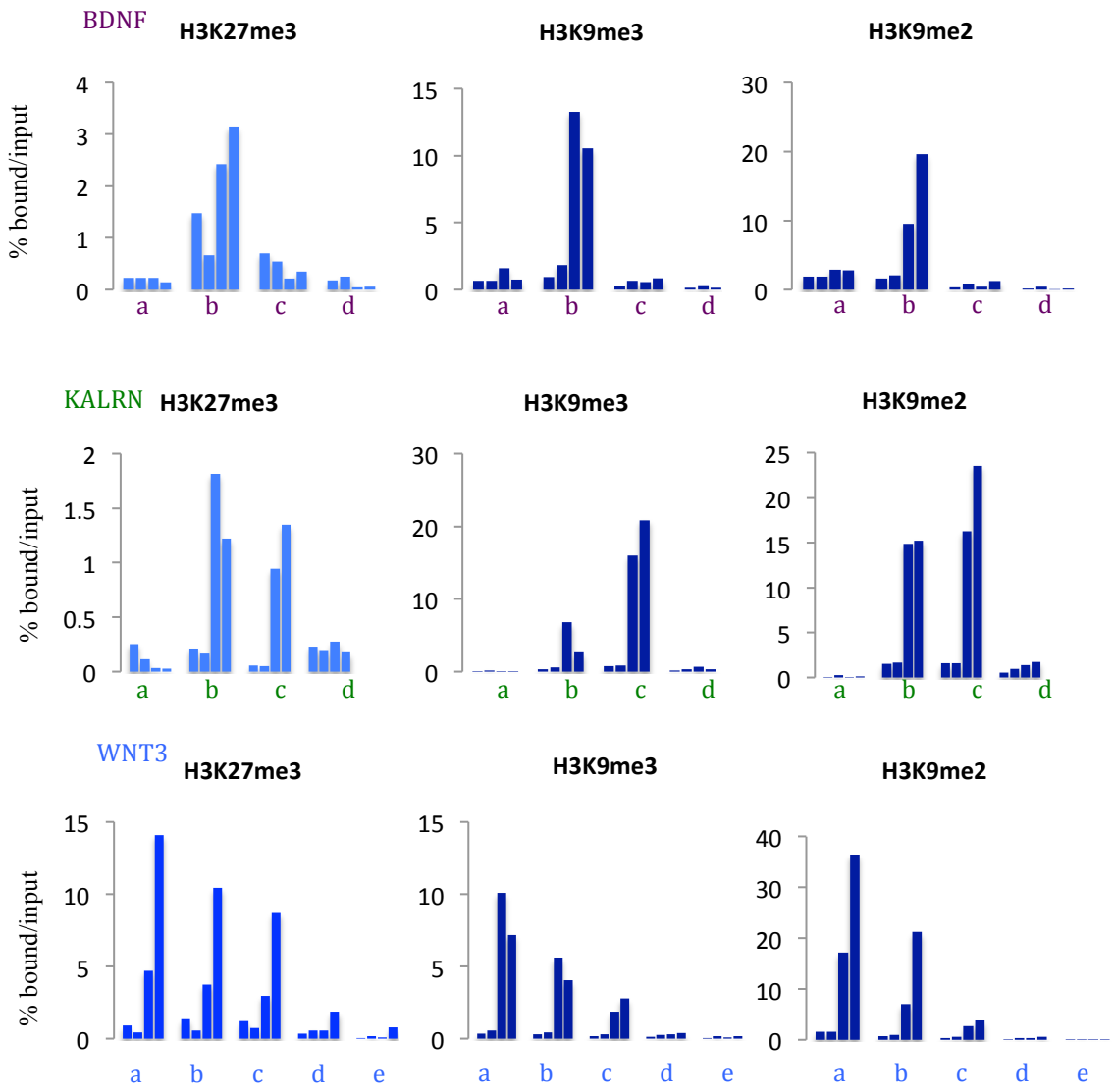

Figure 34. PRDM1 target genes are marked by overlapping repressive histone marks in differentiating NT2-D1. The regions a, b, c, d, e indicate the genomic regions amplified along the target promoters after ChIP (see Fig. 31). Each region was amplified in NT untreated NT2 and 3, 7 and 21 days after ATRA. Each histogram bar corresponds to a single time point (ordered from NT to 21) in the indicated region. In the y, the enrichments are calculated as the percentage on the input chromatin; in the x, the regions selected for primers design (from a to e, see Fig. 31).

We proposed therefore to further extend these observations by looking at other cell model systems where PRDM1 plays analogous functions (e.g. germ cells) in order to broaden this mechanistical insight to a validated model system of PRDM1 function.

These preliminary data supported the hypothesis that PRDM1 target genes are marked by overlapping repressive histone modifications in differentiating cells and it might explain

the mechanism by which the reversible transcriptional regulation mediated by PcG in ESCs is converted in permanent modifications of developmentally important genes during cellular differentiation.

3.5 PRDM1 reinforcement of PcG epigenetic repression in a model of in vitro germ cell differentiation

To investigate whether the proposed mechanism may hold true in a model system where PRDM1 function is biologically relevant we set up a model of in vitro cellular differentiation towards the germ cell lineage by the ectopic expression of deleted in azoospermia-like (Dazl) gene (Fig. 35A), which is an established germ cell developmental regulator. We selected Dazl stably expressing mouse ESC (mESC) clones (Fig. 35B) and we tested them for PRDM1 induction (Fig. 35C). PRDM1 expressing clones were allowed to differentiate by removing ESC medium components (2i medium and LIF) and supplementing it with serum. Progressively the cells stopped proliferating and down regulated pluripotency markers (Fig 35D).

Also in this case, for the validation of the mechanism, we selected as candidates developmentally important genes marked in mouse ESC with bivalent domains and that were both PcG (in mESCs) and PRDM1 (in NT2-D1) target genes (Fig 36A). Among this list of genes we choose GATA4, PAX6 and TAL1 because they were representative factors for development, being implicated in the formation of all the three germ layers: endoderm, ectoderm and mesoderm respectively. We looked at the expression level of these genes in differentiated mESCs verifying that PAX6 and TAL1 were efficiently down regulated when compared with WT mESCs, whereas GATA4 (in Appendix I) showed a strong up regulation (Fig. 36B).

We performed ChIP for post-translational histone modifications and we verified the quality using gapdh, RUNX1 and PU.1 promoters as controls of ChIP quality.

Epigenetic modifications at the promoters of these candidate genes reflected their transcriptional regulation: notably both PAX6 and TAL1 acquired H3K9me2 during

cellular differentiation while GATA4 (in Appendix I) showed undetectable levels of repressive histone mark (Fig 34D). We observed a general enrichment for H3K4me3 in mESC expressing DAZL that might correlate with swapping of cell culture medium from 2i to serum containing medium.

Concluding our mechanistic studies in a germ cell model system corroborated the observations made in NT2-D1 cells. We demonstrated in a biologically significant model system that two developmental important PRDM1 target genes were acquiring definitive repressive marks during cellular differentiation, an important clue since terminally differentiated cells showed different layers of epigenetic repression but the mechanisms responsible for that are still unclear.

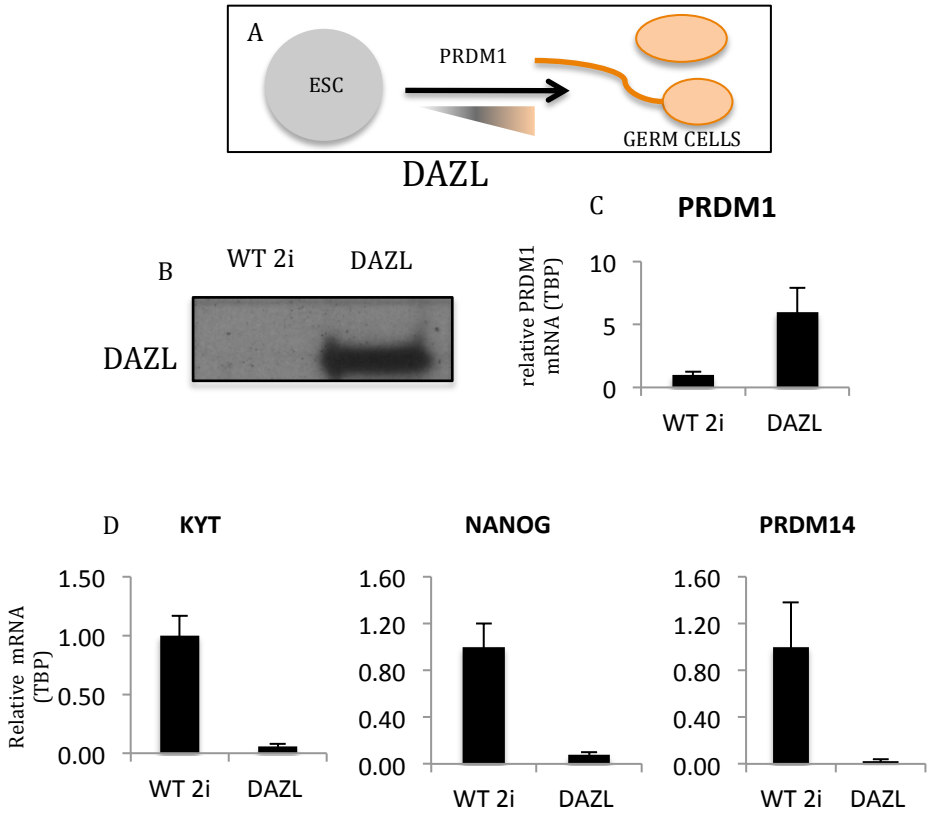

Figure 35. An in vitro model of mouse embryonic stem cells commitment into germ cell lineage. A) Schematic representation of the model system: mouse ESCs over-expressing DAZL are induced to differentiate to the germ cell lineage and up regulate PRDM1. B) DAZL stably expressing clones are selected after ectopic induction in mouse ESC. C) PRDM1 expression is induced in stable clones. D) Differentiated cells down regulate the expression of pluripotency markers. The values are normalized to TBP. 2i indicate that primary murine ESCs were kept in 2i medium.

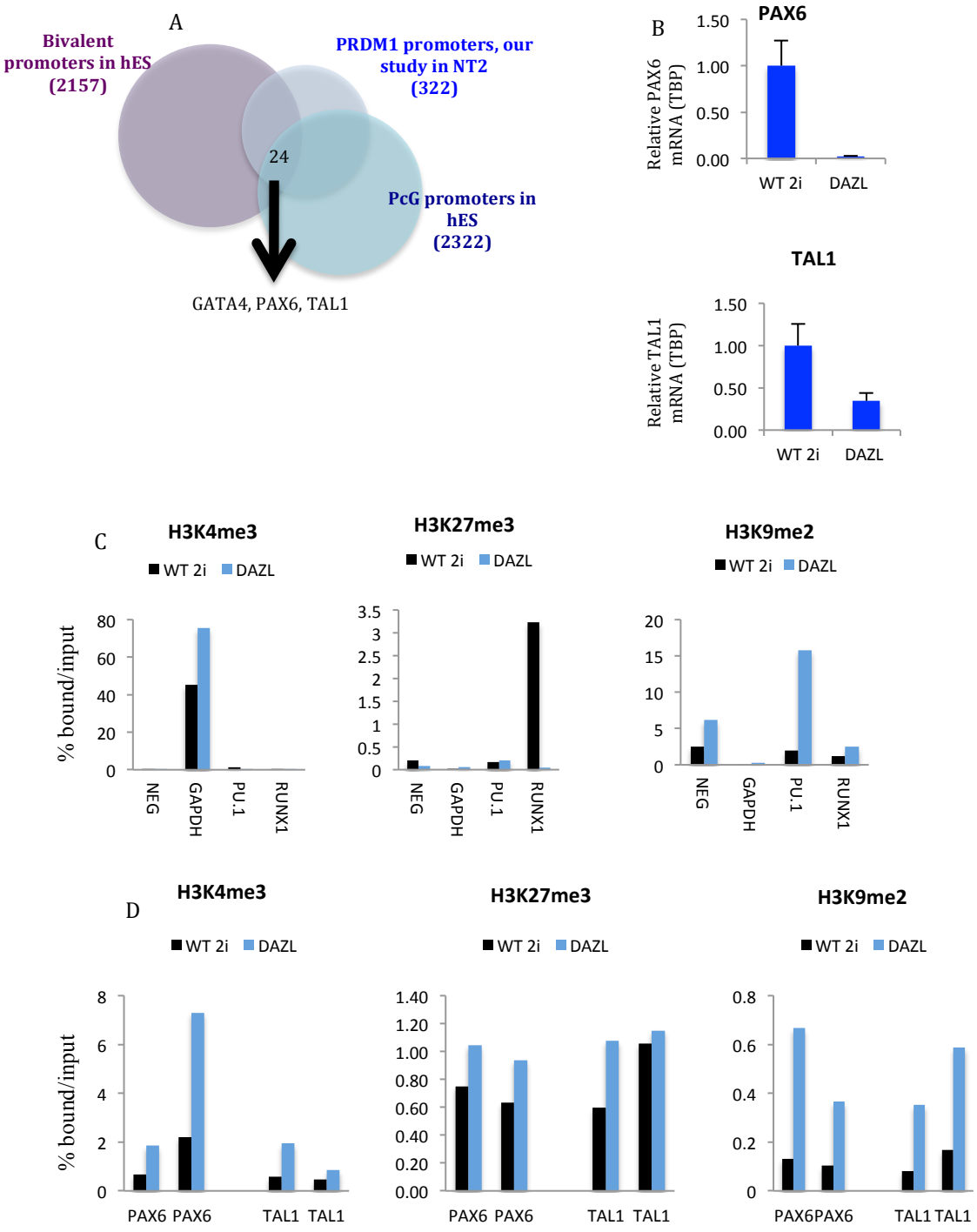

Figure 36. PRDM1 reinforces PcG epigenetic repression during germ cell commitment. A) PRDM1 target promoters in NT2-D1 overlap with bivalent domains and with PcG targets in hESCs. Three of these genes were choose for mechanism validation. B) PAX6 and TAL1 expression was efficiently repressed during germ cell differentiation, while GATA4 was up regulated (see Appendix I). C) Internal controls of H3K4me3 (gapdh) and of H3K27me3 and H3K9me2 (PU.1, RUNX1 and NEG) ChIP efficiency. D) Epigenetic profile of PAX6 and TAL1 promoters in WT and differentiated (DAZL) cells. In the y, the enrichments are calculated as the percentage on the input chromatin; in the x, the regions selected for primers design. GATA4 values are in Appendix I.

3.6 The role of PRDM1 in GBM

Since we achieved evidences for PRDM1 expression in neural progenitors and because PRDM1 is a tumor suppressor in the tissues where it exerts functional activity, we wondered whether it might also be involved in the most common malignant brain tumor of the adulthood that is the glioblastoma multiforme (GBM). In order to investigate this possibility we took advantage of the datasets generated by the large effort of the CANCER GENOME ATLAS (TCGA)[182,203], which described a gene expression-based molecular classification of GBM subtypes. Extrapolating PRDM1 values from this dataset we were able to appreciate that its expression is significantly higher in the GMB subtype named mesenchymal (Fig. 37C). We experimentally supported this observation by testing PRDM1 expression in different samples of GBM. Both PRDM1 isoforms (α and β) were highly expressed in GBM mesenchymal cell line (GBM166) as compared to normal foetal human NPCs (Fig. 37A). PRDM1 was also up regulated in murine GBM initiating cells (Ink4a/Arf -/-; EGFRVIIIhigh NPCs) originated from transformed NSPCs while it was not detected in similarly engineered astrocytes (Fig. 37B). Finally we observed that PRDM1 expression was restricted to a limited number of human GBM derived stem cells, possibly in line with its expression being subtype-dependent. As control, BMI1 - which is a well-known stem cell regulator - was expressed in nearly all of the lines.

Consequently we wanted to directly correlate the effect of PRDM1 deletion during the development of GBM. We exploited this issue by using mouse genetics for the creation of GBM in a WT or conditionally mutant PRDM1 background. In our mouse model of GBM we combined heterozygous germ line mutation of p53 with brain orthotropic inoculation of constitutively active RAS form ($HRas^{V12}$). These mice were also transgenic for tamoxifen inducible Cre ricombinase that was administered by oral gavage in order to obtain PRDM1 conditional deletion (Fig. 38A). We successfully obtained Cre-mediated recombination in the brain of the treated animals (Fig. 38B) meaning that tamoxifen efficiently overcame

blood brain barrier. Some of the treated animals were sacrificed before tumor development (around two months after H-Ras^{V12} inoculation) since they were suffering for unrelated causes (more probably for consequences of tamoxifen toxicity and evident dermatitis).

We are currently collecting the first results of this experiment that are presented in the AppendixII.

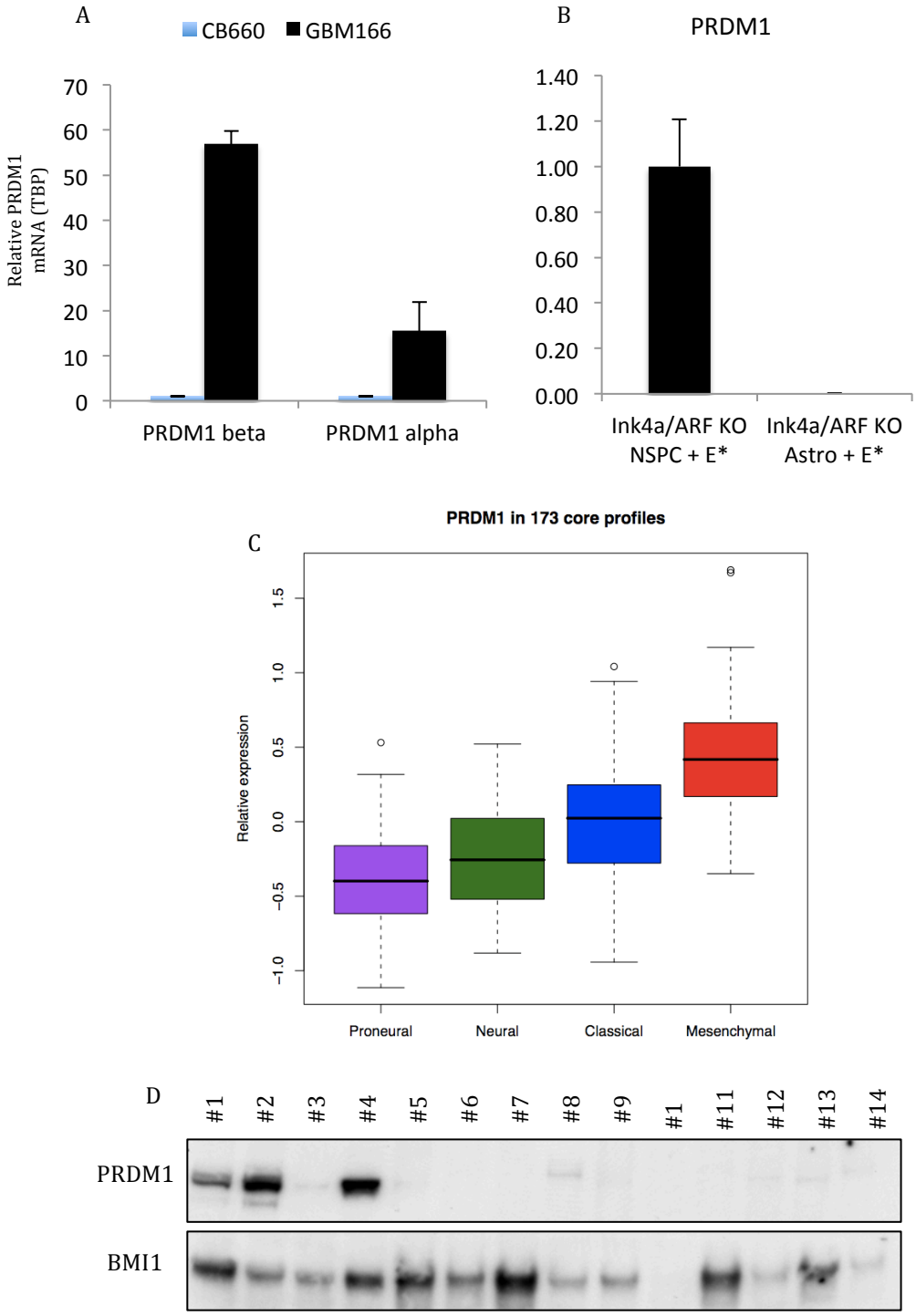

Figure 37. PRDM1 expression in GBM. A) PRDM1 alpha and beta are highly expressed in human mesenchymal GBM cell line (GBM166 – Pollard-Smith-Dirks Cell Stem Cell) while their expression is faint in human foetal neural progenitor cells CB660 (Pollard-Smith-Dirks Cell Stem Cell). B) PRDM1 is strongly up regulated in murine glioma initiating cells derived from transformed NSPc while tumorigenic astrocytes did not express PRDM1. C) PRDM1 expression is significantly higher in a specific subtype of GBM named "Mesenchymal". Source: TCGA D) PRDM1 expression in cancer stem cells derived from different human GBMs.

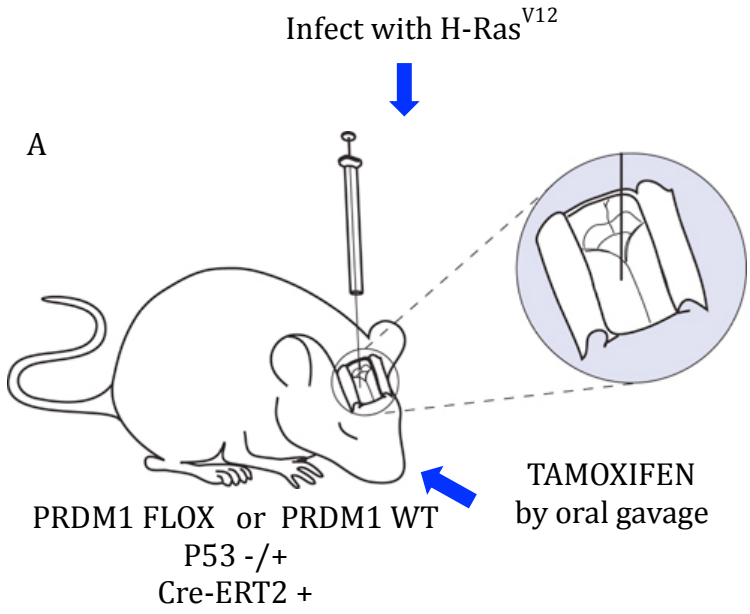

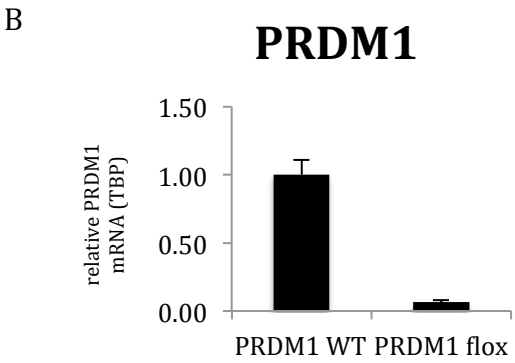

Figure 38. Generation of a spontaneous mouse model of GBM. A) PRDM1FLOX or WT/P53heterozygous/ER-Cre mice were infected by orthotropic inoculation with lentivirus carrying mutated oncogenic HRasV12 (see text). These mice were orally administered with tamoxifen to activate Cre ricombinase in order to delete PRDM1FLOX locus. B) PRDM1 was efficiently deleted in the forebrain of PRDM1-FLOX/P53 heterozygous/ER-CRE comparing with PRDM1 WT mice.

Chapter 4 – DISCUSSION

In our quest for the characterization of the mechanisms by which PRDM1 regulates direct target genes during cell fate commitment, we obtained several molecular and biological hints that shed light on previously unreported PRDM1 function. Below we discuss our findings and the implications for future research.

4.1 PRDM1 is expressed in neural progenitor cells: implications in adult neurogenesis.

Here we presented evidence of PRDM1 expression and function in adult neural progenitor cells of the mouse brain reinforcing the already established role of PRDM1 as a cell fate determinant and extending it to an unexplored tissue: the mammalian brain.

Piece of data in low model organisms for development (zebrafish and Xenopus) pointed out the relevance of PRDM1 in the specification of both peripheral and central nervous system structures. However, in mammals PRDM1 – despite being expressed in the embryonic tissues deputed to anterior patterning – seemed to be dispensable for forebrain and head formation. This observation does not contrast with an important role of PRDM1 in adult stem cells; in fact, other transcriptional regulators such as Bmi1 are also dispensable for embryonic development, yet required for the maintenance of adult neural stem cells. Concerning this, we noted that mice, in which PRDM1 was conditionally deleted in Nestin positive neural progenitor cells, were apparently not compromised in the development. Nonetheless, future studies will be required to elucidate this matter, since we did not perform in deep histopathological analyses to formally exclude its role in embryonic neurogenesis.

Through genetic tracing experiments we clearly demonstrated that PRDM1 is expressed in neural stem and progenitor cells (NSPCs). NSPCs derived from the subventricular zone (SVZ) are a heterogeneous mix of different cell types with variable levels of pluripotency (the ability of self renew and to differentiate in any cell type) and with distinct physical properties. Phenotypical analysis of NSPCs from WT and PRDM1mVenus knock-in mice

was assessed to some extent by using forward scatter (FSC) and side scatter (SSC) parameters (representing cell-size and cellular granularity respectively). Our results highlighted that PRDM1mVenus negative cells were confined in the FSC/SSC$^{mid-low}$ a morphological feature associated with minor ability in neurospheres formation and lower multipotency. Conversely, when compared with the bulk of NSPCs and with negative control (WT NSPCs), Venus-positive cells were found four-fold enriched in the FSC/SSC^{high} population typical of more immature neural stem cells and eight fold enriched in FSC^{low}SSC^{high} a morphologically different population of neural stem cells that increases at later stages of development[204].

Importantly, genetic depletion of PRDM1 in NSPCs further demonstrated that the absence of PRDM1 correlates with a more differentiated phenotype, which was assessed by the ability to form neurospheres in vitro and by gene expression profile experiments (RNA-sequencing and qRT-PCR).

Specifically we used neurosphere formation assay – a culture system in which neural stem and more immature progenitor cells selectively proliferate to form multicellular aggregates, the so called neurospheres – by plating the cells at a very low density and waiting for the formation of secondary derived clones. PRDM1 KO neural stem cells were not properly maintained since they were forming fewer and smaller neurospheres comparing with WT cells. At the second re-plating, in the same growing conditions, KO cells displayed also a different morphology more similar to neural differentiated cells. Anyway keeping the cells in standard plating conditions (at a density of 150 cells per microliter) we easily expanded in culture both WT as well KO NSPCs and we propagated them to investigate genome wide expression changes caused by PRDM1 deletion.

Confirming previous observations, in genome wide expression analyses, we showed that five up regulated genes in PRDM1 KO NSPCs are among the top score cell type specific markers used to defined astrocytes: Aqp4, Gfap, Atp1a2, Ntsr2 and ApoE, while we did not identify any neuronal specific marker and only Mbp for oligodendrocytes. While this is

not surprising, taking into account the prevalence of astrocytic commitment of NSPCs in vitro, nonetheless the genes that are deregulated in PRDM1 KO NSPCs were variably represented in the three major brain cell types – astrocytes, neurons and oligodendrocytes – meaning that PRDM1 dependent genes are expressed in terminally differentiated brain cells. While a major set of the PRDM1-dependent genes as revealed by our RNA-sequencing analysis showed a good concordance with RT-qPCR validation in independent samples, the incomplete validation of our profiles urge reticence when drawing single-gene conclusions without prior validation. Future studies should aim at identifying more precisely genes that depend on PRDM1 for their appropriate expression in vivo, possibly combining several independent replica. Notably, however, we fully recapitulated by gene expression profiles, the more differentiated phenotype of PRDM1-depleted NPCs as being the glial fibrillary acidic protein (Gfap) - a well-known marker of astrocytes and glial cells – the gene more up regulated in CKO cultured cells. Other genes preferentially expressed in astrocytes followed the same trend of Gfap in qRT-PCR (Vegfα, Ndrg2, Acss2, Cav1, Ntsr2) but also a couple of neuronal specific genes were substantially up regulated (Pfkp and Bsg). Moreover we consistently correlated reporter signal localization, genetic tracing and functional ablation experiments, with actual PRDM1 expression in primary cells. In fact, PRDM1 protein was detected in NSPCs derived from adult mice, while it was undetectable in cortical astrocytes. Accordingly, PRDM1 was also down regulated in NSPCs induced to differentiate with BMP4.

Together, our experimental procedures are indicative of a positive role for PRDM1 in neural stem cell self-renewal. Due to the technical challenges to be overcome when blindly analyzing neural stem cells proliferation defects in vivo, the nature and the extent of PRDM1 deletion defects on the adult neurogenesis await future studies, possibly driven by a prior genetic lineage tracing in vivo for PRDM1 expressing cells progeny, which would significantly ease the identification of specific compartments where PRDM1 defects can be reasonably scored.

Furthermore, also the precise mechanism by which PRDM1 may sustain NSPCs self-renewal has not been demonstrated and will require ad hoc experiments. In fact, neurosphere formation could be maintained in higher plating cell density (at a density of 150 cells per microliter). With these conditions we easily expanded in culture both WT as well as KO NSPCs and we easily propagated them.

Two additional observations were interesting in our gene expression analysis. First, the search for statistically enriched canonical pathways performed with IPA tool (Ingenuity System) resulted in a strong representation of terms involved in Glycolisis/Gluconeogenesis, a metabolic pathway characteristic of astrocytes to promote synaptic activity[197]. Second, while PRDM1 consensus sequence (IRFs-like, which contains GAAAG) was not statistically overrepresented, one of the top score matrixes identified was the Hypoxia Inducible Factor 1 alpha (HIF1α). Accordingly Hif1α signaling was the sixth more enriched canonical pathway in PRDM1 dependent genes. Hif1α mediates cellular responses to hypoxia. It is expressed throughout the whole body but in normoxia conditions it is degraded in most cell types and tissues. Interestingly in adult brain neurogenic tissues and in NSPCs this activator it is continuously expressed and stabilized and it is important for the correct neural differentiation[205]. Based on our results we can hypothesize that PRDM1 and HIF1α might be co-expressed in NSPCs and counteract for the regulation of common gene targets but with opposite effects being PRDM1 mainly known as a transcriptional repressor and HIF1α as a transcriptional activator. This represents a common mechanism of PRDM1 target genes regulation already described in plasmacell, where PRDM1 and BCL6 counteract for effector versus memory cell phenotype, or in dendritic cells, where PRDM1 represses whereas IRF8/PU.1 activates CIITA gene. While we will refer for the confirmation of this hypothesis to further experiments it is tempting to speculate that PRDM1 and HIF1α may have opposite outcomes on common targets in NSPCs, and it is intriguing to observe that in PRDM1 KO NSPCs, Vefgα – a HIF1α known target gene – was significantly up regulated.

4.2 PRDM1 regulatory network analysis: implications for target genes regulation during cell fate commitment.

PRDM1 plays critical role in development and structurally it is characterized by an amino terminal PR/SET domain and five C_2H_2 zinc fingers at the carboxyl terminal that mediate DNA binding, nuclear localization and recruitment of histone modification enzymes[163,206]. These properties account for its ability to regulate cell fate decisions and tissue homeostasis by sequence specific DNA binding. Nonetheless still a gap exists between the functional relevance of PRDM1 in many contexts and the complete knowledge of its regulatory network. In specific model systems and through indirect gene expression profile, a set of putative PRDM1 target genes has been reported for germ cells[54]. To date, only few direct target genes have been identified in mammals, possibly due to technical limitations in obtaining high-quality genome wide profiles for this transcription factor.

Indeed, we had to face with diverse technical solutions before being successful in PRDM1 chromatin immunoprecipitation (ChIP). We screened several commercially available and group-restricted antisera in order to identify the one with highest specificity under ChIP conditions. Furthermore, we need to refine our ChIP protocol to account for the low sensitivity of the immunoprecipitation process.

To our knowledge, here we report the first genome wide profile for PRDM1 in mammalian cells.

During plasmacell differentiation, PRDM1 modulates INF-gamma response after viral infection by directly repressing MHC CIITA gene. In this context it was demonstrated, in a luciferase reporter assay, that PRDM1 bind IRF-E sequences and compete with IRF-1/IRF-2 activators for CIITA promoter binding[207]. In our experimental settings (NT2-D1 cells) we found that in differentiating cells PRDM1 binding site is strikingly similar to IRF-E, extending the competitive model of PRDM1 and IRF interaction beyond the INF-gamma mediated induction and extending the number of in vivo PRDM1 direct binding sites. Additional motif discovery and co-expression analysis in NT2-D1, revealed the possible

interaction also between PRDM1 with SP1 and AP2 transcription factors. Notably these proteins also act as general transcriptional activators, reinforcing the concept that PRDM1 may oppose to unwanted transcriptional activation of cell type specific targets.

Together our data represented a solid ground to comprehensively achieve PRDM1 functional network during cellular differentiation. They integrated two genome wide studies (RNAseq and ChIPseq) that extended the current knowledge about the spectrum of PRDM1 biological roles and also contributed to the identification of new PRDM1 binding regions, important for cell fate commitment.

Lineage-commitment is associated with the progressive and specific restriction of genome accessibility[208]. This process has been correlated with the acquisition of repressive histone post-translational modifications. For instance, differentiated embryonic stem cells (ESCs) present large scale regions of H3K9me2, a modification catalyzed by and dependent on the histone lysine methyltransferase G9a[209]. Polycomb group proteins (PcG) regulate the repression of developmentally important genes in order to ensure correct cell fate decisions in part through the deposition of H3K27me3[198,199]. Interestingly, in more differentiated foetal lung fibroblasts, H3K27me3 mark is overlaid by an additional repressive histone post-translational modification, the H3K9me3[201]. Furthermore, PcG target genes in terminally differentiated astrocytes are permanently silenced through DNA methylation[210]. All these reports suggest that PcG mediated repression, which is considered transient and reversible, is reinforced by additional layers of chromatin associated post-translational modifications.

Nonetheless the precise mechanisms by which this may occur have not yet been discovered. PRDM1 directly associate with G9a[38] and here we showed that it binds to PcG target genes in ESCs and that these acquire H3K9me2 and H3K9me3 in differentiated fibroblasts that express PRDM1. It is tempting to speculate that PRDM1 is one of those cell fate transcription factors, which are involved in establishing a definitive transcriptional repressive landscape in terminally differentiated cells.

Our data have been generated in NT2-D1 cells, which are embryonic carcinoma cells (the malignant counterpart of ESCs), capable of differentiating into mature neurons upon to exposure to retinoic acid. While the relation of NT2-D1 with normal cell types is questionable, this model has been successfully used to dissect the mechanistical repression of PcG target genes during neural lineage commitment[211], which acquires confidence into our mechanistical description of BDNF, KALRN and WNT3A repression.

In the attempt of increasing the biological relevance of our findings to a model system where PRDM1 is biological required, we (partly) differentiated mouse ESCs into germ cells, through the over-expression of DAZL, and we used them to evaluate the epigenetic status of developmentally important genes (PcG and PRDM1 common targets). We demonstrated that the expression of TAL1 and PAX6 genes was down regulated after PRDM1 induction and that their promoters acquired higher levels H3K9me2 than control ESCs. Further functional experiments such as RNAi, and genetic rescue, will be required to precisely demonstrate the involvement of PRDM1 in this novel mechanistical detail of transcriptional repression.

4.3 PRDM1 expression and possible involvement in Glioblastoma multiforme.

Since PRDM genes are often tumor suppressors in the tissues where they exert their activity[166] and since adult brain cancers possibly arise from transformed neural stem cells[212], we searched for evidences of PRDM1 in human GBM, the most common form of brain cancer in adults.

Interestingly, not only PRDM1 is highly expressed in GBM[182], but also it significantly correlated with a particular GBM subtype called mesenchymal. In support of this observation we detected high levels of PRDM1 (both human PRDM1 isoforms α and β) expression in a human mesenchymal GBM cell line (GBM166[213]). Furthermore, PRDM1 is expressed in murine GBM initiating cells (Ink4a/Arf-/-; EGFRVIII NPCs), which prompted us to investigate the functional role of PRDM1 in a spontaneous mouse model of GBM.

While experimental, our model system is related to human pathology. The conditional deletion of PRDM1 was obtained by crossing mice carrying floxed PRDM1 alleles with transgenic mice that express Cre recombinase under the control of a tamoxifen inducible promoter, in a p53 heterozygous background, a pathway mutated in approximately 40% of the human GBM 14. We induced tumors using $HRas^{V12}$ that has not been itself directly found mutated in GBM. However, its pathway is up regulated through EGFR and PDGFR amplifications or NF1 mutations[214], and RAS carrying lentivirus generated GBM like lesion in mice[215]. To date, our data are very preliminary but still meaningful. In fact, we obtained tumors from both PRDM1 competent and KO background (see Appendix II), but the extent of GBM penetrance and the preliminary analyses of the lesions suggest a divergence with former literature: PRDM1 seems to be required for tumor initiation, and thus may act as an oncogene in GBM.

This is certainly quite preliminary evidence, and we stress a cautionary note here. Nevertheless, the positive role for PRDM1 in neural stem cells self-renewal, is indeed compatible with our preliminary findings in GBM. It is also worth mentioning that a PRDM1 target gene in NT2-D1, which is also de-regulated in PRDM1 KO NSCs, has been recently found mutated in human GBM. It is the case of the H3f3a gene[216-218]. This gene, which codifies for the replication independent histone variant H3.3, seems to influence the epigenetic pattern of the cancer cells that show a widespread hypomethylation, possibly having a tumor suppressive function. Notably, in human GBM it inversely correlates with PRDM1, which could underpin a functional relationship. We are currently characterizing by histology (neo-angiogenesis, necrosis, mitotic activity) and immunohistochemistry (PRDM1, nestin and other markers to characterize cancer cells expression profile) the generated tumors. Furthermore we are in the process of enlarging our cohort of mice in order to get statistically significant information about the role of PRDM1 in GBM. If our analyses will confirm that functional PRDM1 is required in our spontaneous mouse model of GBM, we would proceed to a more in depth mechanistical dissection.

In conclusion, my study led to the elucidation of PRDM1 target gene regulation, highlighting a role for PRDM1 in stable and heritable gene silencing during differentiation, and provides a resource for further mechanistical studies. Most notably however, the analysis of PRDM1 regulatory network led us to investigate an exciting new hypothesis: the positive regulation for PRDM1 of normal and cancer stem cell self renewal.

REFERENCES

1 Gualdi, R. *et al.* Hepatic specification of the gut endoderm in vitro: cell signaling and transcriptional control. *Genes Dev* **10**, 1670-1682 (1996).

2 Xu, J. *et al.* Pioneer factor interactions and unmethylated CpG dinucleotides mark silent tissue-specific enhancers in embryonic stem cells. *Proc Natl Acad Sci U S A* **104**, 12377-12382, doi:10.1073/pnas.0704579104 (2007).

3 Xu, J. *et al.* Transcriptional competence and the active marking of tissue-specific enhancers by defined transcription factors in embryonic and induced pluripotent stem cells. *Genes Dev* **23**, 2824-2838, doi:10.1101/gad.1861209 (2009).

4 Tenen, D. G. Disruption of differentiation in human cancer: AML shows the way. *Nat Rev Cancer* **3**, 89-101, doi:10.1038/nrc989 (2003).

5 Natoli, G. Maintaining cell identity through global control of genomic organization. *Immunity* **33**, 12-24, doi:10.1016/j.immuni.2010.07.006 (2010).

6 Kallies, A. & Nutt, S. L. Terminal differentiation of lymphocytes depends on Blimp-1. *Curr Opin Immunol* **19**, 156-162, doi:10.1016/j.coi.2007.01.003 (2007).

7 Kallies, A. *et al.* Initiation of plasma-cell differentiation is independent of the transcription factor Blimp-1. *Immunity* **26**, 555-566, doi:10.1016/j.immuni.2007.04.007 (2007).

8 Huang, S. Blimp-1 is the murine homolog of the human transcriptional repressor PRDI-BF1. *Cell* **78**, 9 (1994).

9 Keller, A. D. & Maniatis, T. Identification and characterization of a novel repressor of beta-interferon gene expression. *Genes Dev* **5**, 868-879 (1991).

10 Turner, C. A., Jr., Mack, D. H. & Davis, M. M. Blimp-1, a novel zinc finger-containing protein that can drive the maturation of B lymphocytes into immunoglobulin-secreting cells. *Cell* **77**, 297-306 (1994).

11 Buyse, I. M., Shao, G. & Huang, S. The retinoblastoma protein binds to RIZ, a zinc-finger protein that shares an epitope with the adenovirus E1A protein. *Proc Natl Acad Sci U S A* **92**, 4467-4471 (1995).

12 Fears, S. *et al.* Intergenic splicing of MDS1 and EVI1 occurs in normal tissues as well as in myeloid leukemia and produces a new member of the PR domain family. *Proc Natl Acad Sci U S A* **93**, 1642-1647 (1996).

13 Oliver, P. L. *et al.* Accelerated evolution of the Prdm9 speciation gene across diverse metazoan taxa. *PLoS Genet* **5**, e1000753, doi:10.1371/journal.pgen.1000753 (2009).

14 Sun, X. J. *et al.* Genome-wide survey and developmental expression mapping of zebrafish SET domain-containing genes. *PLoS One* **3**, e1499, doi:10.1371/journal.pone.0001499 (2008).

15 Fumasoni, I. *et al.* Family expansion and gene rearrangements contributed to the functional specialization of PRDM genes in vertebrates. *BMC Evol Biol* **7**, 187, doi:10.1186/1471-2148-7-187 (2007).

16 Allis, C. D. *et al.* New nomenclature for chromatin-modifying enzymes. *Cell* **131**, 633-636, doi:10.1016/j.cell.2007.10.039 (2007).

17 Rea, S. *et al.* Regulation of chromatin structure by site-specific histone H3 methyltransferases. *Nature* **406**, 593-599, doi:10.1038/35020506 (2000).

18 Cao, R. & Zhang, Y. The functions of E(Z)/EZH2-mediated methylation of lysine 27 in histone H3. *Curr Opin Genet Dev* **14**, 155-164, doi:10.1016/j.gde.2004.02.001 (2004).

19 Jenuwein, T., Laible, G., Dorn, R. & Reuter, G. SET domain proteins modulate chromatin domains in eu- and heterochromatin. *Cell Mol Life Sci* **54**, 80-93 (1998).

20 Wilson, J. R. *et al.* Crystal structure and functional analysis of the histone methyltransferase SET7/9. *Cell* **111**, 105-115 (2002).

21 Xiao, B. *et al.* Structure and catalytic mechanism of the human histone methyltransferase SET7/9. *Nature* **421**, 652-656, doi:10.1038/nature01378 (2003).

22 Hamamoto, R. *et al.* SMYD3 encodes a histone methyltransferase involved in the proliferation of cancer cells. *Nat Cell Biol* **6**, 731-740, doi:10.1038/ncb1151 (2004).

23 Trievel, R. C., Beach, B. M., Dirk, L. M., Houtz, R. L. & Hurley, J. H. Structure and catalytic mechanism of a SET domain protein methyltransferase. *Cell* **111**, 91-103 (2002).

24 Manzur, K. L. *et al.* A dimeric viral SET domain methyltransferase specific to Lys27 of histone H3. *Nat Struct Biol* **10**, 187-196, doi:10.1038/nsb898 (2003).

25 Martin, C. & Zhang, Y. The diverse functions of histone lysine methylation. *Nat Rev Mol Cell Biol* **6**, 838-849, doi:10.1038/nrm1761 (2005).

26 Derunes, C. *et al.* Characterization of the PR domain of RIZ1 histone methyltransferase. *Biochem Biophys Res Commun* **333**, 925-934, doi:10.1016/j.bbrc.2005.05.190 (2005).

27 Eom, G. H. *et al.* Histone methyltransferase PRDM8 regulates mouse testis steroidogenesis. *Biochem Biophys Res Commun* **388**, 131-136, doi:10.1016/j.bbrc.2009.07.134 (2009).

28 Hayashi, K., Yoshida, K. & Matsui, Y. A histone H3 methyltransferase controls epigenetic events required for meiotic prophase. *Nature* **438**, 374-378, doi:10.1038/nature04112 (2005).
29 Pinheiro, I. *et al.* Prdm3 and Prdm16 are H3K9me1 Methyltransferases Required for Mammalian Heterochromatin Integrity. *Cell* **150**, 948-960, doi:10.1016/j.cell.2012.06.048 (2012).
30 Davis, C. A. *et al.* PRISM/PRDM6, a transcriptional repressor that promotes the proliferative gene program in smooth muscle cells. *Mol Cell Biol* **26**, 2626-2636, doi:10.1128/MCB.26.7.2626-2636.2006 (2006).
31 Wu, Y. *et al.* PRDM6 is enriched in vascular precursors during development and inhibits endothelial cell proliferation, survival, and differentiation. *J Mol Cell Cardiol* **44**, 47-58, doi:10.1016/j.yjmcc.2007.06.008 (2008).
32 Duan, Z. *et al.* Epigenetic regulation of protein-coding and microRNA genes by the Gfi1-interacting tumor suppressor PRDM5. *Mol Cell Biol* **27**, 6889-6902, doi:10.1128/MCB.00762-07 (2007).
33 Bartholomew, C., Kilbey, A., Clark, A. M. & Walker, M. The Evi-1 proto-oncogene encodes a transcriptional repressor activity associated with transformation. *Oncogene* **14**, 569-577, doi:10.1038/sj.onc.1200864 (1997).
34 Brayer, K. J. & Segal, D. J. Keep your fingers off my DNA: protein-protein interactions mediated by C2H2 zinc finger domains. *Cell Biochem Biophys* **50**, 111-131, doi:10.1007/s12013-008-9008-5 (2008).
35 Cattaneo, F. & Nucifora, G. EVI1 recruits the histone methyltransferase SUV39H1 for transcription repression. *J Cell Biochem* **105**, 344-352, doi:10.1002/jcb.21869 (2008).
36 Kajimura, S. *et al.* Initiation of myoblast to brown fat switch by a PRDM16-C/EBP-beta transcriptional complex. *Nature* **460**, 1154-1158, doi:10.1038/nature08262 (2009).
37 Seale, P. *et al.* PRDM16 controls a brown fat/skeletal muscle switch. *Nature* **454**, 961-967, doi:10.1038/nature07182 (2008).
38 Gyory, I., Wu, J., Fejer, G., Seto, E. & Wright, K. L. PRDI-BF1 recruits the histone H3 methyltransferase G9a in transcriptional silencing. *Nat Immunol* **5**, 299-308, doi:10.1038/ni1046 (2004).
39 Chia, N. Y. *et al.* A genome-wide RNAi screen reveals determinants of human embryonic stem cell identity. *Nature* **468**, 316-320, doi:10.1038/nature09531 (2010).
40 Saitou, M. Germ cell specification in mice. *Curr Opin Genet Dev* **19**, 386-395, doi:10.1016/j.gde.2009.06.003 (2009).
41 Zhang, Y. *et al.* PR-domain-containing Mds1-Evi1 is critical for long-term hematopoietic stem cell function. *Blood* **118**, 3853-3861, doi:10.1182/blood-2011-02-334680 (2011).
42 Chang, D. H., Cattoretti, G. & Calame, K. L. The dynamic expression pattern of B lymphocyte induced maturation protein-1 (Blimp-1) during mouse embryonic development. *Mech Dev* **117**, 305-309 (2002).
43 Aguilo, F. *et al.* Prdm16 is a physiologic regulator of hematopoietic stem cells. *Blood* **117**, 5057-5066, doi:10.1182/blood-2010-08-300145 (2011).
44 Vincent, S. D. *et al.* The zinc finger transcriptional repressor Blimp1/Prdm1 is dispensable for early axis formation but is required for specification of primordial germ cells in the mouse. *Development* **132**, 1315-1325, doi:10.1242/dev.01711 (2005).
45 de Souza, F. S. *et al.* The zinc finger gene Xblimp1 controls anterior endomesodermal cell fate in Spemann's organizer. *Embo J* **18**, 6062-6072, doi:10.1093/emboj/18.21.6062 (1999).
46 Baxendale, S. *et al.* The B-cell maturation factor Blimp-1 specifies vertebrate slow-twitch muscle fiber identity in response to Hedgehog signaling. *Nat Genet* **36**, 88-93, doi:10.1038/ng1280 (2004).
47 Ohinata, Y., Sano, M., Shigeta, M., Yamanaka, K. & Saitou, M. A comprehensive, non-invasive visualization of primordial germ cell development in mice by the Prdm1-mVenus and Dppa3-ECFP double transgenic reporter. *Reproduction* **136**, 503-514, doi:10.1530/REP-08-0053 (2008).
48 Horsley, V. *et al.* Blimp1 defines a progenitor population that governs cellular input to the sebaceous gland. *Cell* **126**, 597-609, doi:10.1016/j.cell.2006.06.048 (2006).
49 Magnusdottir, E. *et al.* Epidermal terminal differentiation depends on B lymphocyte-induced maturation protein-1. *Proc Natl Acad Sci U S A* **104**, 14988-14993, doi:10.1073/pnas.0707323104 (2007).
50 Kuo, T. C. & Calame, K. L. B lymphocyte-induced maturation protein (Blimp)-1, IFN regulatory factor (IRF)-1, and IRF-2 can bind to the same regulatory sites. *J Immunol* **173**, 5556-5563 (2004).
51 Robertson, E. J. *et al.* Blimp1 regulates development of the posterior forelimb, caudal pharyngeal arches, heart and sensory vibrissae in mice. *Development* **134**, 4335-4345, doi:10.1242/dev.012047 (2007).
52 Yabuta, Y., Kurimoto, K., Ohinata, Y., Seki, Y. & Saitou, M. Gene expression dynamics during germline specification in mice identified by quantitative single-cell gene expression profiling. *Biol Reprod* **75**, 705-716, doi:10.1095/biolreprod.106.053686 (2006).
53 Arney, K. L., Erhardt, S., Drewell, R. A. & Surani, M. A. Epigenetic reprogramming of the genome--from the germ line to the embryo and back again. *Int J Dev Biol* **45**, 533-540 (2001).

54 Kurimoto, K., Yamaji, M., Seki, Y. & Saitou, M. Specification of the germ cell lineage in mice: a process orchestrated by the PR-domain proteins, Blimp1 and Prdm14. *Cell Cycle* **7**, 3514-3518 (2008).
55 Saitou, M., Barton, S. C. & Surani, M. A. A molecular programme for the specification of germ cell fate in mice. *Nature* **418**, 293-300, doi:10.1038/nature00927 (2002).
56 Tanaka, S. S. & Matsui, Y. Developmentally regulated expression of mil-1 and mil-2, mouse interferon-induced transmembrane protein like genes, during formation and differentiation of primordial germ cells. *Gene Expr Patterns* **2**, 297-303 (2002).
57 Ohinata, Y. *et al.* Blimp1 is a critical determinant of the germ cell lineage in mice. *Nature* **436**, 207-213, doi:10.1038/nature03813 (2005).
58 Ancelin, K. *et al.* Blimp1 associates with Prmt5 and directs histone arginine methylation in mouse germ cells. *Nat Cell Biol* **8**, 623-630, doi:10.1038/ncb1413 (2006).
59 Seki, Y. *et al.* Extensive and orderly reprogramming of genome-wide chromatin modifications associated with specification and early development of germ cells in mice. *Dev Biol* **278**, 440-458, doi:10.1016/j.ydbio.2004.11.025 (2005).
60 Hajkova, P. *et al.* Chromatin dynamics during epigenetic reprogramming in the mouse germ line. *Nature* **452**, 877-881, doi:10.1038/nature06714 (2008).
61 Yamaji, M. *et al.* Critical function of Prdm14 for the establishment of the germ cell lineage in mice. *Nat Genet* **40**, 1016-1022, doi:10.1038/ng.186 (2008).
62 Assou, S. *et al.* A meta-analysis of human embryonic stem cells transcriptome integrated into a web-based expression atlas. *Stem Cells* **25**, 961-973, doi:10.1634/stemcells.2006-0352 (2007).
63 Tsuneyoshi, N. *et al.* PRDM14 suppresses expression of differentiation marker genes in human embryonic stem cells. *Biochem Biophys Res Commun* **367**, 899-905, doi:10.1016/j.bbrc.2007.12.189 (2008).
64 Shapiro-Shelef, M. *et al.* Blimp-1 is required for the formation of immunoglobulin secreting plasma cells and pre-plasma memory B cells. *Immunity* **19**, 607-620 (2003).
65 Angelin-Duclos, C., Cattoretti, G., Lin, K. I. & Calame, K. Commitment of B lymphocytes to a plasma cell fate is associated with Blimp-1 expression in vivo. *J Immunol* **165**, 5462-5471 (2000).
66 Kallies, A. *et al.* Plasma cell ontogeny defined by quantitative changes in blimp-1 expression. *J Exp Med* **200**, 967-977, doi:10.1084/jem.20040973 (2004).
67 Shapiro-Shelef, M. & Calame, K. Regulation of plasma-cell development. *Nat Rev Immunol* **5**, 230-242, doi:10.1038/nri1572 (2005).
68 Savitsky, D. & Calame, K. B-1 B lymphocytes require Blimp-1 for immunoglobulin secretion. *J Exp Med* **203**, 2305-2314, doi:10.1084/jem.20060411 (2006).
69 Ye, B. H. *et al.* The BCL-6 proto-oncogene controls germinal-centre formation and Th2-type inflammation. *Nat Genet* **16**, 161-170, doi:10.1038/ng0697-161 (1997).
70 Tangye, S. G. & Tarlinton, D. M. Memory B cells: effectors of long-lived immune responses. *Eur J Immunol* **39**, 2065-2075, doi:10.1002/eji.200939531 (2009).
71 Klein, B. *et al.* Survival and proliferation factors of normal and malignant plasma cells. *Int J Hematol* **78**, 106-113 (2003).
72 Shaffer, A. L. *et al.* Blimp-1 orchestrates plasma cell differentiation by extinguishing the mature B cell gene expression program. *Immunity* **17**, 51-62 (2002).
73 Kallies, A. *et al.* Transcriptional repressor Blimp-1 is essential for T cell homeostasis and self-tolerance. *Nat Immunol* **7**, 466-474, doi:10.1038/ni1321 (2006).
74 Martins, G. A. *et al.* Transcriptional repressor Blimp-1 regulates T cell homeostasis and function. *Nat Immunol* **7**, 457-465, doi:10.1038/ni1320 (2006).
75 Cimmino, L. *et al.* Blimp-1 attenuates Th1 differentiation by repression of ifng, tbx21, and bcl6 gene expression. *J Immunol* **181**, 2338-2347 (2008).
76 Rutishauser, R. L. *et al.* Transcriptional repressor Blimp-1 promotes CD8(+) T cell terminal differentiation and represses the acquisition of central memory T cell properties. *Immunity* **31**, 296-308, doi:10.1016/j.immuni.2009.05.014 (2009).
77 Kallies, A., Xin, A., Belz, G. T. & Nutt, S. L. Blimp-1 transcription factor is required for the differentiation of effector CD8(+) T cells and memory responses. *Immunity* **31**, 283-295, doi:10.1016/j.immuni.2009.06.021 (2009).
78 Shin, H. *et al.* A role for the transcriptional repressor Blimp-1 in CD8(+) T cell exhaustion during chronic viral infection. *Immunity* **31**, 309-320, doi:10.1016/j.immuni.2009.06.019 (2009).
79 Chtanova, T. *et al.* T follicular helper cells express a distinctive transcriptional profile, reflecting their role as non-Th1/Th2 effector cells that provide help for B cells. *J Immunol* **173**, 68-78 (2004).
80 Johnston, R. J. *et al.* Bcl6 and Blimp-1 are reciprocal and antagonistic regulators of T follicular helper cell differentiation. *Science* **325**, 1006-1010, doi:10.1126/science.1175870 (2009).
81 Fazilleau, N., McHeyzer-Williams, L. J., Rosen, H. & McHeyzer-Williams, M. G. The function of follicular helper T cells is regulated by the strength of T cell antigen receptor binding. *Nat Immunol* **10**, 375-384, doi:10.1038/ni.1704 (2009).

82 Kallies, A. *et al.* A role for Blimp1 in the transcriptional network controlling natural killer cell maturation. *Blood* **117**, 1869-1879, doi:10.1182/blood-2010-08-303123 (2011).
83 Lin, Y., Wong, K. & Calame, K. Repression of c-myc transcription by Blimp-1, an inducer of terminal B cell differentiation. *Science* **276**, 596-599 (1997).
84 Lin, K. I., Lin, Y. & Calame, K. Repression of c-myc is necessary but not sufficient for terminal differentiation of B lymphocytes in vitro. *Mol Cell Biol* **20**, 8684-8695 (2000).
85 Marsden, V. S. & Strasser, A. Control of apoptosis in the immune system: Bcl-2, BH3-only proteins and more. *Annu Rev Immunol* **21**, 71-105, doi:10.1146/annurev.immunol.21.120601.141029 (2003).
86 Quong, M. W., Romanow, W. J. & Murre, C. E protein function in lymphocyte development. *Annu Rev Immunol* **20**, 301-322, doi:10.1146/annurev.immunol.20.092501.162048 (2002).
87 Kamimura, D. & Bevan, M. J. Endoplasmic reticulum stress regulator XBP-1 contributes to effector CD8+ T cell differentiation during acute infection. *J Immunol* **181**, 5433-5441 (2008).
88 Shaffer, A. L. *et al.* XBP1, downstream of Blimp-1, expands the secretory apparatus and other organelles, and increases protein synthesis in plasma cell differentiation. *Immunity* **21**, 81-93, doi:10.1016/j.immuni.2004.06.010 (2004).
89 Reimold, A. M. *et al.* Transcription factor B cell lineage-specific activator protein regulates the gene for human X-box binding protein 1. *J Exp Med* **183**, 393-401 (1996).
90 Martins, G. & Calame, K. Regulation and functions of Blimp-1 in T and B lymphocytes. *Annu Rev Immunol* **26**, 133-169, doi:10.1146/annurev.immunol.26.021607.090241 (2008).
91 Gong, D. & Malek, T. R. Cytokine-dependent Blimp-1 expression in activated T cells inhibits IL-2 production. *J Immunol* **178**, 242-252 (2007).
92 Martins, G. A., Cimmino, L., Liao, J., Magnusdottir, E. & Calame, K. Blimp-1 directly represses Il2 and the Il2 activator Fos, attenuating T cell proliferation and survival. *J Exp Med* **205**, 1959-1965, doi:10.1084/jem.20080526 (2008).
93 Lin, K. I., Angelin-Duclos, C., Kuo, T. C. & Calame, K. Blimp-1-dependent repression of Pax-5 is required for differentiation of B cells to immunoglobulin M-secreting plasma cells. *Mol Cell Biol* **22**, 4771-4780 (2002).
94 Piskurich, J. F. *et al.* BLIMP-I mediates extinction of major histocompatibility class II transactivator expression in plasma cells. *Nat Immunol* **1**, 526-532, doi:10.1038/82788 (2000).
95 Chen, H. *et al.* Positive regulatory domain I-binding factor 1 mediates repression of the MHC class II transactivator (CIITA) type IV promoter. *Mol Immunol* **44**, 1461-1470, doi:10.1016/j.molimm.2006.04.026 (2007).
96 Keller, A. D. & Maniatis, T. Only two of the five zinc fingers of the eukaryotic transcriptional repressor PRDI-BF1 are required for sequence-specific DNA binding. *Mol Cell Biol* **12**, 1940-1949 (1992).
97 Yu, J., Angelin-Duclos, C., Greenwood, J., Liao, J. & Calame, K. Transcriptional repression by blimp-1 (PRDI-BF1) involves recruitment of histone deacetylase. *Mol Cell Biol* **20**, 2592-2603 (2000).
98 Grunstein, M. Histone acetylation in chromatin structure and transcription. *Nature* **389**, 349-352, doi:10.1038/38664 (1997).
99 Messika, E. J. *et al.* Differential effect of B lymphocyte-induced maturation protein (Blimp-1) expression on cell fate during B cell development. *J Exp Med* **188**, 515-525 (1998).
100 Su, S. T. *et al.* Involvement of histone demethylase LSD1 in Blimp-1-mediated gene repression during plasma cell differentiation. *Mol Cell Biol* **29**, 1421-1431, doi:10.1128/MCB.01158-08 (2009).
101 Wilm, T. P. & Solnica-Krezel, L. Essential roles of a zebrafish prdm1/blimp1 homolog in embryo patterning and organogenesis. *Development* **132**, 393-404, doi:10.1242/dev.01572 (2005).
102 Cornell, R. A. & Eisen, J. S. Delta signaling mediates segregation of neural crest and spinal sensory neurons from zebrafish lateral neural plate. *Development* **127**, 2873-2882 (2000).
103 Knecht, A. K. & Bronner-Fraser, M. Induction of the neural crest: a multigene process. *Nat Rev Genet* **3**, 453-461, doi:10.1038/nrg819 (2002).
104 Rossi, C. C., Kaji, T. & Artinger, K. B. Transcriptional control of Rohon-Beard sensory neuron development at the neural plate border. *Dev Dyn* **238**, 931-943, doi:10.1002/dvdy.21915 (2009).
105 Barth, K. A. *et al.* Bmp activity establishes a gradient of positional information throughout the entire neural plate. *Development* **126**, 4977-4987 (1999).
106 Nguyen, V. H. *et al.* Ventral and lateral regions of the zebrafish gastrula, including the neural crest progenitors, are established by a bmp2b/swirl pathway of genes. *Dev Biol* **199**, 93-110, doi:10.1006/dbio.1998.8927 (1998).
107 Nguyen, V. H. *et al.* Dorsal and intermediate neuronal cell types of the spinal cord are established by a BMP signaling pathway. *Development* **127**, 1209-1220 (2000).
108 Neave, B., Holder, N. & Patient, R. A graded response to BMP-4 spatially coordinates patterning of the mesoderm and ectoderm in the zebrafish. *Mech Dev* **62**, 183-195 (1997).
109 Roy, S. & Ng, T. Blimp-1 specifies neural crest and sensory neuron progenitors in the zebrafish embryo. *Curr Biol* **14**, 1772-1777, doi:10.1016/j.cub.2004.09.046 (2004).

110 Hernandez-Lagunas, L. *et al.* Zebrafish narrowminded disrupts the transcription factor prdm1 and is required for neural crest and sensory neuron specification. *Dev Biol* **278**, 347-357, doi:10.1016/j.ydbio.2004.11.014 (2005).
111 von Hofsten, J. *et al.* Prdm1- and Sox6-mediated transcriptional repression specifies muscle fibre type in the zebrafish embryo. *EMBO Rep* **9**, 683-689, doi:10.1038/embor.2008.73 (2008).
112 Liew, H. P., Choksi, S. P., Wong, K. N. & Roy, S. Specification of vertebrate slow-twitch muscle fiber fate by the transcriptional regulator Blimp1. *Dev Biol* **324**, 226-235, doi:10.1016/j.ydbio.2008.09.020 (2008).
113 Lee, B. C. & Roy, S. Blimp-1 is an essential component of the genetic program controlling development of the pectoral limb bud. *Dev Biol* **300**, 623-634, doi:10.1016/j.ydbio.2006.07.031 (2006).
114 Altman, J. & Das, G. D. Autoradiographic and histological evidence of postnatal hippocampal neurogenesis in rats. *J Comp Neurol* **124**, 319-335 (1965).
115 Doetsch, F., Caille, I., Lim, D. A., Garcia-Verdugo, J. M. & Alvarez-Buylla, A. Subventricular zone astrocytes are neural stem cells in the adult mammalian brain. *Cell* **97**, 703-716 (1999).
116 Palmer, T. D., Takahashi, J. & Gage, F. H. The adult rat hippocampus contains primordial neural stem cells. *Mol Cell Neurosci* **8**, 389-404, doi:10.1006/mcne.1996.0595 (1997).
117 Eriksson, P. S. *et al.* Neurogenesis in the adult human hippocampus. *Nat Med* **4**, 1313-1317, doi:10.1038/3305 (1998).
118 Seri, B. *et al.* Composition and organization of the SCZ: a large germinal layer containing neural stem cells in the adult mammalian brain. *Cereb Cortex* **16 Suppl 1**, i103-111, doi:10.1093/cercor/bhk027 (2006).
119 Kuhn, H. G., Dickinson-Anson, H. & Gage, F. H. Neurogenesis in the dentate gyrus of the adult rat: age-related decrease of neuronal progenitor proliferation. *J Neurosci* **16**, 2027-2033 (1996).
120 Encinas, J. M. & Enikolopov, G. Identifying and quantitating neural stem and progenitor cells in the adult brain. *Methods Cell Biol* **85**, 243-272, doi:10.1016/S0091-679X(08)85011-X (2008).
121 Ni Dhuill, C. M. *et al.* Polysialylated neural cell adhesion molecule expression in the dentate gyrus of the human hippocampal formation from infancy to old age. *J Neurosci Res* **55**, 99-106 (1999).
122 Reynolds, B. A. & Rietze, R. L. Neural stem cells and neurospheres--re-evaluating the relationship. *Nat Methods* **2**, 333-336, doi:10.1038/nmeth758 (2005).
123 Singec, I. *et al.* Defining the actual sensitivity and specificity of the neurosphere assay in stem cell biology. *Nat Methods* **3**, 801-806, doi:10.1038/nmeth926 (2006).
124 Weigmann, A., Corbeil, D., Hellwig, A. & Huttner, W. B. Prominin, a novel microvilli-specific polytopic membrane protein of the apical surface of epithelial cells, is targeted to plasmalemmal protrusions of non-epithelial cells. *Proc Natl Acad Sci U S A* **94**, 12425-12430 (1997).
125 Yin, A. H. *et al.* AC133, a novel marker for human hematopoietic stem and progenitor cells. *Blood* **90**, 5002-5012 (1997).
126 Uchida, N. *et al.* Direct isolation of human central nervous system stem cells. *Proc Natl Acad Sci U S A* **97**, 14720-14725, doi:10.1073/pnas.97.26.14720 (2000).
127 Yu, S., Zhang, J. Z., Zhao, C. L., Zhang, H. Y. & Xu, Q. Isolation and characterization of the CD133+ precursors from the ventricular zone of human fetal brain by magnetic affinity cell sorting. *Biotechnol Lett* **26**, 1131-1136, doi:10.1023/B:BILE.0000035484.64499.ac (2004).
128 Capela, A. & Temple, S. LeX is expressed by principle progenitor cells in the embryonic nervous system, is secreted into their environment and binds Wnt-1. *Dev Biol* **291**, 300-313, doi:10.1016/j.ydbio.2005.12.030 (2006).
129 Corti, S. *et al.* Multipotentiality, homing properties, and pyramidal neurogenesis of CNS-derived LeX(ssea-1)+/CXCR4+ stem cells. *Faseb J* **19**, 1860-1862, doi:10.1096/fj.05-4170fje (2005).
130 Panchision, D. M. *et al.* Optimized flow cytometric analysis of central nervous system tissue reveals novel functional relationships among cells expressing CD133, CD15, and CD24. *Stem Cells* **25**, 1560-1570, doi:10.1634/stemcells.2006-0260 (2007).
131 Keyoung, H. M. *et al.* High-yield selection and extraction of two promoter-defined phenotypes of neural stem cells from the fetal human brain. *Nat Biotechnol* **19**, 843-850, doi:10.1038/nbt0901-843 (2001).
132 Roy, N. S. *et al.* In vitro neurogenesis by progenitor cells isolated from the adult human hippocampus. *Nat Med* **6**, 271-277, doi:10.1038/73119 (2000).
133 Ferri, A. L. *et al.* Sox2 deficiency causes neurodegeneration and impaired neurogenesis in the adult mouse brain. *Development* **131**, 3805-3819, doi:10.1242/dev.01204 (2004).
134 Malas, S. *et al.* Sox1-deficient mice suffer from epilepsy associated with abnormal ventral forebrain development and olfactory cortex hyperexcitability. *Neuroscience* **119**, 421-432 (2003).
135 Rizzoti, K. *et al.* SOX3 is required during the formation of the hypothalamo-pituitary axis. *Nat Genet* **36**, 247-255, doi:10.1038/ng1309 (2004).
136 Graham, V., Khudyakov, J., Ellis, P. & Pevny, L. SOX2 functions to maintain neural progenitor identity. *Neuron* **39**, 749-765 (2003).

137 Wang, T. W. *et al.* Sox3 expression identifies neural progenitors in persistent neonatal and adult mouse forebrain germinative zones. *J Comp Neurol* **497**, 88-100, doi:10.1002/cne.20984 (2006).
138 Fasano, C. A. *et al.* shRNA knockdown of Bmi-1 reveals a critical role for p21-Rb pathway in NSC self-renewal during development. *Cell Stem Cell* **1**, 87-99, doi:10.1016/j.stem.2007.04.001 (2007).
139 Molofsky, A. V. *et al.* Bmi-1 dependence distinguishes neural stem cell self-renewal from progenitor proliferation. *Nature* **425**, 962-967, doi:10.1038/nature02060 (2003).
140 Dahmane, N. *et al.* The Sonic Hedgehog-Gli pathway regulates dorsal brain growth and tumorigenesis. *Development* **128**, 5201-5212 (2001).
141 Kageyama, R., Ohtsuka, T., Hatakeyama, J. & Ohsawa, R. Roles of bHLH genes in neural stem cell differentiation. *Exp Cell Res* **306**, 343-348, doi:10.1016/j.yexcr.2005.03.015 (2005).
142 Hatakeyama, J. *et al.* Hes genes regulate size, shape and histogenesis of the nervous system by control of the timing of neural stem cell differentiation. *Development* **131**, 5539-5550, doi:10.1242/dev.01436 (2004).
143 Okano, H. *et al.* Function of RNA-binding protein Musashi-1 in stem cells. *Exp Cell Res* **306**, 349-356, doi:10.1016/j.yexcr.2005.02.021 (2005).
144 Nieto, M., Schuurmans, C., Britz, O. & Guillemot, F. Neural bHLH genes control the neuronal versus glial fate decision in cortical progenitors. *Neuron* **29**, 401-413 (2001).
145 Mao, Y. *et al.* Disrupted in schizophrenia 1 regulates neuronal progenitor proliferation via modulation of GSK3beta/beta-catenin signaling. *Cell* **136**, 1017-1031, doi:10.1016/j.cell.2008.12.044 (2009).
146 Kuwabara, T. *et al.* Wnt-mediated activation of NeuroD1 and retro-elements during adult neurogenesis. *Nat Neurosci* **12**, 1097-1105, doi:10.1038/nn.2360 (2009).
147 Lo, L., Sommer, L. & Anderson, D. J. MASH1 maintains competence for BMP2-induced neuronal differentiation in post-migratory neural crest cells. *Curr Biol* **7**, 440-450 (1997).
148 Paris, M., Wang, W. H., Shin, M. H., Franklin, D. S. & Andrisani, O. M. Homeodomain transcription factor Phox2a, via cyclic AMP-mediated activation, induces p27Kip1 transcription, coordinating neural progenitor cell cycle exit and differentiation. *Mol Cell Biol* **26**, 8826-8839, doi:10.1128/MCB.00575-06 (2006).
149 Cau, E., Gradwohl, G., Fode, C. & Guillemot, F. Mash1 activates a cascade of bHLH regulators in olfactory neuron progenitors. *Development* **124**, 1611-1621 (1997).
150 Bel-Vialar, S., Medevielle, F. & Pituello, F. The on/off of Pax6 controls the tempo of neuronal differentiation in the developing spinal cord. *Dev Biol* **305**, 659-673, doi:10.1016/j.ydbio.2007.02.012 (2007).
151 Fior, R. & Henrique, D. A novel hes5/hes6 circuitry of negative regulation controls Notch activity during neurogenesis. *Dev Biol* **281**, 318-333, doi:10.1016/j.ydbio.2005.03.017 (2005).
152 Sun, Y. *et al.* Neurogenin promotes neurogenesis and inhibits glial differentiation by independent mechanisms. *Cell* **104**, 365-376 (2001).
153 Nakashima, K. *et al.* Synergistic signaling in fetal brain by STAT3-Smad1 complex bridged by p300. *Science* **284**, 479-482 (1999).
154 Abematsu, M. *et al.* Basic fibroblast growth factor endows dorsal telencephalic neural progenitors with the ability to differentiate into oligodendrocytes but not gamma-aminobutyric acidergic neurons. *J Neurosci Res* **83**, 731-743, doi:10.1002/jnr.20762 (2006).
155 Kinameri, E. *et al.* Prdm proto-oncogene transcription factor family expression and interaction with the Notch-Hes pathway in mouse neurogenesis. *PLoS One* **3**, e3859, doi:10.1371/journal.pone.0003859 (2008).
156 Huang, S. Histone methyltransferases, diet nutrients and tumour suppressors. *Nat Rev Cancer* **2**, 469-476, doi:10.1038/nrc819 (2002).
157 Liu, Z. Y. *et al.* Retinoblastoma protein-interacting zinc-finger gene 1 (RIZ1) dysregulation in human malignant meningiomas. *Oncogene*, doi:10.1038/onc.2012.155 (2012).
158 Morishita, K. *et al.* Retroviral activation of a novel gene encoding a zinc finger protein in IL-3-dependent myeloid leukemia cell lines. *Cell* **54**, 831-840 (1988).
159 Liu, L., Shao, G., Steele-Perkins, G. & Huang, S. The retinoblastoma interacting zinc finger gene RIZ produces a PR domain-lacking product through an internal promoter. *J Biol Chem* **272**, 2984-2991 (1997).
160 Gyory, I., Fejer, G., Ghosh, N., Seto, E. & Wright, K. L. Identification of a functionally impaired positive regulatory domain I binding factor 1 transcription repressor in myeloma cell lines. *J Immunol* **170**, 3125-3133 (2003).
161 Fichelson, S. *et al.* Evi-1 expression in leukemic patients with rearrangements of the 3q25-q28 chromosomal region. *Leukemia* **6**, 93-99 (1992).
162 He, L. *et al.* RIZ1, but not the alternative RIZ2 product of the same gene, is underexpressed in breast cancer, and forced RIZ1 expression causes G2-M cell cycle arrest and/or apoptosis. *Cancer Res* **58**, 4238-4244 (1998).
163 Bikoff, E. K., Morgan, M. A. & Robertson, E. J. An expanding job description for Blimp-1/PRDM1. *Curr Opin Genet Dev* **19**, 379-385, doi:10.1016/j.gde.2009.05.005 (2009).

164 Alizadeh, A. A. *et al.* Distinct types of diffuse large B-cell lymphoma identified by gene expression profiling. *Nature* **403**, 503-511, doi:10.1038/35000501 (2000).
165 Pasqualucci, L. *et al.* Inactivation of the PRDM1/BLIMP1 gene in diffuse large B cell lymphoma. *J Exp Med* **203**, 311-317, doi:10.1084/jem.20052204 (2006).
166 Tam, W. *et al.* Mutational analysis of PRDM1 indicates a tumor-suppressor role in diffuse large B-cell lymphomas. *Blood* **107**, 4090-4100, doi:10.1182/blood-2005-09-3778 (2006).
167 Sasaki, Y. *et al.* Canonical NF-kappaB activity, dispensable for B cell development, replaces BAFF-receptor signals and promotes B cell proliferation upon activation. *Immunity* **24**, 729-739, doi:10.1016/j.immuni.2006.04.005 (2006).
168 Staudt, L. M. Oncogenic activation of NF-kappaB. *Cold Spring Harb Perspect Biol* **2**, a000109, doi:10.1101/cshperspect.a000109 (2010).
169 Bhakar, A. L. *et al.* Constitutive nuclear factor-kappa B activity is required for central neuron survival. *J Neurosci* **22**, 8466-8475 (2002).
170 Mandelbaum, J. *et al.* BLIMP1 is a tumor suppressor gene frequently disrupted in activated B cell-like diffuse large B cell lymphoma. *Cancer Cell* **18**, 568-579, doi:10.1016/j.ccr.2010.10.030 (2010).
171 Calado, D. P. *et al.* Constitutive canonical NF-kappaB activation cooperates with disruption of BLIMP1 in the pathogenesis of activated B cell-like diffuse large cell lymphoma. *Cancer Cell* **18**, 580-589, doi:10.1016/j.ccr.2010.11.024 (2010).
172 Liu, Y. Y. *et al.* Rituximab plus CHOP (R-CHOP) overcomes PRDM1-associated resistance to chemotherapy in patients with diffuse large B-cell lymphoma. *Blood* **110**, 339-344, doi:10.1182/blood-2006-09-049189 (2007).
173 Jiang, G. L. & Huang, S. The yin-yang of PR-domain family genes in tumorigenesis. *Histol Histopathol* **15**, 109-117 (2000).
174 Zhang, Y. W. *et al.* Loss of promoter methylation contributes to the expression of functionally impaired PRDM1beta isoform in diffuse large B-cell lymphoma. *Int J Hematol* **92**, 439-444, doi:10.1007/s12185-010-0689-3 (2010).
175 Zhao, W. L. *et al.* PRDM1 is involved in chemoresistance of T-cell lymphoma and down-regulated by the proteasome inhibitor. *Blood* **111**, 3867-3871, doi:10.1182/blood-2007-08-108654 (2008).
176 Garcia, J. F. *et al.* PRDM1/BLIMP-1 expression in multiple B and T-cell lymphoma. *Haematologica* **91**, 467-474 (2006).
177 Feiden, S. & Feiden, W. [WHO classification of tumours of the CNS: revised edition of 2007 with critical comments on the typing und grading of common-type diffuse gliomas]. *Pathologe* **29**, 411-421, doi:10.1007/s00292-008-1064-5 (2008).
178 Miller, C. R. & Perry, A. Glioblastoma. *Arch Pathol Lab Med* **131**, 397-406, doi:10.1043/1543-2165(2007)131[397:G]2.0.CO;2 (2007).
179 Biernat, W., Huang, H., Yokoo, H., Kleihues, P. & Ohgaki, H. Predominant expression of mutant EGFR (EGFRvIII) is rare in primary glioblastomas. *Brain Pathol* **14**, 131-136 (2004).
180 Ohgaki, H. & Kleihues, P. Population-based studies on incidence, survival rates, and genetic alterations in astrocytic and oligodendroglial gliomas. *J Neuropathol Exp Neurol* **64**, 479-489 (2005).
181 Dang, L., Jin, S. & Su, S. M. IDH mutations in glioma and acute myeloid leukemia. *Trends Mol Med* **16**, 387-397, doi:10.1016/j.molmed.2010.07.002 (2010).
182 Verhaak, R. G. *et al.* Integrated genomic analysis identifies clinically relevant subtypes of glioblastoma characterized by abnormalities in PDGFRA, IDH1, EGFR, and NF1. *Cancer Cell* **17**, 98-110, doi:10.1016/j.ccr.2009.12.020 (2010).
183 Phillips, H. S. *et al.* Molecular subclasses of high-grade glioma predict prognosis, delineate a pattern of disease progression, and resemble stages in neurogenesis. *Cancer Cell* **9**, 157-173, doi:10.1016/j.ccr.2006.02.019 (2006).
184 Sanai, N., Alvarez-Buylla, A. & Berger, M. S. Neural stem cells and the origin of gliomas. *N Engl J Med* **353**, 811-822, doi:10.1056/NEJMra043666 (2005).
185 Beroukhim, R. *et al.* Assessing the significance of chromosomal aberrations in cancer: methodology and application to glioma. *Proc Natl Acad Sci U S A* **104**, 20007-20012, doi:10.1073/pnas.0710052104 (2007).
186 Mermel, C. H. *et al.* GISTIC2.0 facilitates sensitive and confident localization of the targets of focal somatic copy-number alteration in human cancers. *Genome Biol* **12**, R41, doi:10.1186/gb-2011-12-4-r41 (2011).
187 Parsons, D. W. *et al.* An integrated genomic analysis of human glioblastoma multiforme. *Science* **321**, 1807-1812, doi:10.1126/science.1164382 (2008).
188 Carro, M. S. *et al.* The transcriptional network for mesenchymal transformation of brain tumours. *Nature* **463**, 318-325, doi:10.1038/nature08712 (2010).
189 Bhat, K. P. *et al.* The transcriptional coactivator TAZ regulates mesenchymal differentiation in malignant glioma. *Genes Dev* **25**, 2594-2609, doi:10.1101/gad.176800.111 (2011).
190 Sanai, N. Integrated genomic analysis identifies clinically relevant subtypes of glioblastoma. *World Neurosurg* **74**, 4-5, doi:10.1016/j.wneu.2010.08.011 (2010).

191 Gorovets, D. *et al.* IDH mutation and neuroglial developmental features define clinically distinct subclasses of lower grade diffuse astrocytic glioma. *Clin Cancer Res* **18**, 2490-2501, doi:10.1158/1078-0432.CCR-11-2977 (2012).
192 Nishikawa, R. Standard therapy for glioblastoma--a review of where we are. *Neurol Med Chir (Tokyo)* **50**, 713-719 (2010).
193 Stupp, R. *et al.* Effects of radiotherapy with concomitant and adjuvant temozolomide versus radiotherapy alone on survival in glioblastoma in a randomised phase III study: 5-year analysis of the EORTC-NCIC trial. *Lancet Oncol* **10**, 459-466, doi:10.1016/S1470-2045(09)70025-7 (2009).
194 Weller, M. *et al.* MGMT promoter methylation in malignant gliomas: ready for personalized medicine? *Nat Rev Neurol* **6**, 39-51, doi:10.1038/nrneurol.2009.197 (2010).
195 Brandes, A. A. *et al.* MGMT promoter methylation status can predict the incidence and outcome of pseudoprogression after concomitant radiochemotherapy in newly diagnosed glioblastoma patients. *J Clin Oncol* **26**, 2192-2197, doi:10.1200/JCO.2007.14.8163 (2008).
196 Labussiere, M. *et al.* All the 1p19q codeleted gliomas are mutated on IDH1 or IDH2. *Neurology* **74**, 1886-1890, doi:10.1212/WNL.0b013e3181e1cf3a (2010).
197 Cahoy, J. D. *et al.* A transcriptome database for astrocytes, neurons, and oligodendrocytes: a new resource for understanding brain development and function. *J Neurosci* **28**, 264-278, doi:10.1523/JNEUROSCI.4178-07.2008 (2008).
198 Lee, T. I. *et al.* Control of developmental regulators by Polycomb in human embryonic stem cells. *Cell* **125**, 301-313, doi:10.1016/j.cell.2006.02.043 (2006).
199 Boyer, L. A. *et al.* Polycomb complexes repress developmental regulators in murine embryonic stem cells. *Nature* **441**, 349-353, doi:10.1038/nature04733 (2006).
200 Kim, J. *et al.* A Myc network accounts for similarities between embryonic stem and cancer cell transcription programs. *Cell* **143**, 313-324, doi:10.1016/j.cell.2010.09.010 (2010).
201 Hawkins, R. D. *et al.* Distinct epigenomic landscapes of pluripotent and lineage-committed human cells. *Cell Stem Cell* **6**, 479-491, doi:10.1016/j.stem.2010.03.018 (2010).
202 O'Geen, H. *et al.* Genome-wide analysis of KAP1 binding suggests autoregulation of KRAB-ZNFs. *PLoS Genet* **3**, e89, doi:10.1371/journal.pgen.0030089 (2007).
203 Comprehensive genomic characterization defines human glioblastoma genes and core pathways. *Nature* **455**, 1061-1068, doi:10.1038/nature07385 (2008).
204 Narayanan, G. *et al.* Single-Cell mRNA Profiling Identifies Progenitor Subclasses in Neurospheres. *Stem Cells Dev*, doi:10.1089/scd.2012.0232 (2012).
205 Milosevic, J. *et al.* Lack of hypoxia-inducible factor-1 alpha impairs midbrain neural precursor cells involving vascular endothelial growth factor signaling. *J Neurosci* **27**, 412-421, doi:10.1523/JNEUROSCI.2482-06.2007 (2007).
206 Nutt, S. L., Fairfax, K. A. & Kallies, A. BLIMP1 guides the fate of effector B and T cells. *Nat Rev Immunol* **7**, 923-927, doi:10.1038/nri2204 (2007).
207 Tooze, R. M., Stephenson, S. & Doody, G. M. Repression of IFN-gamma induction of class II transactivator: a role for PRDM1/Blimp-1 in regulation of cytokine signaling. *J Immunol* **177**, 4584-4593 (2006).
208 Gargiulo, G. *et al.* NA-Seq: a discovery tool for the analysis of chromatin structure and dynamics during differentiation. *Dev Cell* **16**, 466-481, doi:10.1016/j.devcel.2009.02.002 (2009).
209 Wen, B., Wu, H., Shinkai, Y., Irizarry, R. A. & Feinberg, A. P. Large histone H3 lysine 9 dimethylated chromatin blocks distinguish differentiated from embryonic stem cells. *Nat Genet* **41**, 246-250, doi:10.1038/ng.297 (2009).
210 Mohn, F. *et al.* Lineage-specific polycomb targets and de novo DNA methylation define restriction and potential of neuronal progenitors. *Mol Cell* **30**, 755-766, doi:10.1016/j.molcel.2008.05.007 (2008).
211 Bracken, A. P. *et al.* The Polycomb group proteins bind throughout the INK4A-ARF locus and are disassociated in senescent cells. *Genes Dev* **21**, 525-530, doi:10.1101/gad.415507 (2007).
212 Kriegstein, A. & Alvarez-Buylla, A. The glial nature of embryonic and adult neural stem cells. *Annu Rev Neurosci* **32**, 149-184, doi:10.1146/annurev.neuro.051508.135600 (2009).
213 Pollard, S. M. *et al.* Glioma stem cell lines expanded in adherent culture have tumor-specific phenotypes and are suitable for chemical and genetic screens. *Cell Stem Cell* **4**, 568-580, doi:10.1016/j.stem.2009.03.014 (2009).
214 Chen, J., McKay, R. M. & Parada, L. F. Malignant glioma: lessons from genomics, mouse models, and stem cells. *Cell* **149**, 36-47, doi:10.1016/j.cell.2012.03.009 (2012).
215 Marumoto, T. *et al.* Development of a novel mouse glioma model using lentiviral vectors. *Nat Med* **15**, 110-116, doi:10.1038/nm.1863 (2009).
216 Sturm, D. *et al.* Hotspot Mutations in H3F3A and IDH1 Define Distinct Epigenetic and Biological Subgroups of Glioblastoma. *Cancer Cell* **22**, 425-437, doi:10.1016/j.ccr.2012.08.024 (2012).
217 Wu, G. *et al.* Somatic histone H3 alterations in pediatric diffuse intrinsic pontine gliomas and non-brainstem glioblastomas. *Nat Genet* **44**, 251-253, doi:10.1038/ng.1102 (2012).

218 Schwartzentruber, J. *et al.* Driver mutations in histone H3.3 and chromatin remodelling genes in paediatric glioblastoma. *Nature* **482**, 226-231, doi:10.1038/nature10833 (2012).

Appendix I

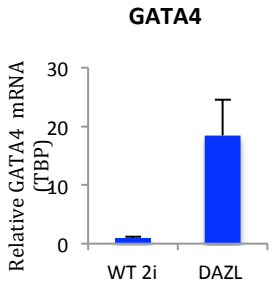

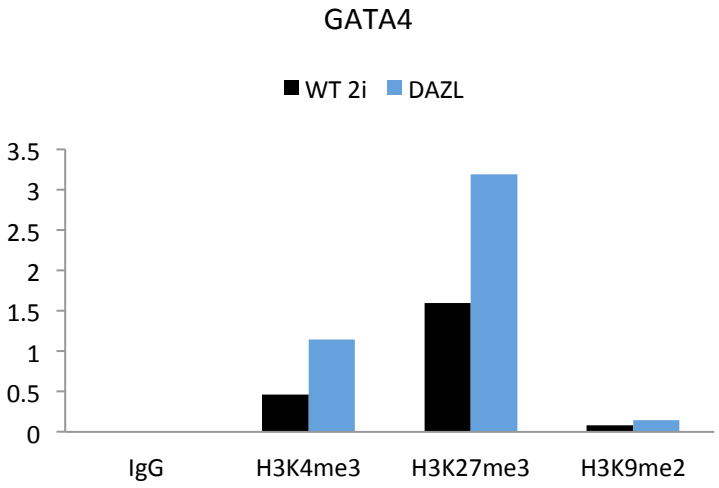

Common PRDM1 and PcG target gene GATA 4, differently from PAX6 and TAL1, is up regulated in DAZL induced mESC differentiation. Accordingly with expression data, the promoter does not acquire repressive histone marks duringcellular differentiation.

Appendix II

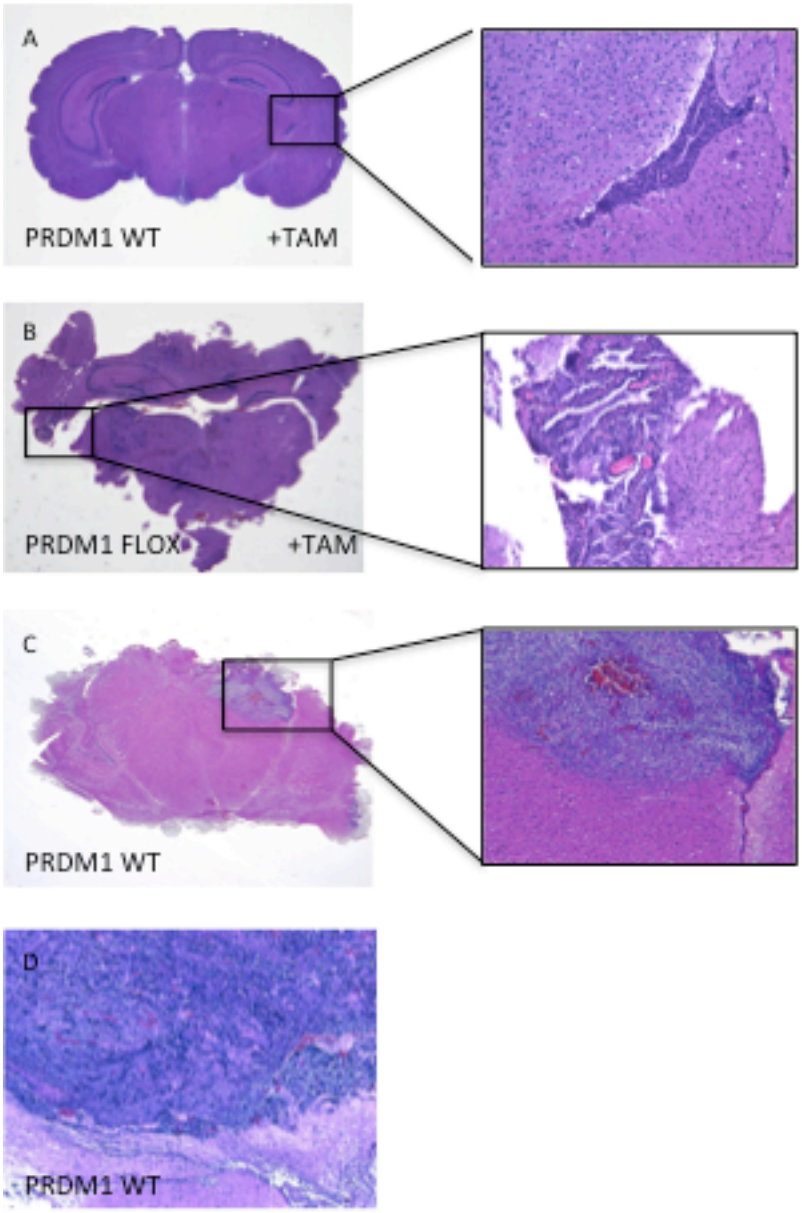

Histological features of mouse brains showing initial or evident signs of high grade glioma. The brain in A and B were collected from mice that prematurely died for other causes. In both the cases hematoxylin and eosin staining revealed signs of tumor formation such as areas of rapidly proliferating cells and in B also of hemorrhages. The images in C) and D) referred to full blown tumors obtained around four months after H-RASV12 inoculation. Since now we collected tumors only from mice with PRDM1 WT background but we are still collecting results and phenotypically analyzing them.